2004

Stress effects on ferromagnetic materials: investigation of stainless steel and nickel

Lu Li
Iowa State University

NOTE TO USERS

Stress effects on ferromagnetic materials – investigation of stainless steel and nickel

by

Lu Li

A dissertation submitted to the graduate faculty

in partial fulfillment of the requirements for the degree of

DOCTOR OF PHILOSOPHY

Major: Electrical Engineering
Program of Study Committee:
David. C. Jiles, Major Professor
John Bowler
Mani Mina
Robert J. Weber
Bulent S. Biner

Iowa State University

Ames, Iowa

2004

Graduate College
Iowa State University

This is to certify that the doctoral dissertation of

Lu Li

has met the dissertation requirements of Iowa State University

Signature was redacted for privacy.

Major Professor

Signature was redacted for privacy.

For the Major Program

TABLE OF CONTENTS

LIST OF TABLES

LIST OF FIGURES

ACKNOWLEDGMENTS

My foremost thanks go to my major advisers Dr. David C. Jiles. I thank him for his insights and suggestions that helped to shape my research skills. The feedback he gave to me contributed greatly to this dissertation.

I would also like to express my gratitude to my graduate committee members, Drs. John Bowler, Mani Mina, Robert J. Weber, and Bulent S. Biner for their generous contributions of time and effort during this research project and for providing me with valuable comments on earlier versions of this dissertation.

My special thanks also go to Dr. C.C.H. Lo for helping me further understand concepts in magnetic materials. I appreciate the valuable discussions and suggestions he gave to me.

In addition, I am grateful to all the professors, scientists, and graduate students in the magnetism program at Iowa State University, whose presences and fun-loving spirits made the otherwise grueling experience tolerable. I enjoyed all the vivid discussions we had on various topics and had lots of fun being a member of this fantastic group. During many discussions regarding my dissertation I received several valuable comments from: Dr. Yevgen Melikhov, Dr. Seong-Jae Lee, and Yuping Shen.

I feel a deep sense of gratitude to my parents who formed part of my vision and taught me the good things that really matter in life. I am grateful for my dear sisters and brothers for rendering me the sense and the value of sisterhood and brotherhood.

Last but not least, I thank my wife, Wenzheng Qiu, for always being there when I needed her most, and for the love and support she gave to me through all these years.

CHAPTER 1. GENERAL INTRODUCTION

This work reports on the recent investigation on the stress dependent hysteresis and magnetomechanical effects of ferromagnetic materials. The magnetic properties of several materials, such as nickel, both cold-worked and annealed, and steel, under various stresses were measured and modeled using an improved model theory. Chapter 1 gives a general introduction to magnetism, including domain theory and magnetization processes. The stress affected hysteresis and previous hysteresis models are introduced in chapter 2. Measurements on different samples and the extension of existing models are described in chapter 3. Chapter 4 gives detailed description of magnetomechanical effects. The existing models and the early approach to this field are also introduced. Chapter 5 shows the measurements of magnetomechanical effects and the simulation results based on the extended magnetomechanical model. The limitations of the revised model are also discussed. Chapter 6 draws the general conclusion and gives suggestion for future study. Reprints of paper published on hysteresis and magnetomechanical effects out of this work are included in the Appendix.

Chapter 1 begins with introduction of magnetism and its applications. Then the domain theory is explained followed by the explanation of magnetostriction and the magnetization process which is an important concept through the whole study.

1.1 Magnetism and its applications

Magnetism has been known to human beings for more than three thousand years. Magnets are substances that attract some other magnetic materials and are generally made from iron, cobalt or nickel. Alloys of Fe-Ni and few other elements added to them also show magnetism. Some rare earth elements also show magnetism. Practically alloys of Sm-Co or NdFeB are used as permanent magnets.

Magnets attract materials like Fe, Ni, Co. These materials are called magnetic materials. Some materials like copper, aluminum, gold, tin are not attracted to magnets and these materials are called non-magnetic materials.

Naturally occurring iron ores called lodestones are magnetic. They are used to make magnets with convenient shapes and sizes for use. Shapes of magnets can vary as a disc, a bar magnet or a horse shoe magnet.

On the macroscopic scale, magnets are associated with a pair of poles known as a dipole, consisting of the north pole and the south pole. If a bar magnet is hung freely, it will come to rest with its north pole facing the magnetic north. If one tries to displace it, again it will rotate and align itself to the magnetic north. In real life, the compass needle is made up of a magnet and it is widely used to find directions especially by navigators.

As mentioned above, a magnet has two poles – a north pole and a south pole. All the properties of magnets arise because of their poles. A magnetic pole cannot be isolated, that is to say we do not know of monopoles existing in isolation.

Magnetic effects can be induced on substances that can then become magnetic themselves. The substances mostly are made of magnetic materials like iron, cobalt or nickel.

Handling or breaking, heating, etc may reduce or destroy magnetism of ferromagnetic materials. Such effects are called demagnetizing effects. In order to minimize demagnetizing effects, a permanent magnet is always kept stuck to soft iron materials called keepers. These keepers help the poles to stay apart and not get stuck to each other or bang against each other.

An electric current also produces a magnetic field. This was first discovered by Oersted in 1820.

Applications of induced electric and magnetic fields are many. The most important use of magnets is in electric motors. All electric motors use electromagnets. These motors run refrigerators, vacuum cleaners, washing machines, compact disc players, blenders, drills, cars etc. Audiotape and videotape players have electromagnets called heads that record and read information on tapes or disks covered with tiny magnetic particles. Magnets in speakers transform the signal into a sound by making the speakers vibrate. An electromagnet called a deflection yoke in TV picture tubes helps form images on a screen. Huge electro-magnets are used to lift heavy iron objects such as cars; maglev trains run on electromagnets. Basic electricity generation also depends on the induced electric and magnetic fields.

An atom has negatively charged electrons orbiting around the positively charged nucleus. Each circulating electron can be visualized as a current loop. Thus electrons

produce magnetic fields around themselves. In an atom, a pair of electrons in the same orbit revolves in clockwise and anti-clockwise directions. This cancels the magnetic field produced by one electron with that produced by the other. Therefore only unpaired electrons are able to produce magnetic fields. The larger the number of unpaired of electrons, the larger will be the magnetic field surrounding the atoms. As seen in case of solenoids, the magnetic field generated by an orbiting electron is along the axis of the orbit.

In substances like copper, bismuth and other "non-magnetic" elements, the atomic magnetic field is non-existent because of paired electrons. In substances like aluminum, platinum, there are unpaired electrons; they exhibit weak magnetic fields. At ordinary temperatures, the magnetic directions of atoms are random. Hence these materials show only very weak magnetic behavior at ordinary temperatures. If an external magnetic field is applied, the atomic magnets get aligned with respect to the direction of the applied magnetic field. This behavior is enhanced at low temperatures as the random motion of the atoms is reduced. Thus the substances which show weak magnetic behavior on application of a magnetic field are called paramagnetic substances (Strictly speaking, a ferromagnet with low saturation magnetization might show "weak" magnetic behavior under an applied field. The main difference between paramagnetic and ferromagnetic materials is the absence and presence of spontaneous magnetization below the magnetic transformation temperature). When the field is removed, these substances show no magnetic alignment or net magnetization.

On the other hand substances like iron, nickel and cobalt show very high degree of alignment and magnetic behavior with the application of an external magnetic field. Even when the external magnetic field is removed, these substances retain magnetic alignment. These substances are called ferromagnetic materials. Ferromagnetic properties may be lost at high temperatures, as random alignment of atoms is increased due to thermal energy. Thus electron orbit alignments or spin alignments are essential to the magnetic behavior of a material. If by any method, the atomic alignment is disturbed or is made random, the material will lose its magnetism. This is the reason why breaking or heating a magnet destroys magnetism.

The unit of measuring magnetic field in the M.K.S. System is Tesla (T). In C.G.S system it is Gauss (g). 1 tesla = 10^4 gauss. The density of magnetic lines of force or flux is measured in M.K.S System is Weber (Wb). One Weber is the magnetic flux obtained in a circuit of one turn that produces a voltage of 1 volt, when the magnetic flux is reduced at a uniform rate in one second. In the C.G.S system, the magnetic flux is measured in Maxwell (Mx). 1 Wb = 10^8 Mx. Also 1 T = 1 Wb/m^2.

1.2 Domain theory

A remarkable property of ferromagnetic materials is not only that they have a spontaneous magnetization, but rather that their magnetization can be influenced by the application of very low magnetic fields. Even the earth's field can cause magnetization changes even though the inter-atomic exchange forces responsible for the spontaneous

magnetization are equivalent to a field of about 1000 T, almost 100 million times greater than the earth's field.

What allows this to occur is the fact that the sample is actually composed of small regions called magnetic domains, within each of which the local magnetization is saturated, but the directions of magnetization from one domain to the next one not necessarily parallel. Domains are small (1-100's microns), but much larger than atomic distances.

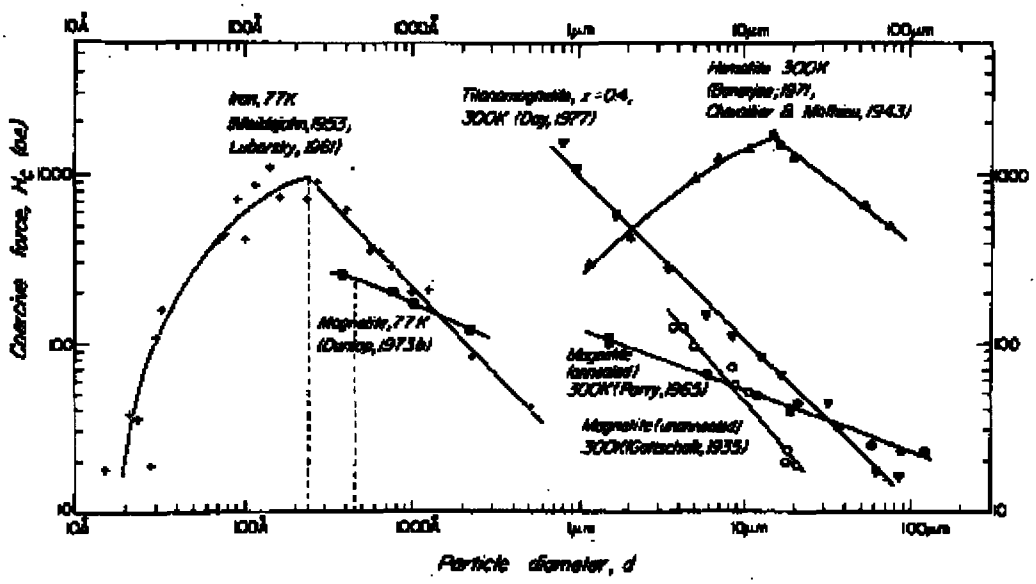

Figure 1.1 The variation of H_c with grain size.

The existence of domains is suggested by the observation that some magnetic properties, and in particular, coercivity and remanence, vary greatly with grain size. This is best illustrated in the Figure 1.1 below, which shows the variation of Hc with grain size.

As symbolic notation in literature, the magnetic behavior can be subdivided on the basis of grain size into four ranges

SPM: superparamagnetic

SD: single domain

PSD: pseudo-single domain

MD: multidomain

The maximum coercivity for a given material occurs within its SD range. For larger grain sizes, coercivity decreases as the grain subdivides into domains. For smaller grain sizes, coercivity again decreases, but this time due to the randomizing effects of thermal energy.

Domains constitute a fundamental concept in magnetism. A ferromagnetic or ferrimagnetic material may be generally defined as one that possesses a spontaneous magnetization, $\boldsymbol{M_s}$, dependent on temperature, but only slightly dependent on applied field. The theory of ferromagnetism, based on the consideration of electronic exchange forces, predicts the alignment of electron spin and can even determine the magnitude of $\boldsymbol{M_s}$, but says nothing about the direction of $\boldsymbol{M_s}$. Experimentally, it is observed that for a homogeneous specimen at constant temperature, the magnitude of $\boldsymbol{M_s}$ is uniform but the direction of $\boldsymbol{M_s}$ is in general not uniform from one region (i.e. a magnetic domain) to another (on a scale of microns to millimeters). Uniformity of direction is attained only by applying a large enough field to drive the domains out of the sample, or by reducing the particle's dimensions to small enough size to prevent domain formation.

Domains are formed for the following reason. Consider a large single crystal. Suppose it is uniformly magnetized, and hence a single domain. Surface charges will form on the ends due to the magnetization and are themselves a second source of a magnetic field (the demagnetizing field). The energy associated with the surface charge distribution is called the magnetostatic energy. It is just the volume integral of the field over all space.

The magnetostatic energy can be approximately halved if the magnetization splits into two domains magnetized in opposite directions. This subdivision into more and more domains can not continue indefinitely because the transition region between domains (called a domain wall) requires energy to be produced and maintained. Eventually an equilibrium number of domains will be reached for a given particle size.

Domain walls are interfaces between regions in which the magnetization has different directions. Within the wall, the magnetization must change direction from that in one domain to that in the other domain. Domain walls have a finite width that is determined principally by exchange and magnetocrystalline energy. Consider a domain wall in which the magnetization changes by 180°, Figure 1.2. The change in magnetization within the wall can be gradual as in (a) or abrupt as in (b).

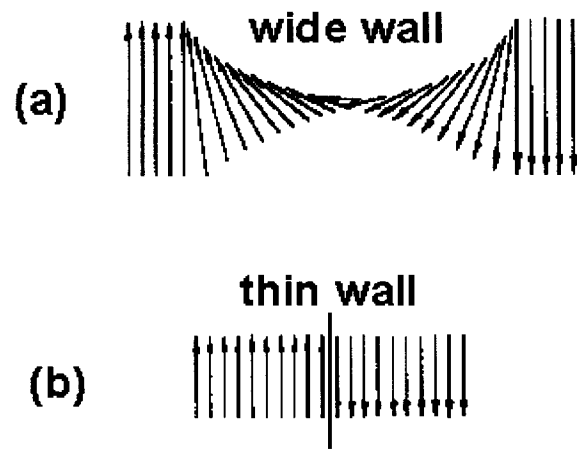

Figure 1.2 Structure of domain walls.

The exchange energy acts to keep spins parallel and can be kept small if the 180° rotation takes place gradually, over many atomic units. The exchange energy is small in the case of thick domain wall (e.g. (a)) but large for thin domain walls (e.g. (b)).

However, in (a), the spins within the wall are no longer aligned along an easy axis of magnetization. This produces an anisotropy energy, which is high in (a) but low in (b).

The exchange energy tends to make the wall as wide as possible whereas the anisotropy tends to make the wall as thin as possible. As a result of this competition between exchange and anisotropy energies, the domain wall has a finite width (on the order of 100 nm) and an associated surface energy.

The interplay between long range and short range effects results in the domain states being grain-size dependent. In addition, the number of domains for a given grain size depends on the magnitudes of the exchange, magnetocrystalline, and saturation magnetization. As mentioned before, these properties are dependent on temperature as

well as composition. Hence domain states in different magnetic minerals (magnetite and hematite) will have different grain size dependence. The domain states will also vary with temperature for a single grain size. However, as a guideline, the larger the grain size the more domains it contains.

As the grain size decreases, a critical size will be reached where the grain can no longer accommodate a wall because it becomes energetically unfavorable. Below this critical size, the grain contains a single domain (SD). An SD grain is uniformly magnetized to its saturation magnetization.

SD grains are very important. To change the magnetization of a MD grain, all you need to do is translate the domain wall, an energetically easy process, which can be accomplished in relatively low fields. Thus MD grains are magnetically soft with low values of coercivity and remanence.

However, the only way to change the magnetization of a SD grain is to rotate the entire magnetization of the grain, an energetically difficult process. Thus, SD grains are magnetically hard and have high coercivities and remanence. Here is an example of an SD and MD grain as characterized by hysteresis loops, Figure 1.3.

The critical size for SD behavior depends on several factors including, the saturation magnetization and the shape of the grain. Most estimates of the SD-MD transition size are based on simplified theoretical calculations. For magnetite, the best estimate for the transition size is about 80 nm. For hematite, the transition size from SD to MD is much larger (15 mm), primarily because the saturation magnetization is about 200 times lower than for magnetite.

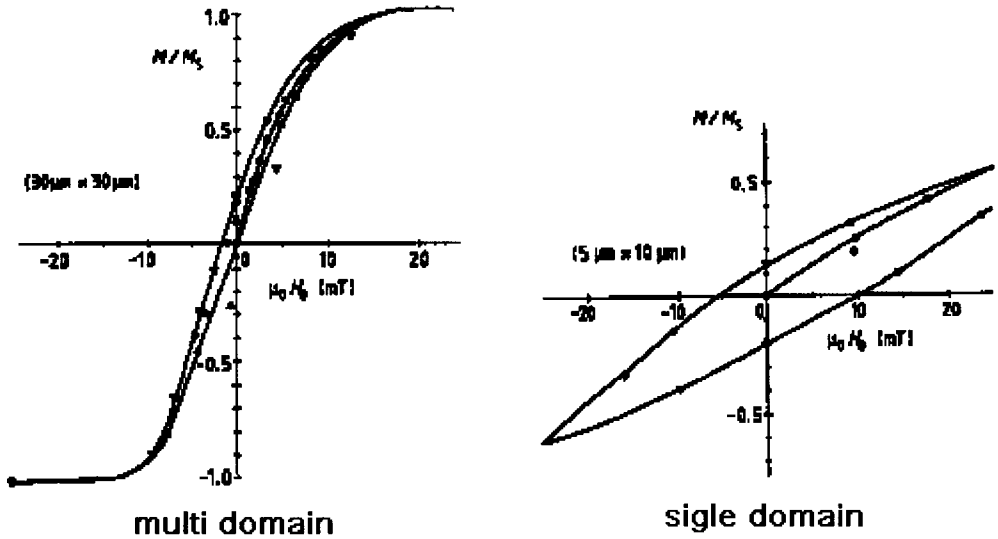

Figure 1.3 Single domain and multi domain hysteresis loops.

The distinction between SD and MD is straightforward. However, small MD grains exhibit a mixture of SD-like (high remanence) and MD-like (low coercivity) behavior. For magnetite, this behavior occurs in the size range between 0.1-20 mm.

There has been much theoretical and experimental work on PSD grains. Some current thinking is that small MD particles that contain just a few domains may actually have difficulty nucleating domains. In some cases MD grains exist in metastable SD states. The transformation of one domain state into another, such as addition or loss of domains, is called transdomain transformation.

The importance of PSD behavior in magnetite is that the grain size range for PSD behavior covers the range in sizes that most commonly occur in natural samples.

As particle size continues to decrease within the SD range, another critical threshold is reached, at which remanence and coercivity go to zero. When this happens, the grain becomes superparamagnetic. This is the superparamagetic limit.

An SD particle of volume v has a uniform magnetization directed along the easy axis of magnetization. If v is small enough, or the temperature is high enough, thermal energy (kT) will be sufficient to overcome the anisotropy energy separating the spin up and spin down magnetization states and causing a spontaneous reversal of magnetization.

Initial susceptibility is measured in a low AC or DC field (<1mT) and is defined as the ratio of *M/H*. Initial susceptibility is due to reversible displacements of mobile domain walls in MD particles or moment rotation in SD particles. In the latter case, low fields are not very effective in rotating SD moments. Therefore, susceptibilities in SD and PSD grains are usually lower than that of MD grains.

However, what is actually measured in the laboratory is the apparent susceptibility, χ_o, not the intrinsic susceptibility, χ_i. The difference is due to the effects of self-demagnetization.

Remember, inside a grain, the applied field, $\boldsymbol{H}$, is modified by the demagnetizing field resulting from surface charges. The magnitude of the demagnetizing field is $N\boldsymbol{M}$. N is called demagnetizing factor. N is weakly related to grain shape and domain state. It is usually assumed to be a constant, independent of grain size. If this is so, low-field susceptibility can be used as a reliable measure of magnetite content.

A small fraction of SPM particles can contribute significantly to the room temperature susceptibility of SD or MD grains. Calculations show SPM susceptibility can be 10-100 times that of an equivalent amount of SD grains.

The shape of a hysteresis loop is determined partly by the domain state. Loops for SD materials are typically wider than loops for MD materials. This is just a reflection

of the higher coercivity and remanence in SD material. The hysteresis loop parameters, M_r/M_s and $H_r/H_c>$, have proven very useful in distinguishing domain state. In fact, M_r/M_s is a definitive test for differentiating between SD and non-SD particles.

1.3 Magnetostriction

The changes of magnetization of a ferromagnetic material are strongly related to the changes in dimensions of the material. The dimension of a ferromagnetic material may change under some circumstances and the resulting strain is called magnetostriction. There are two main types of magnetostriction: spontaneous magnetostriction arising from the ordering of magnetic moments into domains at the Curie temperature, and field-induced magnetostriction. In both cases, the magnetostriction λ is simply defined as the fractional change in length.

$$\lambda = \frac{\Delta l}{l} \tag{1.1}$$

Spontaneous magnetostriction within domains arises from the creation of domains as the temperature of the ferromagnet passes through the Curie (or ordering) temperature. Field-induced magnetostriction arises when domains that have spontaneous magnetostriction are reoriented under the action of a magnetic field. Magnetostriction can be measured by using resistive strain gauges, as described in chapter 3.

When a ferromagnetic material's temperature is higher than its Curie point, the disordered magnetic moments have completely random alignment. But when it is cooled through its Curie point, the magnetic moments become ordered over volumes containing

large numbers of atoms. These volumes in which all moments lie parallel are called domains, as described in chapter 1. The direction of spontaneous magnetization M_s varies from domain to domain through the material to ensure that the bulk magnetization is zero. These domains with ordered magnet moments change the dimension of the material and this change is the reason for spontaneous magnetostriction.

As for the field-induced magnetostriction, the most important thing is the saturation magnetostriction, which is the fractional change in length between a demagnetized ferromagnetic specimen and the same specimen in a magnetic field sufficiently strong to saturate the magnetization along the field direction. So the value of λ measured at magnetic saturation is called the saturation magnetostriction.

Table 1.1 Magnetostriction coefficients of iron and nickel.

Material	λ_{100} (10^{-6})	λ_{111} (10^{-6})
Iron	21	-21
Nickel	-46	-24

The magnetostrictions or spontaneous strains are defined along each of the principal axes of the crystal. For cubic materials there are two independent magnetostriction constants λ_{100} and λ_{111}. λ_{100} is the saturation magnetostriction measured along the <100> direction and λ_{111} is the saturation magnetostriction along the <111> direction. They can be determined by saturating the magnetostriction along the axis of interest and then at right angles. The magnetostriction constants λ_{100} and λ_{111} of iron and nickel are listed in Table 1.1. The saturation magnetostriction λ_s undergone by a single

domain, single cubic crystal in a direction defined by $\beta_1, \beta_2, \beta_3$ relative to the field directions in which the saturation magnetostriction is measured, when it changes from the demagnetized state to saturation in a direction defined by the cosines $\alpha_1, \alpha_2, \alpha_3$ relative to the field directions of the axis along which the magnetic moments are saturated, is given by

$$\begin{aligned}\lambda_s = &\frac{3}{2}\lambda_{100}(\alpha_1^2\beta_1^2 + \alpha_2^2\beta_2^2 + \alpha_3^2\beta_3^2 - \frac{1}{3}) \\ &+ 3\lambda_{111}(\alpha_1\alpha_2\beta_1\beta_2 + \alpha_2\alpha_3\beta_2\beta_3 + \alpha_3\alpha_1\beta_3\beta_1),\end{aligned} \tag{1.2}$$

Usually we will wish to know the saturation magnetostriction in the same direction as the field in which case the above expression reduces to

$$\lambda_s = \lambda_{100} + 3(\lambda_{111} - \lambda_{100})(\alpha_1^2\alpha_2^2 + \alpha_2^2\alpha_3^2 + \alpha_3^2\alpha_1^2). \tag{1.3}$$

The saturation magnetostriction of a hexagonal crystal is given by the following equation:

$$\begin{aligned}\lambda_s = &\lambda_A[(\alpha_1\beta_1 + \alpha_2\beta_2)^2 - (\alpha_1\beta_1 + \alpha_2\beta_2)\alpha_3\beta_3] \\ &+ \lambda_B[(1-\alpha_3^2)(1-\beta_3^2) - (\alpha_1\beta_1 + \alpha_2\beta_2)^2] \\ &+ \lambda_C[(1-\alpha_3^2)\beta_3^2 - (\alpha_1\beta_1 + \alpha_2\beta_2)\alpha_3\beta_3] \\ &+ 4\lambda_D(\alpha_1\beta_1 + \alpha_2\beta_2)\alpha_3\beta_3\end{aligned}, \tag{1.4}$$

where the direction cosines in the above equation are not relative to the hexagonal axes, but to orthogonal axes *x*, *y*, *z*. The magnetostriction constants of cobalt are:

$$\lambda_A = -45\times10^{-6} \qquad \lambda_B = -95\times10^{-6}$$
$$\lambda_C = 110\times10^{-6} \qquad \lambda_D = -100\times10^{-6}$$

The behavior of the magnetostriction of an assembly of domains, a polycrystal for example, can only be calculated by averaging the effects. This is not possible in general

and therefore it is assumed that the material consists of a large number of domains and hence that the strain is uniform in all directions.

The magnetostriction constants are usually very small: λ_s is typically of the order of 10^{-5}, and they usually decrease in absolute magnitude as the temperature increases and reaches zero at the Curie point. Although the direct magnetostrictive effect is small, there exists an inverse effect which causes such properties as permeability and the size of the hysteresis loop to be dependent on stress in many materials. Magnetostriction therefore has many practical consequences. Highly magnetostrictive materials, that is materials with saturation magnetostrictions of beyond a few hundred parts per million, are invariably rather exotic alloys of rare earth metals alloyed often with transition metals such as iron, cobalt or nickel. The rare earths provide the high magnetostriction and the transition metals the high Curie temperatures. These materials find practical applications today mostly in actuators and in magnetic sensors.

1.4 Magnetization processes

A ferromagnetic material that is not subjected to a large applied stress contains many domains because the existence of a single domain is normally energetically unfavorable due to the high magnetostatic energy associated with a single domain sample. When the magnetostatic energy exceeds the energy required for domain wall formation, multiple domains will form in the material thereby reducing the magnetostatic energy.

Under the action of an applied magnetic field, the orientations and sizes of these magnetic domains will change. These changes in magnetization under an applied magnetic field can be either reversible or irreversible, depending on the domain processes involved. A reversible change in magnetization is the one in which after application and removal of a magnetic field, the magnetization returns to its original value. More often both reversible and irreversible changes occur together, so that on removal of the field the magnetization does not return to its initial value.

It is often suggested in an oversimplified way that the magnetic hysteresis curve of a ferromagnetic material can be interpreted in terms of four distinct (sometimes these regions are not so distinctive) regions, as illustrated in Figure 1.4.

(i) Starting from zero field, a narrow field region "1" where domain walls move reversibly and will return to their original position if the field is removed.

(ii) A low-field region "2", where domain walls move irreversibly as they overcome barriers presented by pinning sites in the microstructure.

(iii) An intermediate-field region "3", where domain nucleation and annihilation occurs.

(iv) A high-field region "4", where further increase in magnetization is predominantly due to rotation of the magnetization vectors within individual domains and little domain wall motion occurs.

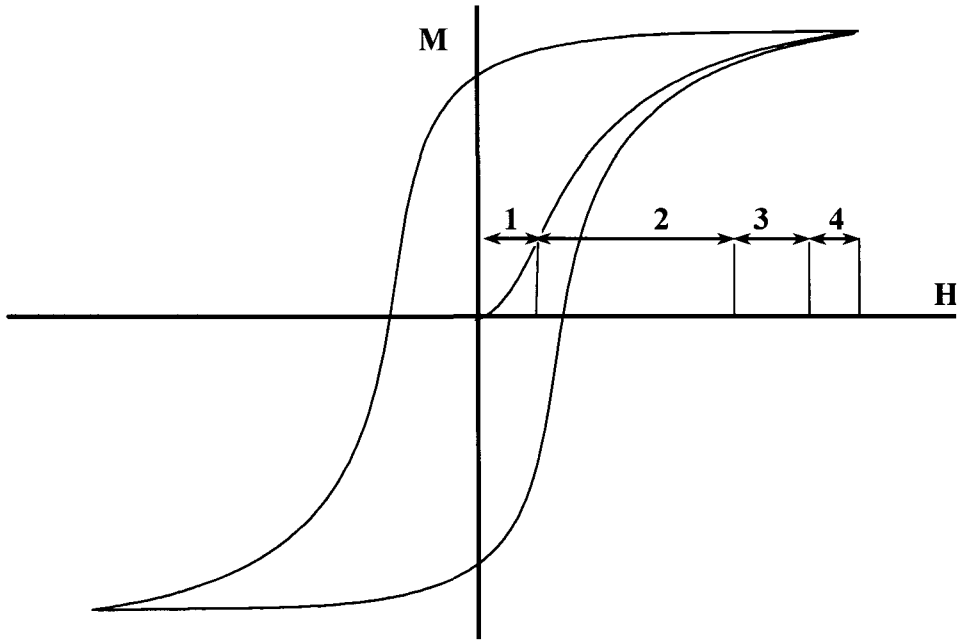

Figure 1.4 Magnetization curve and the classification of the magnetization mechanisms.

The properties of the material's magnetization have lots of applications. The hysteresis of magnetization versus magnetic field in ferromagnets is used in magnetic recording. Without hysteresis the magnetic state of the material in zero field would be independent of the field that it had last experienced. However in hysteretic systems the remanent magnetization acts as a memory of the last field, both in magnitude and direction, experienced by the magnetic material. Therefore data, either in digital form for computers and related devices, or analog signals as in sound recording, can be stored in the form of magnetic imprints on magnetic media. The magnetic recording media must have high saturation magnetization to give as large a signal as possible during the reading process. The coercivity must be sufficient to prevent erasure, but small enough to allow the material to be reused for recording.

CHAPTER 2. STRESS DEPENDENCE OF HYSTERESIS AND ANHYSTERETIC MAGNETIZATION

It is known to be a complex task to describe the behavior of magnetic materials under the influence of an applied field and its field exposure history by hysteresis modeling. The complexity arises because of the multiplicity of magnetization processes that can occur simultaneously within a magnetic material. These processes can be both reversible and irreversible, and can arise from domain magnetization rotation or domain boundary motion or both, so that at least four types of magnetization process are usually taking place at any given time. An even more exact analysis would also include the increase in spontaneous magnetization within the domains as field is increased (although the effect is relatively smaller), and the counteracting effects of temperature which as it is increased has the effect of reducing spontaneous magnetization.

Reliable magnetic modeling of the behavior of ferromagnetic materials has great impact on the field of magnetism [1, 2, 3, 4]. In most cases the models that are proposed concentrate on a limited subset of the processes. For example the widely used Preisach model focuses only on irreversible switching processes of an assembly of single domain switching elements called hysterons. The Stoner-Wohlfarth model focuses only on the rotational magnetization processes (both reversible and irreversible) in non-interacting single domain particles. The models developed by Neel and others concentrate on domain wall dynamics and its relationship with microstructure such as the density of defects that act as pinning sites for domain walls. The stochastic process models of Bertotti are

similarly directed towards the discontinuous motion of domain walls. The micromagnetic models based on the Landau-Lifshitz-Gilbert equation consider the reorientation of a small number of spins, much less than the numbers of spins which comprise a typical single domain in a magnetic material.

The reliable description of the magnetization processes in materials, founded on a secure physical basis, is therefore of great scientific interest. Such description must take advantage of the average collective behavior of the electron spins, however; since any attempt to simply scale up a calculation of all active magnetic moments (e.g. through a scaling up of the Landau-Lifschitz-Gilbert model to a full samples of perhaps $10^{23} \sim 10^{26}$ spins) is beyond the computational capabilities at present.

This chapter gives detailed mathematical description of hysteresis and the anhysteretic magnetization in section 2.2 after introducing the phenomenon of hysteresis of magnetic materials in section 2.1. The previous models of hysteresis are also discussed in section 2.3. It ends with the dissertation of stress effects on the magnetic materials in section 2.4.

2.1 Introduction to hysteresis and the anhysteretic

Generally speaking, the hysteresis is caused by energy barriers and imperfections in the material. The imperfections, whether in the form of dislocations or impurity elements in the metal, cause an increase in the energy lost during the magnetization process, in the form of a kind of internal friction, which give rise to hysteresis. Another

mechanism which gives rise to hysteresis is caused by magnetocrystalline anisotropy. Ferromagnetic materials with higher anisotropy have greater hysteresis. In an anisotropic solid, certain crystallographic axes are favored by the magnetic moments which will lie along these directions as this leads to a lower energy. The magnetic moments can be dislodged from the direction they are occupying by application of a magnetic field but when this occurs they jump to crystallographically equivalent axes which are closer to the field direction, and hence of lower energy. This results in discontinuous and irreversible rotation of the magnetic moments which leads to a kind of switching action.

It is conventional to discuss the properties of ferromagnetic materials in terms of various parameters associated with the hysteresis loop and anhysteretic curve of the material. Figure 2.1 shows such a typical sigmoid-shaped hysteresis loop, together with the definition of customary parameters. B_s is the saturation magnetic induction corresponding to saturation magnetization M_s. The remanence B_r is defined as the flux density remaining in the material when the applied field in the material is brought from its maximum value back to zero. The coercivity H_c is the amount of field in the opposite direction that has to be applied before the remaining flux density in the material is finally brought back to zero.

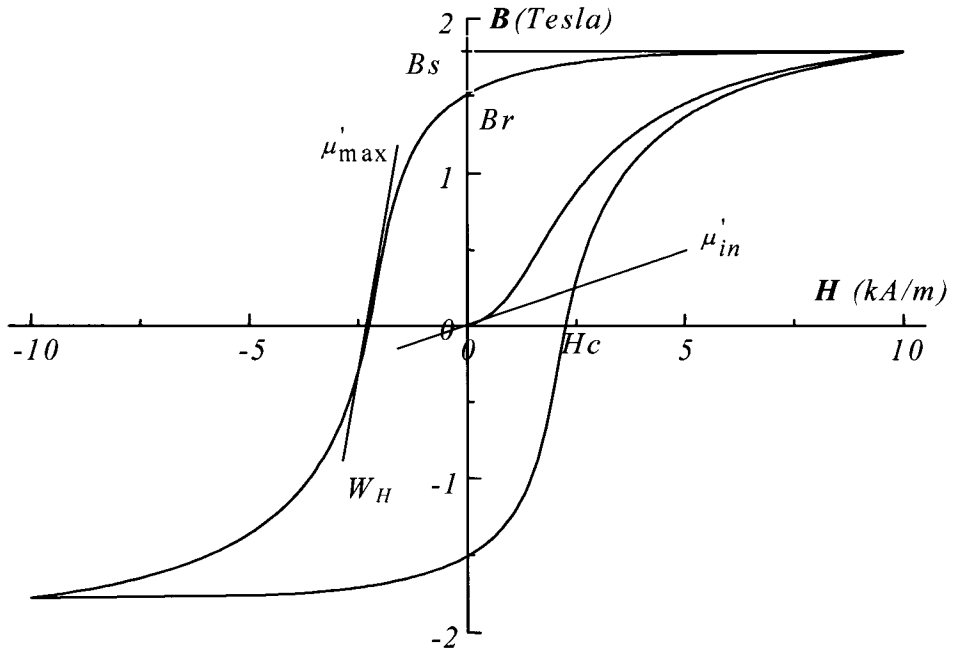

Figure 2.1 A typical hysteresis loop of a ferromagnetic material.

The slope of the magnetic induction versus magnetic field curve (*B-H* curve), known as the differential permeability μ', is typically a maximum at the coercive field H_c, and so the maximum differential permeability $\mu'_{\max}$ is another characteristic of the hysteresis loop. The path taken on the *B-H* plot when a demagnetized specimen is subjected to a maximum field is known as the initial magnetization curve, and the slope of the initial magnetization curve as the field begins to increase from $H = 0$, $B = 0$ is known as the initial permeability μ'_{in}.

The area enclosed by the hysteresis loop is the hysteresis loss W_H. The loop area is the magnetic energy that is dissipated per unit volume if the material is completely cycled around one loop. The energy loss is associated with irreversible motion of magnetic domain walls or irreversible rotation of domain magnetization inside the

material and appears in the material as heat. The hysteresis is thus due to irreversible thermodynamic changes that develop as a result of magnetization. The changes of magnetization are caused by domain wall motion and rotation. Both of these processes can be manifested as either reversible or irreversible mechanisms, and the transition from reversible to irreversible is dependent on the amplitude of the magnetic field.

Hence the five parameters, coercivity, remanence, hysteresis loss, initial permeability, maximum permeability and saturation magnetization, can be used to characterize the bulk magnetic properties of a material.

Table 2.1 shows magnetic properties of various high-permeability ferromagnetic materials.

Table 2.1 Typical value of high-permeability ferromagnetic materials (after D. C. Jiles "Introduction to Magnetism and Magnetic Materials" second edition 1998).

Material	μ_{max}	B_s ***(T)***	W_H ***(J/m^3)***	H_c ***(A/m)***
Purified iron	180000	2.15	30	4
Iron	5000	2.15	500	80
Cold rolled steel	180	2.1	-	144
45 Permalloy	2500	1.6	120	24
78 Permalloy	8000	1.07	20	4
Mumetal	20000	0.65	-	4
Ferroxcube	1000	2.5	-	8

One effect that has to be addressed is the problem of demagnetizing effects due to finite geometries and magnetic pole formation at both ends of the specimen. This effect

leads to a reduction in effective local field in the material by $N_d \boldsymbol{M}$, where N_d is known as the demagnetizing factor and is dependent on the shape of the sample.

One important bulk property of interest which is not contained in the hysteresis plot is the magnetostriction. This is the change in length of a material either as a result of magnetic order (spontaneous magnetostriction) or the action of a magnetic field (field-induced magnetostriction). The magnetostriction is introduced in Chapter 1.

Figure 2.2 shows a typical anhysteretic curve, together with the definition of customary parameters.

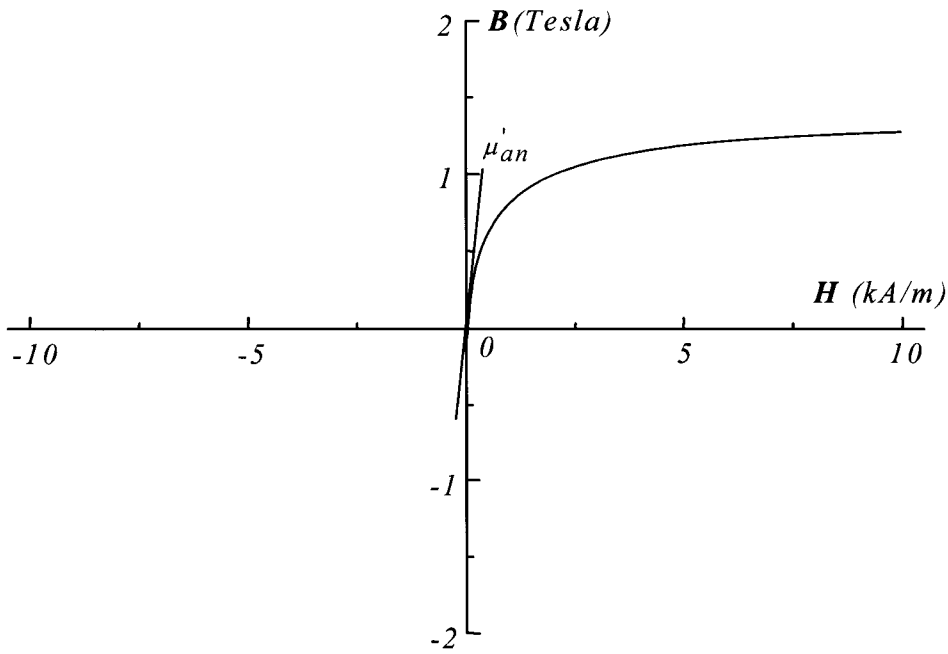

Figure 2.2 A typical anhysteretic curve of a ferromagnetic material.

The slope of the anhysteretic magnetic induction versus magnetic field curve at $H = 0$, $B = 0$ is typically a maximum, and so the maximum differential permeability μ'_{an} is an important characteristic of the anhysteretic curve.

Ferromagnetic hysteresis is related to the irreversible stochastic motion of magnetic domain walls during the magnetization process. The intrinsically random nature of domain wall motion is a consequence of the pinning process caused by lattice defects, inclusions, or interactions between different domain walls. Magnetic and thermal treatments, applied stresses, and many other factors may affect the properties of the pinning sites. Because of this, a detailed description of the various microscopic magnetization processes, and of the related hysteretic behavior, remains a very difficult task. But a good understanding of these will help to predict the material's magnetic properties.

2.2 Mathematical description of hysteresis

The initial magnetization curve, as shown in Figure 2.1, is the variation of magnetization with field obtained when a d.c. field is first applied to a demagnetized ferromagnet. It was noticed by Rayleigh [5] that in the low-field region of the initial magnetization curve the permeability could be represented by an equation of the form

$$\mu(H) = \mu(0) + vH, \tag{2.1}$$

which leads to the following parabolic dependence of $\boldsymbol{B}$ on $\boldsymbol{H}$ along the initial magnetization curve

$$B(H) = \mu(0)H + vH^2. \tag{2.2}$$

According to Rayleigh the term $\mu(0)H$ represented the reversible change in magnetic induction while the term vH^2 represented the irreversible change in magnetic

induction. Furthermore, Rayleigh indicated that low-amplitude hysteresis loops could be represented by parabolic curves which have a reversible differential permeability at the loop tips which is equal to μ(0) as show in Figure 2.3. It follows from this assumption and the Rayleigh law that in the low-field region the small-amplitude hysteresis loops can be described by an equation of the form

$$B = [\mu(0) + \nu H_m]H \pm \left(\frac{\nu}{2}\right)\left(H_m^2 - H^2\right), \tag{2.3}$$

where H_m is the maximum field at the lop tip. Low-amplitude hysteresis loops for which this parabolic relation applies are known as Rayleigh loops. It must be remembered of course that these relations only hold true in the low-field region. As $\boldsymbol{H_m}$ is increased the parabolic relation breaks down. In order to model the hysteresis behavior over a wider range of $\boldsymbol{H}$ it is necessary to gain further insight into the microscopic mechanisms occurring within the material.

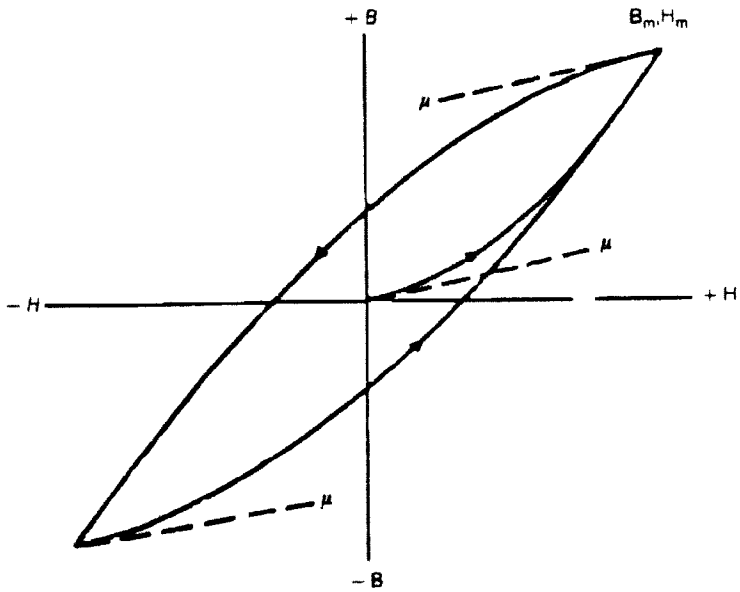

Figure 2.3 Hysteresis loops of low-field amplitude in the Rayleigh region.

In the high-field region the magnetization approaches saturation. The high-field behavior can be modeled by the law of approach to saturation as given by Becker and Doring [6] and Bozorth [7]. This is expressed in the form of a series,

$$M = M_s\left(1 - \frac{a}{H} - \frac{b}{H^2} - \ldots\right). \tag{2.4}$$

A quantitative relationship between magnetization $\boldsymbol{M}$ and magnetic field $\boldsymbol{H}$ is clearly highly desirable since any such equation provides a means of telling how the magnetization or magnetic induction of a material will change with field. An empirical relationship between $\boldsymbol{M}$ and $\boldsymbol{H}$ along the anhysteretic magnetization curve was suggested by Fröhlich [8] and Kennelly[9]. This equation can be written in the form of a series

$$M = M_s\left[1 - \frac{cM_s}{H} + \left(\frac{cM_s}{H}\right)^2 \ldots\right]. \tag{2.5}$$

This is the form of equation used by Weiss [10] for finding M_s from magnetization curves by extrapolation, using only the terms up to $1/H$.

It is interesting to note that this law which was only derived at high magnetizations is also very similar to the series form of the law of approach to saturation relation. The reason for this is that at high fields the initial magnetization curve, the upper and lower branches of the hysteresis loop and the anhysteretic magnetization approach each other asymptotically.

2.3 Previous models of hysteresis

Early investigators in the field of magnetism considered several possible explanations for the phenomenon of ferromagnetic hysteresis. These hypotheses fell broadly into two categories [11], one of which suggested that a frictional type force was responsible and the other which considered hysteresis as due entirely to the strong mutual interactions between the individual magnetic moments.

In the past there have been many model equations to simulate the magnetization data. According to the review by Cullity [12], the algebraic model expressions fall into three categories: high field magnetization curves of single crystals, as in the work of Williams [13]; high field magnetization curves of polycrystals which are governed by the law of approach to saturation as indicated by Chikazumi [14]; low field magnetization curves and hysteresis loops of polycrystalline specimens which exhibit Rayleigh loops [5].

The previous model equations either use an extremely complicated mathematical function to describe the behavior to any arbitrary level of accuracy but with little or no theoretical basis, or alternatively use a simple function obtained from first principles to simulate the behavior with a good theoretical foundation but without sufficient accuracy.

According to Jiles and Atherton [11], there are two methods to approach theoretically the problem of describing and modeling hysteresis. One is the calculations based on the Preisach- Nëel model [15, 16, 17], the other is based on the micromagnetics theory of Brown [18] and Aharoni [19]. However a serious drawback of the Preisach model is its arbitrary nature. The micromagnetic model does not yield a simple equation

of state for a ferromagnet which is the objective of the present work and consequently this method will not be considered further here.

The changes in magnetization arising from the application of a magnetic field to a ferromagnet can be either reversible or irreversible depending on the domain processes involved. A reversible change in magnetization is one in which after application and removal of a magnetic field, the magnetization returns to its original value. In ferromagnetic materials this only occurs for small field increments. An irreversible change in magnetization is one in which after application and removal of a magnetic field, the magnetization does not return to its initial value.

Jiles-Atherton model is the basis of this research work. So let's introduce this model first. Since the anhysteretic magnetization model equation has fewer model parameters, we will introduce the anhysteretic function first.

Inside a ferromagnetic material, there is coupling between the domains. According to the model this coupling can be represented as a coupling to the bulk magnetization $\boldsymbol{M}$ and this is called the effective field. This effective field is analogous to the Weiss mean field experienced by the individual magnetic moments within a domain.

The response of the magnetization to this effective field in the absence of hysteresis can be expressed as

$$M_{an}(H_e) = M_s f(H_e), \tag{2.6}$$

where f is an single-valued function of H_e which takes the value zero when H_e is zero and takes the value unity as H_e tends to infinity. M_s is the saturation magnetization. The form of this function varies depending on such factors as anisotropy, structure of the

material. Although Equation (2.6) is an implicit function since $H_e=H+\alpha M_{an}$, it represents a single-valued relation between magnetic field H and magnetization M_{an}. An example is shown in Figure 2.4. As for the anhysteretic function, the model uses the modified Langevin expression $L(H_e)$ [20] as the arbitrary function $M_s f(H_e)$. This therefore leads to an expression for the anhysteretic magnetization in the from of

$$M_{an}(H_e) = M_s\left[\coth\left(\frac{H_e}{a}\right) - \frac{a}{H_e}\right], \tag{2.7}$$

where a is a parameter with dimensions of magnetic field which characterizes the general shape of the anhysteretic magnetization curve.

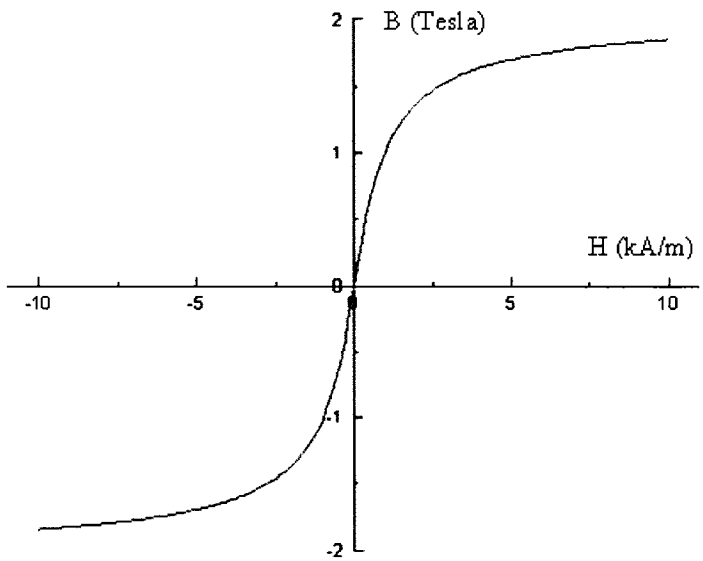

Figure 2.4 Anhysteretic magnetization curve for isotropic material.

It is stated that the magnetization $\boldsymbol{M}$ can be calculated as the sum of two components, an irreversible component $\boldsymbol{M_{irr}}$ and a reversible component $\boldsymbol{M_{rev}}$. Based on the anhysteretic function, the model equations for the hysteresis loop can be expressed as

$$\frac{dM_{irr}}{dH} = \frac{1}{\delta k/\mu_0 - \alpha(M_{an} - M)}(M_{an} - M), \tag{2.8}$$

$$\frac{dM_{rev}}{dH} = c\left(\frac{dM_{an}}{dH} - \frac{dM}{dH}\right), \tag{2.9}$$

$$\frac{dM}{dH} = \frac{1}{(1+c)}\frac{1}{\delta k/\mu_0 - \alpha(M_{an} - M)}(M_{an} - M) + \left(\frac{c}{1+c}\right)\frac{dM_{an}}{dH}, \tag{2.10}$$

where δ takes the value +1 when H increase in the positive direction, $dH/dt>0$, and -1 when H increases in the negative direction, $dH/dt<0$, ensuring that the pinning opposes changes in magnetization. The coefficient k is not constrained to be constant and may vary as a function of M and H. Nevertheless, the form of the solution remains the same whether k is constant or not, only the shape is modified by variable k. α is a mean field parameter representing inter-domain coupling, which has to be determined experimentally. The value of the coefficient c is determined experimentally by the ratio of the initial differential susceptibilities of the normal and anhysteretic magnetization curves.

After solving the first order differential equation numerically, a sigmoid-shaped hysteresis loop can be obtained. Through changing the parameters and the form of anisotropy, this model is able to model the magnetization of soft magnetic materials, hard magnetic materials and anhysteretic magnetization. Figure 2.5 shows three typical modeled hysteresis curves.

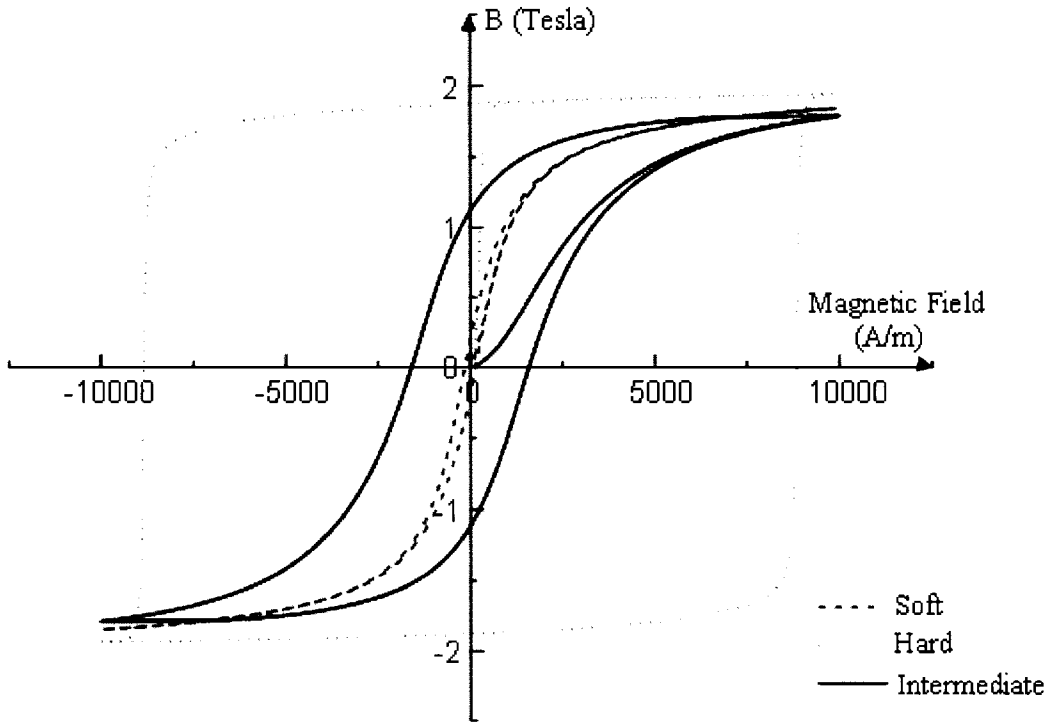

Figure 2.5 Hysteresis curves of soft, hard, and intermediate magnetic materials.

2.4 Stress effects on hysteresis

The effect of stress on magnetization is normally referred to as the magneto-mechanical effect. It has been shown experimentally that there is a close relationship between the magnetostriction λ of a material and its magnetic behavior under stress.

Stress can create an easy axis of magnetization. Therefore, when stress (residual or applied) is present, stress induced anisotropy must be considered along with any other anisotropies that may exist, such as magnetocrystalline anisotropy. Stress causes a uniaxial anisotropy, and the corresponding magnetoelastic energy E_{me} is defined as

$$E_{me} = -\frac{3}{2}\lambda_{100}\sigma(\alpha_1^2\gamma_1^2 + \alpha_2^2\gamma_2^2 + \alpha_3^2\gamma_3^2)$$

$$-3\lambda_{111}\sigma(\alpha_1\alpha_2\gamma_1\gamma_2+\alpha_2\alpha_3\gamma_2\gamma_3+\alpha_3\alpha_1\gamma_3\gamma_1), \qquad (2.11)$$

where σ is the stress, α_1, α_2, α_3 are the direction cosines of M, and γ_1, γ_2, γ_3 are the direction cosines of σ with respect to the crystal axes.

More than that, the effect of changing stress on the magnetization of a magnetic material leads to behavior in which the magnetization has been observed to increase or decrease under exposure to the same stress under the same external applied field. This indicates that the phenomenon is dependent on more than simply the external influences of stress σ and magnetic field H. In fact, the behavior also depends on the magnetization history of the specimen, which for major hysteresis loops can be expressed in terms of the displacement from the anhysteretic ($M_{an} - M$). This, together with the field H and stress σ, specifies the state of the material on a major hysteresis loop.

It is convenient to discuss the stress dependent magnetostriction first.

2.4.1 Stress dependent magnetostriction

The magnetostriction of bulk material depends on the domain configuration throughout the material. Since the magnetostriction must be symmetric about $M = 0$, a simple series expansion gives [21]

$$\lambda = \sum_{i=0}^{\infty} \gamma_i M^{2i} \qquad (2.12)$$

If we use a simplified approximation to the magnetostriction by including the terms up to $i = 2$ and ignoring the constant term ($i = 0$), which is simply the elastic strain and does not play an active role in the magnetomechanical effect, this gives

$$\lambda = \gamma_1 M^2 + \gamma_2 M^4 . \qquad (2.13)$$

The stress-dependence of magnetostriction curve λ (M, σ) can be described in terms of the stress dependence of γ_1 and γ_2 using a Taylor series expansion,

$$\gamma_i(\sigma) = \gamma_i(0) + \sum_{n=1}^{\infty} \frac{\sigma^n}{n!} \gamma_i^n(0), \tag{2.14}$$

where $\gamma_i^n(0)$ is the nth derivative of γ_i with respect to stress at σ = 0. Using only the terms up to n = 1, and applying the above Equation (2.13) and (2.14) to the magnetostriction, the magnetostriction is then given by

$$\lambda = \sum_{i=0}^{\infty} \gamma_i(\sigma) M^{2i} \approx [\gamma_{11} + \gamma_{12}(\sigma)]M^2 + [\gamma_{21} + \gamma_{22}(\sigma)]M^4. \tag{2.15}$$

Thus by truncating the series, the magnetostriction can be decomposed by two parts, quadratic and quartic part. And each part has its stress dependent and stress-independent components. Experimental data shows that this assumption can be used for mild steel, nickel and other magnetic samples.

2.4.2 Stress dependent anhysteretic magnetization

As described in previous work [22], an applied uniaxial stress σ acts in some respects like an applied magnetic field operating through the magnetostriction λ. This additional field H_σ can be thought as an effective field introduced by stress. The effective magnetic field causes a change in magnetization. This means that a correction needs to be made to the anhysteretic magnetization discussed previously, as a result of the application of stress.

Consequently H_σ, the component of the effective field due to stress, is

$$H_\sigma = \frac{3}{2}\frac{\sigma}{\mu_o}\left(\frac{d\lambda}{dM}\right)_\sigma = \frac{3}{2}\frac{\sigma_o}{\mu_o}\left(\frac{d\lambda}{dM}\right)_\sigma \left(\cos^2\theta - \upsilon\sin^2\theta\right), \tag{2.16}$$

where θ is the angle between the axis of the applied stress σ_o and the axis of the magnetic field H and υ is Poisson's ratio. According to the effective field theory, the effects of stress have been incorporated into the equivalent effective field. It is therefore implicit in this description of the theory that the anhysteretic magnetization under a field H and stress σ, is identical to the anhysteretic magnetization under an equivalent effective magnetic field

$$H_{eff} = H + \alpha M + \frac{3}{2}\frac{\sigma}{\mu_o}\left(\frac{d\lambda}{dM}\right)_\sigma . \tag{2.17}$$

In other words, the change in energy of the magnetization in a particular direction can be described either in terms of the stress or, equivalently, in terms of the effective magnetic field that causes the same change in energy. This is the basic idea of the Jiles-Atherton hysteresis model which considers the stress effects.

Hence, in the isotropic limit, the stress-dependence of the anhysteretic magnetization curve can be determined from the equation

$$M_{an} = M_S\left[\coth\left(\frac{H + \alpha M + \frac{3}{2}\frac{\sigma}{\mu_o}\left(\frac{d\lambda}{dM}\right)_\sigma}{\mathrm{a}}\right) - \frac{\mathrm{a}}{H + \alpha M + \frac{3}{2}\frac{\sigma}{\mu_o}\left(\frac{d\lambda}{dM}\right)_\sigma}\right], \tag{2.18}$$

where $a=k_BT/\mu_0 m$ in which k_B is Boltzmann's constant, T is the temperature, and m is the magnetic moment of a typical domain. Obviously this is a modification of Equation (2.7) due to the effect of stress.

In the uniaxial magnetic case, the stress-dependence of the anhysteretic magnetization curve can be determined as the hyperbolic function

$$M_{an} = M_S \tanh\left(\frac{H + \alpha M + \frac{3}{2}\frac{\sigma}{\mu_o}\left(\frac{d\lambda}{dM}\right)_\sigma}{a}\right), \tag{2.19}$$

In the planar case, the stress-dependence of the anhysteretic magnetization curve can be described by the expressions of the Langevin function given by Jiles *et al* for the one-, two and three-dimensional cases [23].

2.4.3 Stress dependent hysteresis

It has been shown in previous studies [24, 25] that the effect of an applied stress σ on magnetization M of ferromagnetic materials can to some extent be treated as an effective field given by

$$H_\sigma = \frac{3}{2}\frac{\sigma}{\mu_\circ}\left(\frac{d\lambda}{dM}\right), \tag{2.20}$$

where λ is the magnetostriction and μ_o is the permeability of free space. If the magnetostriction can be described by an equation of the form $\lambda = \gamma M^2$, where γ is a coefficient dependent on σ, the total magnetic field sensed by a domain can then be written in the form,

$$H_{eff} = H + \alpha M + \frac{3\gamma\sigma}{\mu_\circ} M = H + \alpha_{eff} M, \tag{2.21}$$

where $\alpha_{eff} = \alpha + 3\gamma\sigma/\mu_0$, and α is a mean field parameter representing inter-domain coupling [26] and H is the true applied field. So the stress effects are coupled into the effective field and can be calculated by Equation (2.8), (2.9) and (2.10).

CHAPTER 3. MEASUREMENT AND MODELING OF HYSTERESIS AND ANHYSTERETIC MAGNETIZATION

Modeling of magnetization processes has a wide impact because of its practical utility in engineering applications of magnetic materials where their performance characteristic of magnetic materials can be described and, if the theoretical model is physically sound, properties and performance outside of a known range of conditions can also be successfully predicted. It would also be very useful to be able to predict the changes of the magnetic properties due to other physical quantities like applied and residual stresses, fatigue, temperature, or irradiation, for example. Moreover, engineering applications require the integration of the model into system design software and therefore need fast computation and efficient parameter identification strategies.

In this work mathematical comparison was demonstrated between the hysteresis models, originally published by Jiles and Atherton (JAM) and model law of approach to saturation. The objective was to examine the mathematical structure of the model and identify the correspondences.

This chapter begins with the measurements of hysteresis and anhysteretic magnetization. Then the stress dependent model parameters are discussed in detail and a set of mathematical expression of the model parameters are given. Finally simulations based on these model equations and stress dependent parameters are shown for different materials, such as nickel and stainless steel.

3.1 Measurement of hysteresis and anhysteretic magnetization

In order to get better understanding of properties of ferromagnetic material and verify the generality of the model, measurement on different samples is essential. A series of experiments were conducted on stainless steel 410 and nickel samples (both cold-worked and annealed) which have different magnetostrictive properties.

The anhysteretic can be measured by cycling the magnetization by applying an alternating field of gradually decreasing amplitude superimposed on the d.c. field of interest. As the a.c. field was cycled the hysteresis was gradually removed and the magnetization converged on the anhysteretic value for the prevailing d.c. field strength. The major hysteresis loops are obtained by cycling the *H* field (d.c. field) at progressively increasing amplitudes starting from the demagnetized state.

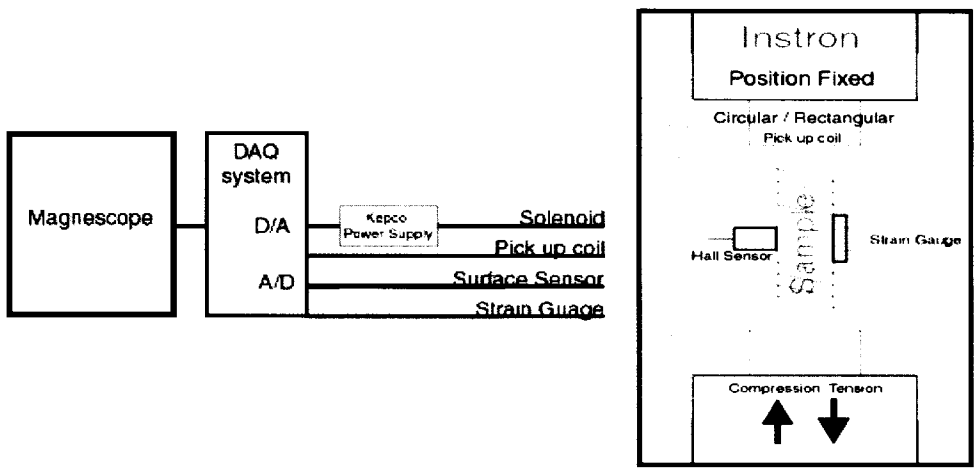

Figure 3.1 Hysteresis loop and anhysteretic curve measurement.

Figure 3.1 shows the configuration of equipment for measurement. The tensile testing machine (Model 8500, Instron, Inc.) was used to apply stress on the samples; solenoid to vary the applied magnetic field; pickup coil to collect magnetic induction

signals; hall sensor to get the sample surface magnetic field; strain gauge to record the magnetostriction. The *H* field was measured locally on the surface of the sample at the center of the long axis of solenoid, making use of the fact that *H* tangential is continuous across the surface and assuming that *H* is uniform inside the sample. The sample can be steel, nickel or other materials. The experiment involved applying an external stress to the materials at up to 60% of the estimated yield strength.

The objective of this measurement was to perform systematic experimental studies of the connection between micro-structural changes due to stress and magnetic properties of ferromagnetic Fe-based materials and nickel. The nickel rod sample was 140mm length and 8mm diameter. All the measurements were conducted within the sample's elastic limit in order to make a completely reversible process. An initial measurement was carried out using the computer controlled Magnescope to obtain the stress-strain curve for the material and for the purpose of obtaining preliminary hysteresis data under both tensile and compressive loading conditions. The same procedure was conducted again for the same nickel sample but after it was annealed at 1000^{o}C for one hour.

After annealing, the nickel sample's yield point was lower than the cold-worked one. The yield point of the nickel sample before annealing is around 300MPa, while the annealed one is around 75MPa. For this annealed nickel sample with 99.9% purity, the yield strength is around 50MPa.

The stainless steel 410 was a dog-bone like sample with 24mm in length, 12.5mm in width and 7.5mm in depth. The tensile strength of 410 stainless is around 750MPa.

All the measured procedures are the same as for that of nickel samples. One should note that nickel has a negative magnetostriction, while iron and steel has positive ones.

Figure 3.2 shows the strain versus stress curve for nickel (both cold-worked and annealed) and steel samples within their elastic ranges. During these initial trials, surface-hysteresis measurements were carried out using the Magnescope. The results, including the coercivity and remanence all carried out under positive (tensile) and negative (compressive) loading conditions, are shown in Figure 3.3, Figure 3.4 and Figure 3.5. From the figures one can see that coercivity results exhibit linear behavior under compressive loads and nonlinearities under tension, but probably offer an adequate measurement tool under limited conditions. The remanence also shows a linear function dependence on loads within a limited load range.

For cold-worked nickel, the magnetic coercivity appears to be particularly sensitive to applied load but exhibits a non-linear response over 100MPa under tensile stress, which is also seen in the magnetic remanence results over 150MPa, under either tensile or compressive stress. For annealed nickel, coercivity will lose linearity over 20MPa, while remanence will lose linearity over 20MPa in both tensile and compressive stress. For steel, coercivity retains linearity within 100MPa, under either tensile or compressive stress; while remanence will lose linearity beyond 100MPa in both directions.

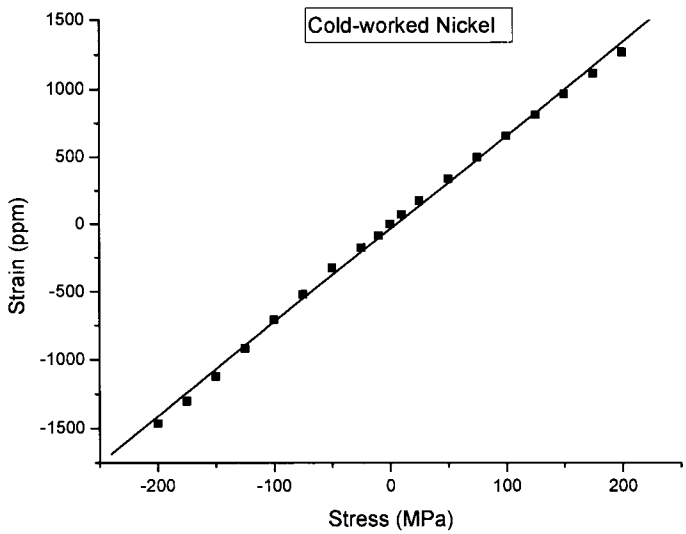
Cold-worked Nickel
Strain (ppm)
Stress (MPa)
1500
1000
500
0
-500
-1000
-1500
-200
-100
0
100
200

(a)

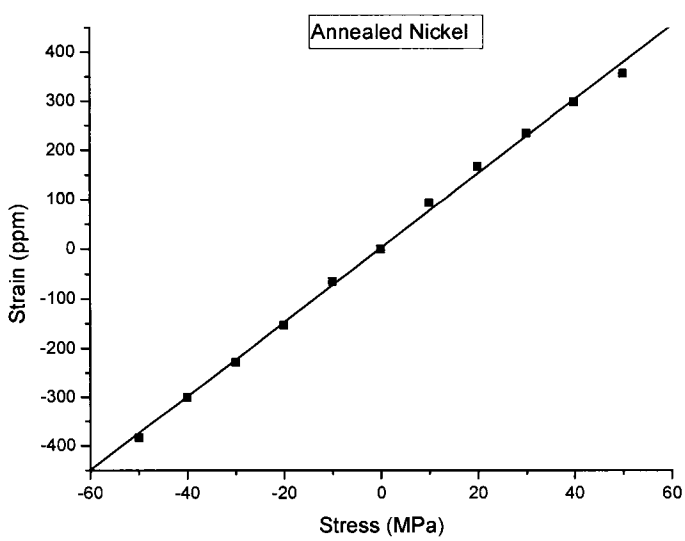
Annealed Nickel
Strain (ppm)
Stress (MPa)
400
300
200
100
0
-100
-200
-300
-400
-60
-40
-20
0
20
40
60

(b)

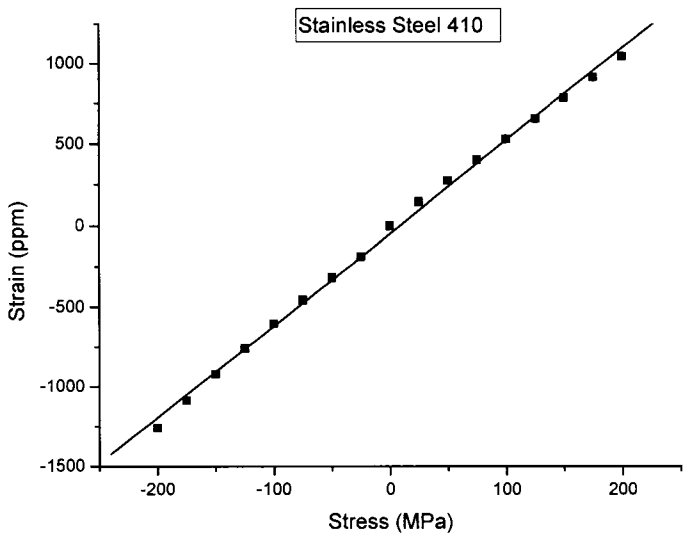

(c)

Figure 3.2 Stress-strain curves for nickel and steel sample. (a) cold-worked nickel; (b) annealed nickel; (c) steel.

(b)

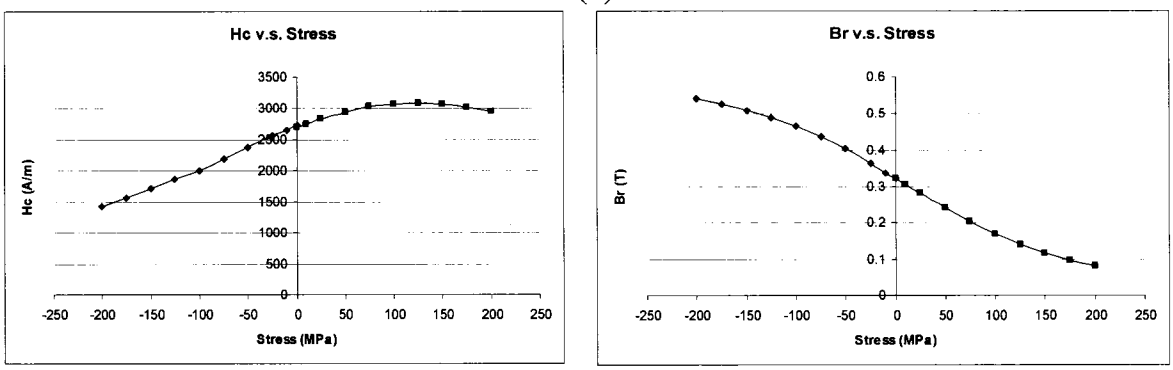

(a) (b)

Figure 3.3 Hysteresis data for Ni (cold-worked) obtained up to 200MPa. (a) Coercivity versus stress; (b) Remanence versus stress.

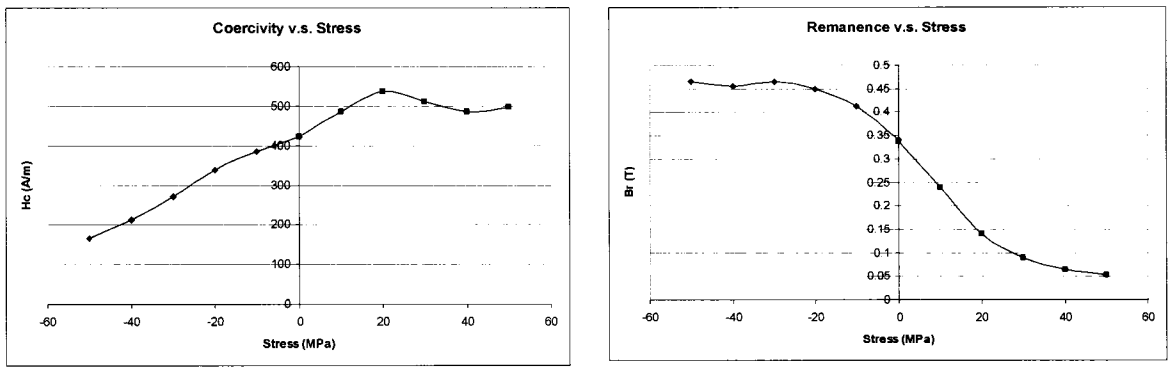

(a) (b)

Figure 3.4 Hysteresis data for Ni (annealed) obtained up to 50MPa.
(a) Coercivity versus stress; (b) Remanence versus stress.

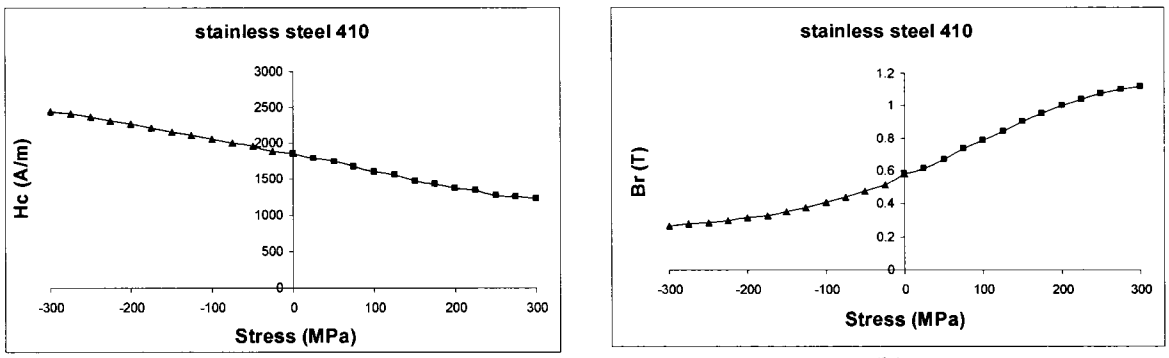

(a) (b)

Figure 3.5 Hysteresis data for steel obtained up to 300MPa.
(a) Coercivity versus stress; (b) Remanence versus stress.

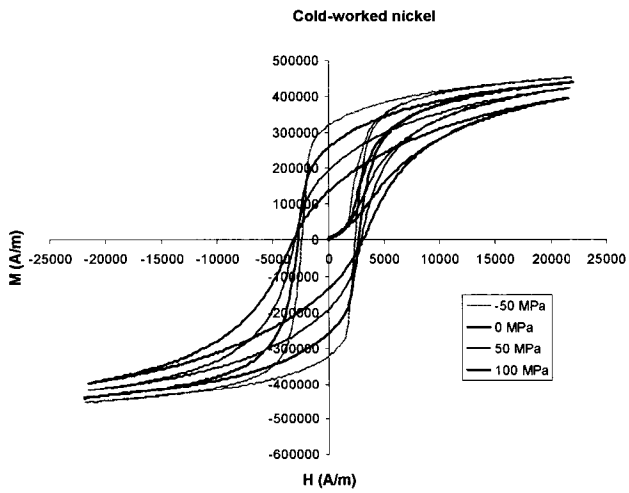

(a)

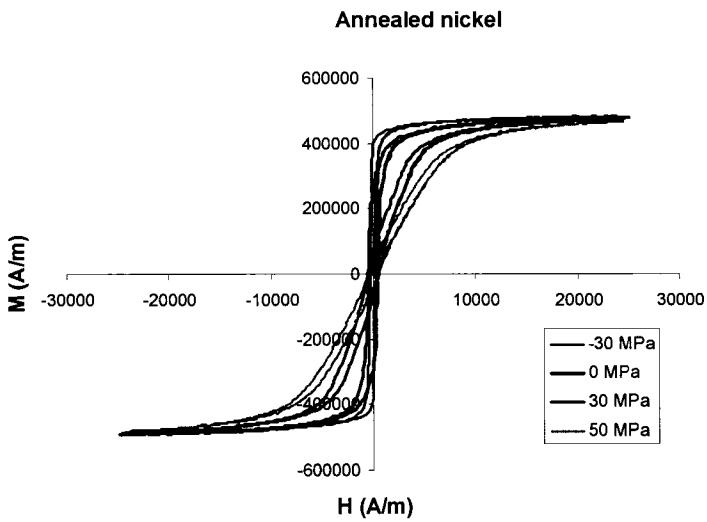

(b)

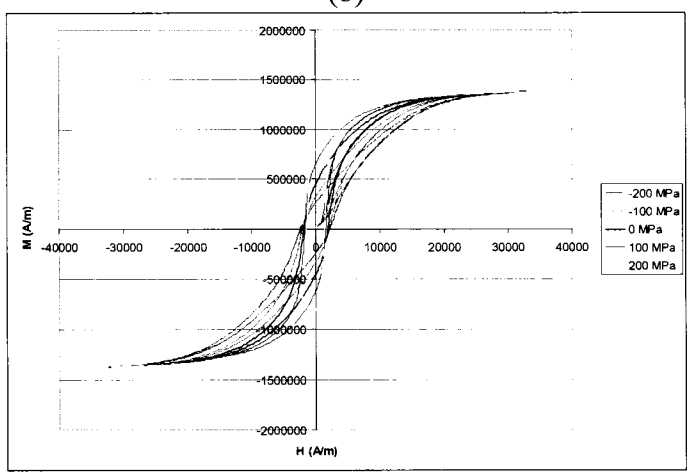

(c)

Figure 3.6 Hysteresis loops for nickel and steel samples.
(a) cold-worked nickel; (b) annealed nickel; (c) steel.

Figure 3.6 is the measured hysteresis loops of nickel (cold-worked and annealed) and steel samples. In order to make the figures clearer, only some of the measured hysteresis loops under several stress levels are drawn, for example hysteresis loops under -50, 0, 50 and 100MPa are shown on the figures for cold-worked nickel sample.

Comparison of Figure 3.6 (a) with (b) will lead to a conclusion that nickel will change from hard-magnetic to soft-magnetic material after annealing since the hysteresis

loss becomes quite small. The coercivity and remanence of all the samples are affected strongly by stress, but the coercivity is affected less than the remanence if the relative percentage values are compared. Increasing tensile stress reduces the permeability of nickel sample which has a negative magnetostriction; while it makes the hysteresis loops of steel sample which has positive magnetostriction become more vertical. Increasing the compressive stress will have the opposite effect on the permeability.

Figure 3.7 is the measured anhysteretic curves of nickel (cold-worked and annealed) and steel samples. The noise signal was obvious when measurement on anhysteretic magnetization was conducted. Also due to the integration capability of flux meter, anhysteretic magnetization under some stress level can not obtained as expected. This resulted in un-smooth curve and data with singularity.

Similar results are obtained by comparing the figures. Various stresses make the anhysteretic curves go upward or downward, with the same trend of hysteresis loops. It can be understood easily since the anhysteretic curve lies between the upper and lower branches of the hysteresis loop.

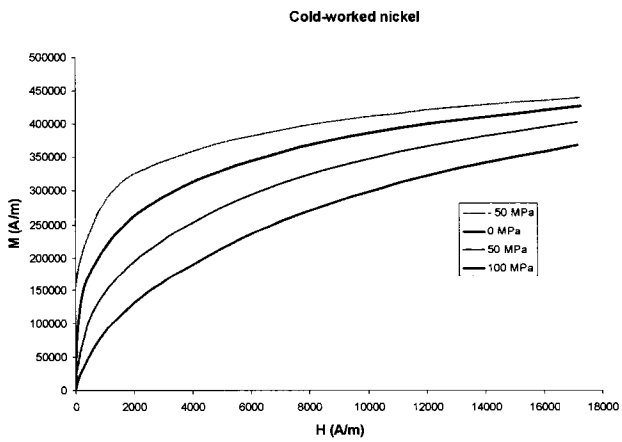

(a)

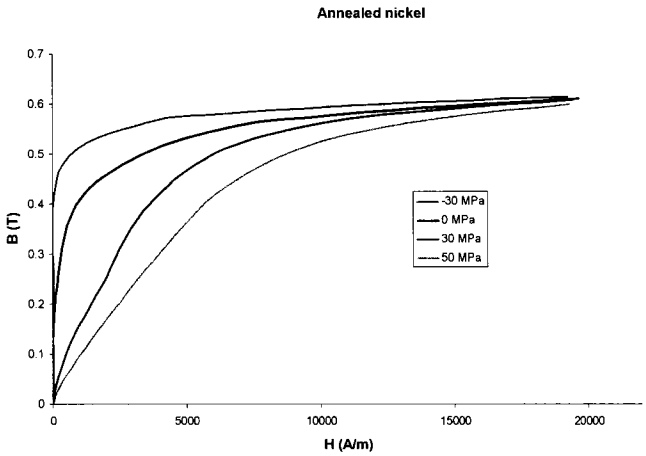

(b)

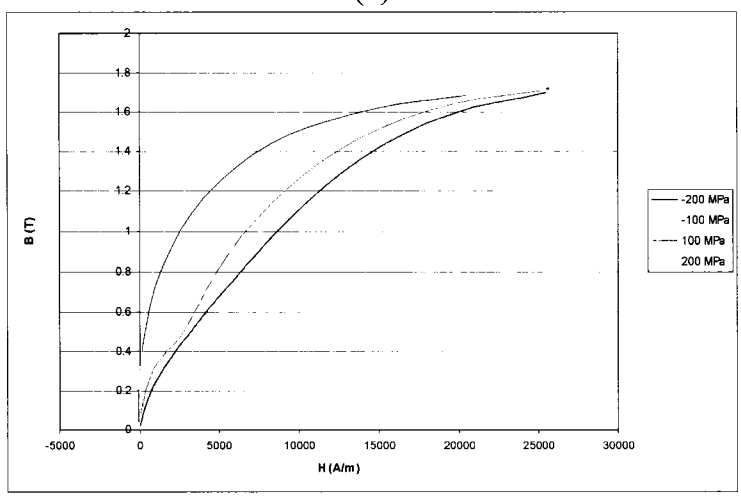

(c)

Figure 3.7 Anhysteretic curves for nickel and steel samples.
(a) cold-worked nickel; (b) annealed nickel; (c) steel.

3.2 Model of stress dependent hysteresis

This section presents a modified model which provides a description of the effects of stress on both hysteresis loops and anhysteretic magnetization curves. It has been proposed in previous studies that an applied stress can be treated as an effective field

operating through the magnetoelastic coupling [27,28]. The theory of magnetomechanical effect based on this approach has been found useful in describing the effects of varying stress on magnetization [24] and anhysteretic magnetization curves. This approach nevertheless cannot always completely describe the stress dependence of hysteresis loop properties such as coercivity and remanence [29]. In this study the magnetomechanical hysteresis model has been extended by taking into account the effect of applied stresses on domain wall pinning. The extended model has been found to reproduce the stress dependence of magnetic properties, such as coercivity and remanence, on applied stress.

An accurate model description of the effects of stress on magnetic properties of materials has become increasingly important in quantitative analysis of magnetic measurement results, and to the development of magnetostrictive sensors for nondestructive evaluation applications. The model of the magnetomechanical effect developed in the previous work provides the basis for describing changes of magnetization under stresses. However there is a need to further improve the model to deal with materials which have different magnetomechanical properties or anisotropy. This study has recently performed modeling studies to investigate how stress induced magnetic anisotropy affects hysteretic and anhysteretic magnetization curves as they approach saturation. The result of this work has led to an improved model which takes into account the stress dependence of the input model parameters. The extended model was validated with respect to its capability for describing the changes of magnetization in response to varying mechanical stress under constant applied fields, and to varying magnetic field under constant applied stresses. Simulation results are compared to the

measurement results obtained from materials with both positive and negative magnetostrictions, including steel and nickel.

The previous model mentioned in chapter 2 needs several parameters to do this kind of simulation. The model parameters include domain density, domain coupling, loss coefficient, reversibility constant, and demagnetizing factor. Domain density stands for the number density of a typical domain within the specimen; Loss coefficient is the strength of pinning site; domain coupling describes how strongly the magnetic moment can be coupled to the magnetization; reversibility stands for what fraction of the magnetization change is reversible; while demagnetizing factor takes into account the demagnetizing effects caused by domain surface charges and other reasons. Among these parameters, domain coupling, domain density, and loss coefficient are the most important, because they will decide what the curve shape looks like. The original model assumes there is one model parameter - domain coupling – which is stress dependent. The other two are independent of stress. The drawbacks of the original model are that when stress is increased, towards either tensile or compressive direction, the calculated hysteresis and anhysteretic data, especially the hysteresis loss, are inconsistent from the experimental data. The calculated anhysteretic permeability at the original point also decreases faster than the measured one. On the other hand, the simulation of hysteresis loops and anhysteretic curves at high stress level have deformed shapes, which means the calculated shapes are far from the measured ones. Since the model equation of anhysteretic magnetization has only two model parameters, i.e. domain coupling and domain density, a reasonable hypothesis is that not only the domain coupling is stress

dependent as utilized by the original model, the domain density is also stress dependent. On the other hand, since the loss coefficient is related to hysteresis loss, the changing of hysteresis loss under various stresses, which can be seen from Figure 3.6, means the loss coefficient is also stress dependent.

3.2.1 Stress dependent domain coupling α_{eff}

It has been shown in chapter 2, Equation (2.21) that stress can affect the domain coupling parameter by effective field theory. In order to discuss it conveniently, we list the equation for the effective field here again.

$$H_{eff} = H + \alpha M + \frac{3\gamma\sigma}{\mu_0} M = H + \alpha_{eff} M \quad , \tag{3.1}$$

where $\alpha_{eff} = \alpha + 3\gamma\sigma/\mu_0$, and α is a mean field parameter representing inter-domain coupling [26] and H is the true applied field. As discussed previously in chapter 2, the domain coupling at zero stress can be obtained from the experimental data.

Considering the symmetric parabola shape of the typical magnetostriction curve as shown in Figure 3.8, and keeping Equation (2.15) in mind, it is reasonable to use an approximation to the magnetostriction by including the power terms up to 2 and ignoring the constant term, which is simply the elastic strain and does not play an active role in the magnetomechanical effect [21].

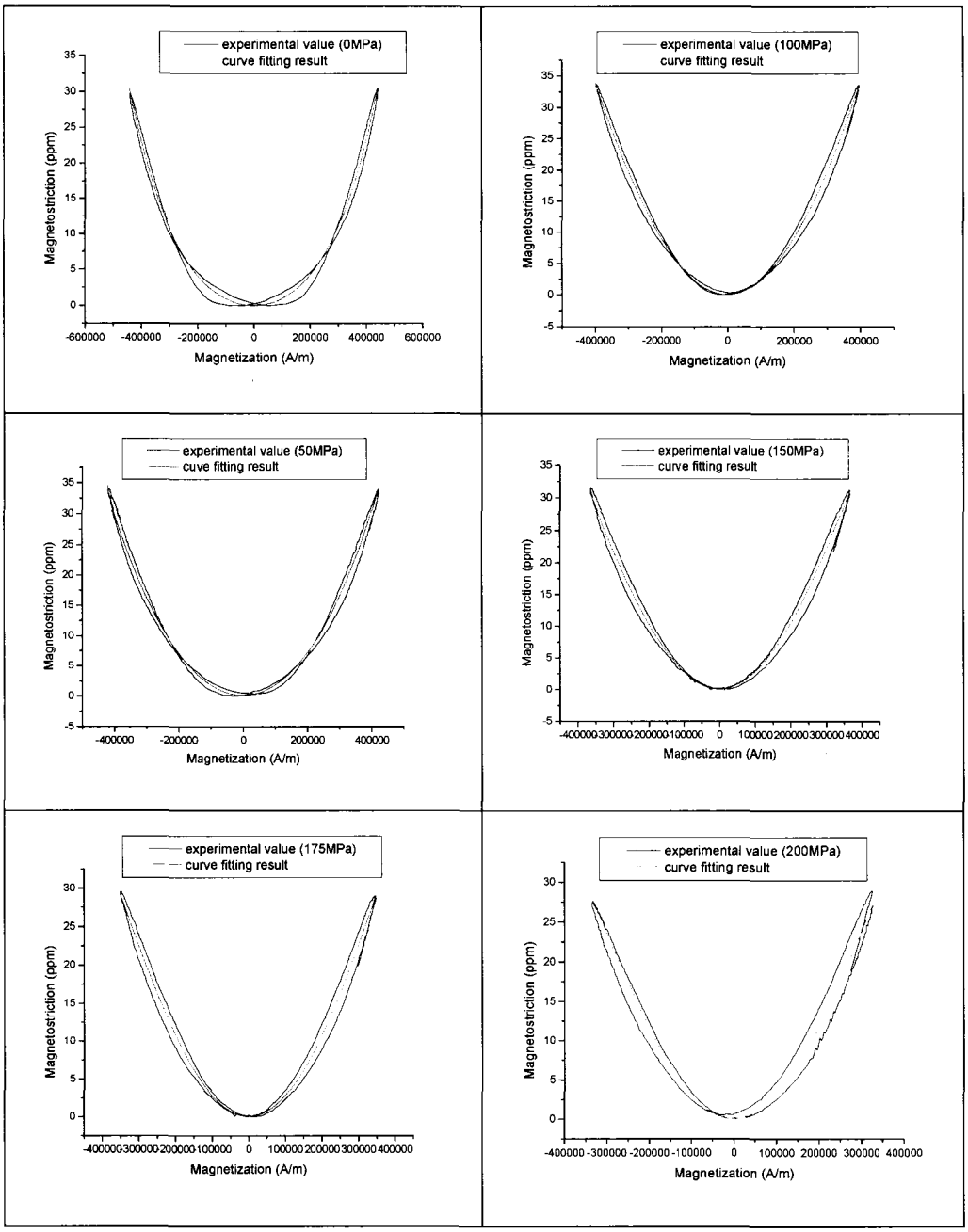

Figure 3.8 Curve fitting results of magnetostriction against magnetization at various tensile stress levels for nickel sample.

The stress-dependence of the magnetostriction curve λ (M, σ) can be described in terms of the stress dependence of γ_1 and γ_2 using a Taylor series expansion as described

by Equation (2.15). Then, $\gamma_{11} \sim \gamma_{22}$ can be obtained from curve fitting from γ_1 and γ_2 versus stress graphs, as seen in Figure 3.9.

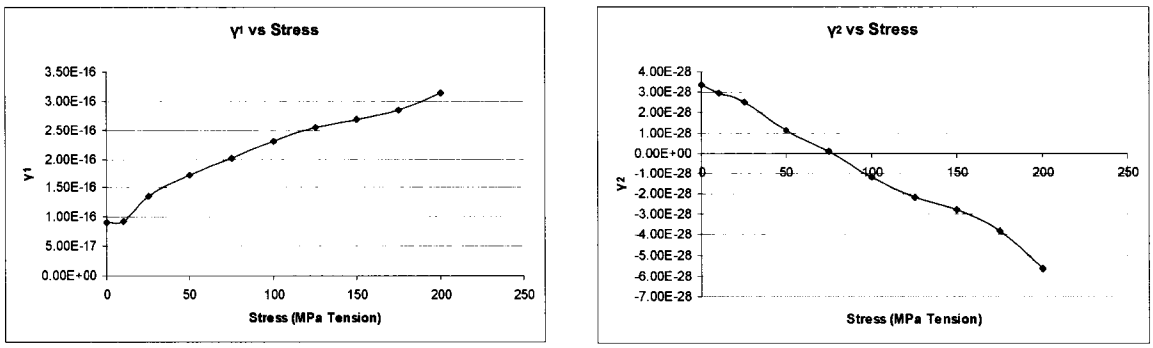

Figure 3.9 Curve fitting to calculate magnetostriction.

The parameters, γ_1 and γ_2, in Equation (2.13) are approximately linearly proportional to stress, Figure 3.9. That is to say the hypothesis of Equation (2.15) is consistent with the experimental result. Table 3.1 shows the results obtained on nickel using this method.

Table 3.1 Linear curve fitting from 0MPa to 200MPa for $\gamma_{11} \sim \gamma_{22}$

γ_{11} (m^2A^{-2})	γ_{12} ($m^2A^{-2}Pa^{-1}$)	γ_{21} (m^4A^{-4})	γ_{22} ($m^4A^{-4}Pa^{-1}$)
1.03E-16	1.11E-18	3.38E-28	-4.34E-30

Hence, the domain coupling parameter which comes from stress dependent magnetostriction is also stress dependent and there is a way to calculate it from the experimental data.

3.2.2 Stress dependent loss coefficient k_{eff}

The applied stress changes the anisotropy energies of domains due to the magnetoelastic coupling, and this in turn alters the levels of local energy barriers that a domain wall needs to overcome before it moves irreversibly from one pinning site to another. Therefore the strengths of pinning sites for domain walls become dependent on the applied stress. For simplicity in the isotropic case, consider a domain wall separating two domains which are magnetized along and at an arbitrary angle θ to the stress direction respectively. Under an applied stress σ, the magnetoelastic energies of the domains are

$$E_1 = -\frac{3}{2}\lambda_s\sigma, \tag{3.2}$$

$$E_2 = -\frac{3}{2}\lambda_s\sigma\cos^2\theta, \tag{3.3}$$

where λ_s is the saturation magnetostriction. The energy needed for the domain wall to overcome the pinning site is therefore changed by

$$\Delta E = -\frac{3}{2}\lambda_s\sigma\left(1-\cos^2\theta\right). \tag{3.4}$$

Under a constant or zero applied magnetic field the domain wall may break away from the pinning site and move across the energetically unfavorable domain if the internal field is large enough to overcome the pinning force. This causes irreversible changes in magnetization.

For those domain walls which remain pinned after a constant stress σ has been applied, the energy needed to overcome the pinning site becomes dependent on σ because the domains separated by the domain wall will have different magnetoelastic

energies. As a result the coercivity of the material changes with the applied stress. This effect can be described using the equation based on the theory of ferromagnetic hysteresis [30]. According to this theory the energy E_{pin} dissipated through pinning and unpinning of a domain wall is proportional to the change in magnetization and the pinning coefficient $k_0 = n_0 \langle \varepsilon_0 \rangle / 2m$, where m is magnetic moment, n_0 is the pinning site density and $\langle \varepsilon_0 \rangle$ is the average pinning energy without applied stress. Since the applied stress alters the pinning energy on either side of a domain wall as given in Equation (3.4), the pinning coefficient (denoted by k_{eff}) becomes dependent on stress and can be written as

$$\begin{aligned} k_{eff} &= n(\sigma) \ \langle \varepsilon_0 - \tfrac{3}{2} \lambda_s \sigma (1 - \cos^2 \theta) \rangle \ / 2m \\ &\cong n_0 \langle \varepsilon_0 \rangle / 2m \ - \ n_0 \langle \tfrac{3}{2} \lambda_s \sigma (1 - \cos^2 \theta) \rangle / 2m \ , \\ &= \ k_0 \ - n_0 \langle \tfrac{3}{2} \lambda_s \sigma (1 - \cos^2 \theta) \rangle / 2m \end{aligned} \qquad (3.5)$$

where $\langle \ \rangle$ is the value averaged over all the pinning sites and k_{eff} is dependent on σ because the applied stress changes the orientation of domain magnetization with respect to the stress axis (i.e. θ is a function of σ). Equation (3.5) was derived based on the assumption that the density of pinning sites (dislocations, secondary phases and precipitates) remains unchanged under applied stresses within the elastic limit of the material. Accordingly the stress-induced change in the pinning coefficient is determined by the product of λ_s and σ. For materials with positive λ_s (e.g. iron at low field strengths) k_{eff} decreases with tension but increases with compression, while for materials with negative λ_s (e.g. nickel) k_{eff} shows the opposite dependence on stress. It is expected that for soft magnetic materials coercivity exhibits a stress dependence similar to that of k_{eff},

since in soft magnetic materials the pinning coefficient k is approximately equal to coercivity [31]. The stress dependence of coercivity predicted by the current model is consistent with that observed in the previous studies on steel [25, 26] and nickel [32].

This relation can be testified by a curve fitting process based on the experimental data. The coercivity and remanence of the simulated hysteresis loops exhibited stress dependence consistent with that of the experimental data as shown in Figure 3.10.

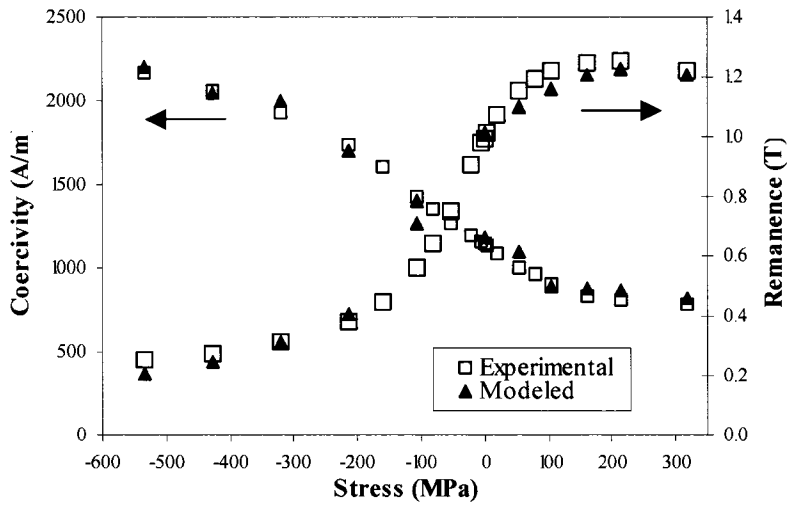

Figure 3.10 Measure and modeled coercivity and remanence in AISI 410 stainless steel as a function of stress.

As shown in Figure 3.11, the pinning coefficient k_{eff} appears to vary approximately linearly with stress within the range of -533 MPa to 200 MPa. This experimental result is consistent with that predicted by Equation (3.5). On the other hand k_{eff} becomes relatively insensitive to stress beyond 200 MPa. A possible explanation is that application of large tensile stress favors a domain structure in which domains are magnetized along the stress axis and hence have the same magnetoelastic energy. As a result the magnetoelastic energy does not contribute further to the strength of domain

wall pinning and therefore k_{eff} becomes less sensitive to further changes in the applied stress.

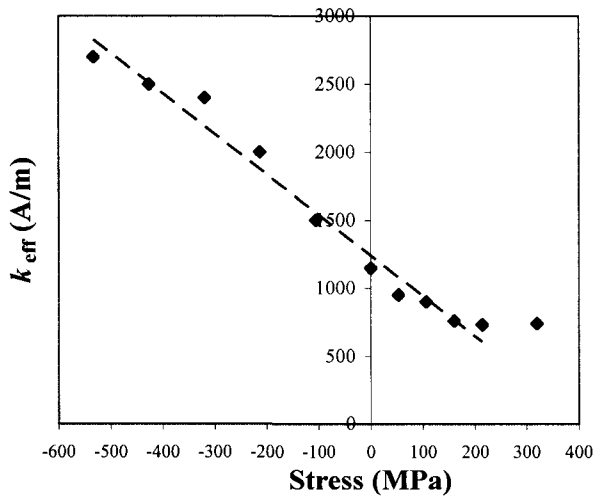

Figure 3.11 The pinning coefficient k_{eff} plotted against applied stress σ for steel sample.

Figure 3.12 shows another example of k_{eff} by best curve fitting for nickel samples.

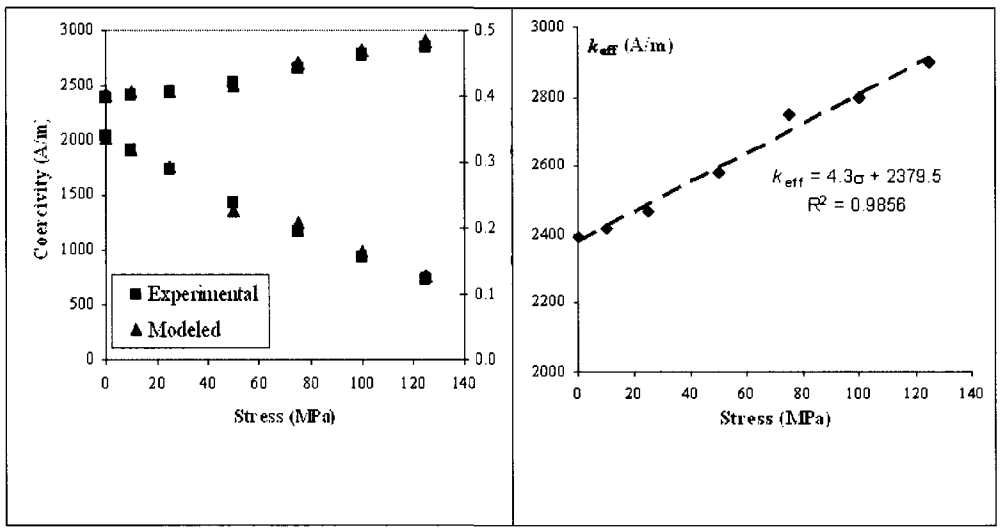

Figure 3.12 The pinning coefficient k_{eff} plotted against applied stress σ for nickel sample.

Hence, the loss coefficient parameter is also stress dependent and there is a way to estimate it from experimental data.

3.2.3 Stress dependent domain density a_{eff}

The law of approach to saturation is a well-known mathematical model for describing the behavior of ferromagnets at high magnetic field strengths which has the additional advantage that it can be linked to anisotropy through one of the terms in the mathematical expression of the law. In this work the recent and more comprehensive model of the magnetization process was compared with the law of approach to saturation in terms of the capability to describe the dependence of the magnetization curve in the high field regime. The comparison leads to relations between the parameters of the model and the interpretation of certain aspects of the model in terms of anisotropy. It is shown that the effects of anisotropy can be incorporated directly into the model without any additional assumptions.

First we concentrate on the parameter relations at stronger fields much larger than H_c, where most of the irreversible domain processes are finished. The magnetization behavior under compressive and tensile applied stress, as predicted by the models, has been studied and the results are compared to hysteresis measurements of nickel and steel samples under applied stress.

The Law of Approach (LA) to saturation [33, 34,14] describes the dependence of magnetization on the applied field $H >> H_c$ near the saturation magnetization M_s (which is close to the spontaneous magnetization at a temperature T well below the Curie temperature T_C) according to the equation

$$M = M_s\left(1 - \frac{a}{H} - \frac{b}{H^2} - \ldots\right). \tag{3.6}$$

Using the reduced magnetization $m = M/M_s$ and the demagnetizing field $H_d = N_d M$ (N_d is an average geometric demagnetizing factor), and neglecting the a/H term and the H^{-n} terms with $n > 2$ in the LA and considering the difference between the inner and external fields ($H_i = H_{ext} + N_d m M_s$) we find for $0 \le m < 1$

$$H = \sqrt{\frac{b}{1-m}} + N_d m M_s \,, \tag{3.7}$$

where the parameter $b = \varepsilon H_k^2$ is related to the fictive anisotropy field $H_k = 2K_u/\mu_0 M_s$ (K_u is uniaxial anisotropy constant) and ε is a microscopic constant considering the crystal geometry; ε is either 1/15 [35] for isotropic hexagonal structure or 8/105 for isotropic cubic structure, depending on the crystal geometry and assuming that higher order anisotropy constants can be neglected; $\varepsilon = 0.02$ in iron, for example [36].

Two ideas for relating the parameters to anisotropy are considered. At a certain field H_a, which is a fraction n of H_k, i.e. $n = H_k / H_a$ we find $m_a = 1 - n^2 \varepsilon$ from Equation (3.7), where $m_a = M(H_a)/M_s$. Without considering N_d — because it does not affect the parameter relations with anisotropy — we then compare the differential susceptibility $\chi_a' = dM / dH$ at $M_a = M(H_a)$ and the reversible work $\omega_a = \mu_0 \int_{M_a}^{M_s} H dM$ of Equation (3.7) with Equation (3.8). This implies that $M(H_a)$ is approximately the same in LA and JAM, which is not *a priori* fulfilled in a wider field range but should be satisfied for $H_c << H_a < H_k$. The validity of our assumptions is supported by numerical analysis. Figure 3.13 shows the quantities used in the following calculations schematically for a typical magnetization curve.

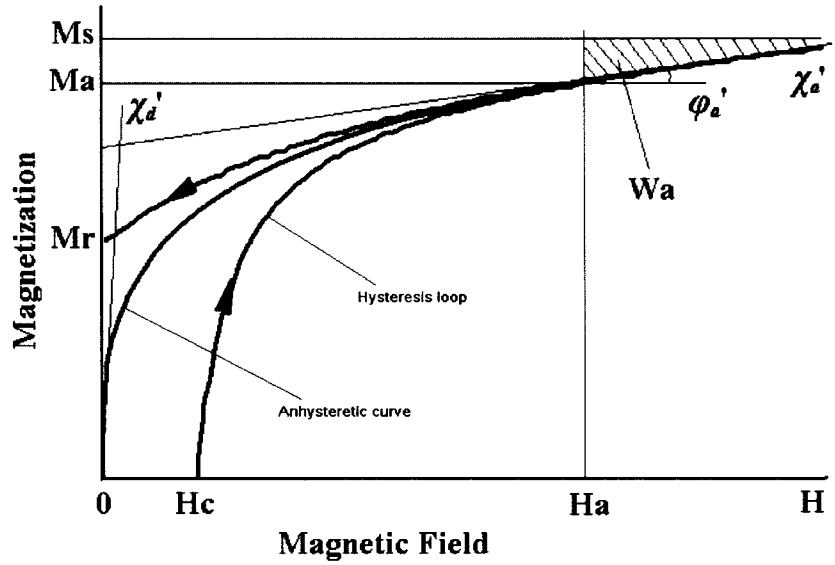

Figure 3.13 Typical magnetization curve (first quadrant only) with M_s, H_c, M_a, H_a, w_a, and χ_a'.

The LA works very well for isotropic hard magnetic materials, where the term b/H^2 is dominant. There the relation between b and H_k is clearly described and usually $H_k >> H_d$ which allows neglecting the demagnetizing field. For soft and amorphous magnetic materials the situation is completely different. For soft magnetic materials often H_k is small and the effect of H_d is very important for the shape of the hysteresis loop. In materials where the magnetostriction is large, the magnetoelastic energy becomes important, which is especially the case in soft magnetic materials. This leads in amorphous materials to a complex behavior, there the constants a and b are scaled with magnetostriction depending on the magnitude of the exchange length [36]. Therefore, the question which type of analysis is suitable, or which parameters are negligible, needs the consideration of the individual material.

The magnetization curve at $H >> H_c$ is close to the anhysteretic magnetization function $M = M_s \tanh[(H + (\alpha - N_d)M)/a]$, which gives

$$H = \frac{a}{2}\ln\frac{1+m}{1-m} - M_s m(\alpha - N_d) \tag{3.8}$$

in the JAM, where the parameters a and α are related to the pseudo domain size (or domain density) and domain coupling, respectively [11]. Using a Langevin function L for $M = M_s L[(H + \alpha M)/a]$ will yield similar results as the following considerations, however, some analytical results are impossible to obtain.

Considering the derivatives with respect to m at $m = m_a = 1 - n^2\varepsilon$ of Equation (3.7) and (3.8),

$$\frac{dH}{dm} = \frac{a}{n^2\varepsilon(2 - n^2\varepsilon)} - (\alpha - N_d)M_s \tag{3.9}$$

which leads to

$$a\frac{2n}{2 - n_2\varepsilon} - \alpha M_s 2n^3\varepsilon = H_k \tag{3.10}$$

which analytically indicates a single linear relationship between a and H_k only if $\alpha = 0$ or m is assumed to change much less than H, for example when m is close to saturation (i.e. ~1): $\Delta M << \Delta H$. Using the functions f_a and f_α to represent the various terms in Equation (3.10), yields

$$f_a a - f_\alpha M_s \alpha = H_k. \tag{3.11}$$

These functions may degenerate to the linear approximations

$$a = a_c + c_a H_k \tag{3.12}$$

and

$$\alpha = \alpha_c + c_\alpha \frac{H_k}{M_s}, \tag{3.13}$$

where a_c and α_c are independent of H_k, c_a and c_α are microscopic proportionality constants, related to the crystal structure or microstructure. Figure 3.14 shows the dependence of c_a on ε, n, and α.

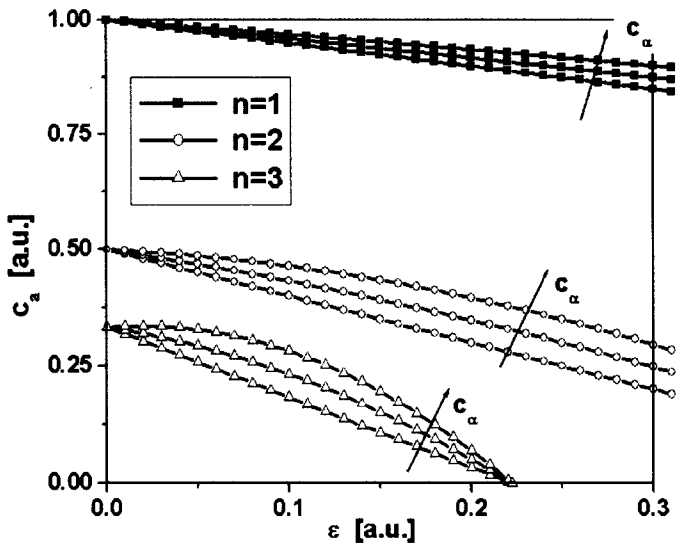

Figure 3.14 Consideration of $1/\chi_a'$; c_a versus ε, depending on n=1, n =2, n= 3, and $c_\alpha = 0$, $c_\alpha = 0.05$, $c_\alpha = 0.1$ with $a_c = 0$ and $\alpha_c = 0$.

The integral of Equation (3.7) with respect to m is

$$\int_{m_a}^{} (H - H_a) dm = H_k n \varepsilon, \tag{3.14}$$

and of Equation (3.8) is

$$\int_{m_a}^{} (H - H_a) dm = a \ln \frac{2}{2 - n^2 \varepsilon} - M_s \alpha \frac{n^4 \varepsilon^2}{2} \tag{3.15}$$

These lead to a similar relationship between a, α, and H_k as compared to Equation (3.10):

$$a\frac{\ln\dfrac{2}{2-n^2\varepsilon}}{n\varepsilon}-\alpha M_s\frac{n^3\varepsilon}{2}=H_k. \tag{3.16}$$

Figure 3.15 shows the general dependence of c_a on ε, n, and $\alpha M_s/H_k$.

The comparison of χ_a' and ω_a relations leads to the following: Considering $n^2\varepsilon <<$ 1, we find in the case of equal χ_a'

$$c_a=\frac{1}{n},\ c_\alpha=\frac{1}{8n}. \tag{3.17}$$

and in the case of equal ω_a

$$c_a=\frac{2}{n},\ c_\alpha=\frac{1}{2n}. \tag{3.18}$$

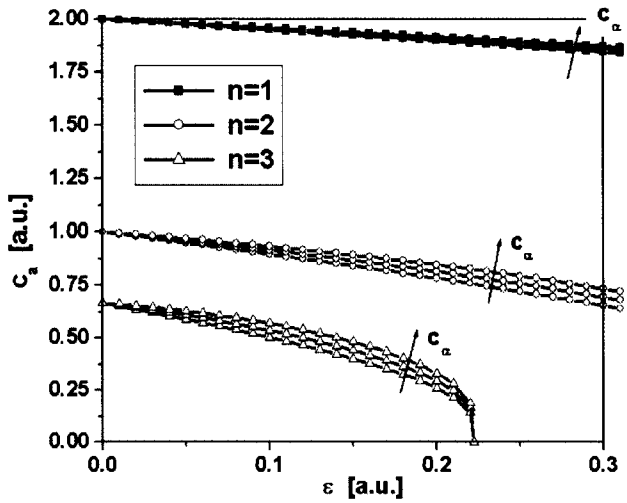

Figure 3.15 Consideration of ω_a; c_a versus ε, depending on $n = 1$, $n = 2$, $n = 3$, and $c_a = 0$, $c_a = 0.05$, $c_a = 0.1$ with $a_c = 0$ and $\alpha_c = 0$.

To fulfill equality for χ_a' and w_a is impossible; the equations above represent the upper and lower limits for the relations, respectively.

In general, one can say that the energy surface of applied stress appears to be the same as that of first order uniaxial anisotropy. Magnitude and sign of the "stress anisotropy constant" depend on $\lambda_s\sigma$ (magnetostriction constant and applied stress, respectively). In the following we consider only stresses below the elastic limit.

There will be mainly two different cases observed in experiments (but there will be a variety of intermediate cases, of course), depending on the relation between magnetocrystalline anisotropy energy and strain energy.

Assume that $\boldsymbol{H}$ and $\sigma > 0$ are parallel. In both cases, the changing anisotropy field will cause a change of the domain structure, as the domain wall energy $\gamma_w \propto \sqrt{A\mu_0 M_s H_k}$ depends on the exchange stiffness constant A and the anisotropy energy, represented by $\mu_0 M_s H_k$. Decreasing γ_w will result in a refinement of the domain structure [37, 38, 39], because the domain size in bulk materials (in the demagnetized state) is mainly a function of the ratio of wall energy and magnetostatic energy.

If $0 < K_u << \lambda_s\sigma$ then the easy directions will change, e.g., if $\lambda_s < 0$ then the domains will more likely align perpendicular to σ (or parallel to σ, if $\lambda_s > 0$), thus changing the average component of $\boldsymbol{M_s}$ of the domains with respect to $\boldsymbol{H}$. This might be the case for amorphous materials or for crystalline materials with comparable large magnetostriction.

If $K_u >> \lambda_s\sigma$ then the easy directions will not be so strongly affected by σ, but a refinement of the domain structure will still occur. This might be the case for crystalline materials with comparable low magnetostriction. For example to reduce the anomalous

eddy current losses, the effect is utilized to decrease the domain width in grain oriented FeSi steel sheets.

In principle, the physical interpretation with respect to the JAM parameters can be argued as following. Using the magnetic moment m of a pseudo domain, the parameter a is

$$a = \frac{k_B T}{\mu_0 m}, \tag{3.19}$$

where k_B is the Boltzmann constant. If the average domain moment with respect to H changes, then a will change according to the Equation (3.19); e.g., if $\lambda_s \sigma < 0$ then a will increase with increasing σ. On the other hand, increasing domain refinement (decreasing average domain size) may lead to a decreasing coupling coefficient α.

3.3 Simulation of hysteresis

Stress-induced changes in magnetization were simulated using the improved model equation of the magnetomechanical effect. The input model parameters were determined by measuring hysteresis loops and magnetostriction curves under various applied stresses using the Magnescope. The stress-strain curve of the sample was also measured to determine the mechanical properties such as the Young's modulus for use in the simulations.

Several parameters should be known before attempting to calculate the model results by the above mentioned theory. These parameters include domain density a, pinning coefficient k, domain coupling α, reversibility c, maximum applied magnetic

field H_m, maximum applied stress, Poisson's ratio, Young's modulus, the angle between applied stress and applied magnetic field, stress related constant ε and the four magnetostriction coefficients described in Equation (2.15). Hysteresis parameters such as domain density, pinning coefficient, domain coupling, and reversibility can be calculated from a predetermined set of slopes and intercepts taken from experimentally measured hysteresis curves [40]. The details will be discussed in chapter 5.

Based on the model theory described in chapter 2 and the stress dependent model parameters - domain density a, pinning coefficient k, domain coupling α, - simulations of cold-worked nickel sample are shown in Figure 3.16. Although the modeled result under 100MPa is different from the experimental data at loop tip, in general the calculated results agree with the experimental data both quantitatively and qualitatively.

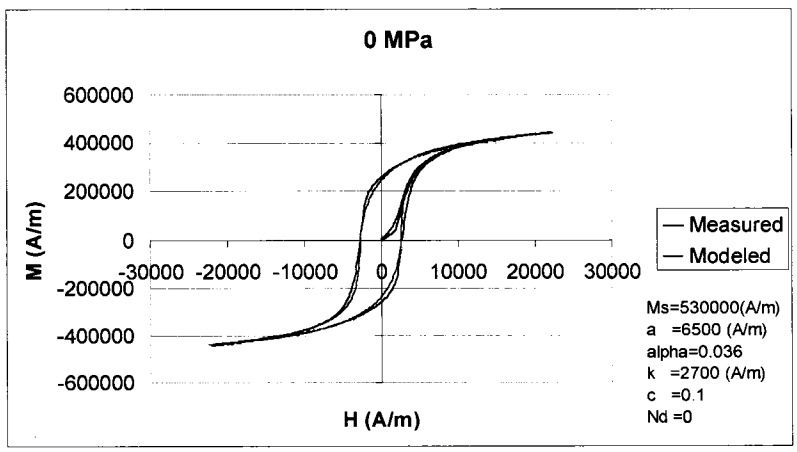

(a)

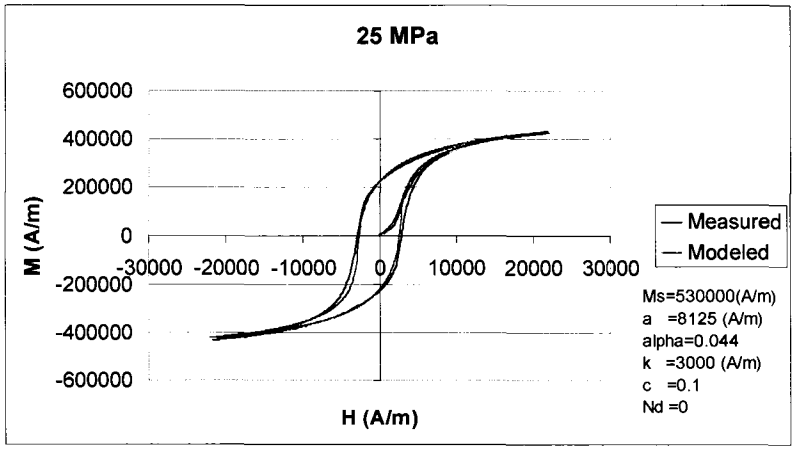
25 MPa
600000
400000
200000
0
-200000
-400000
-600000
-30000 -20000 -10000 0 10000 20000 30000
M (A/m)
H (A/m)
Measured
Modeled
Ms=530000(A/m)
a =8125 (A/m)
alpha=0.044
k =3000 (A/m)
c =0.1
Nd =0

(b)

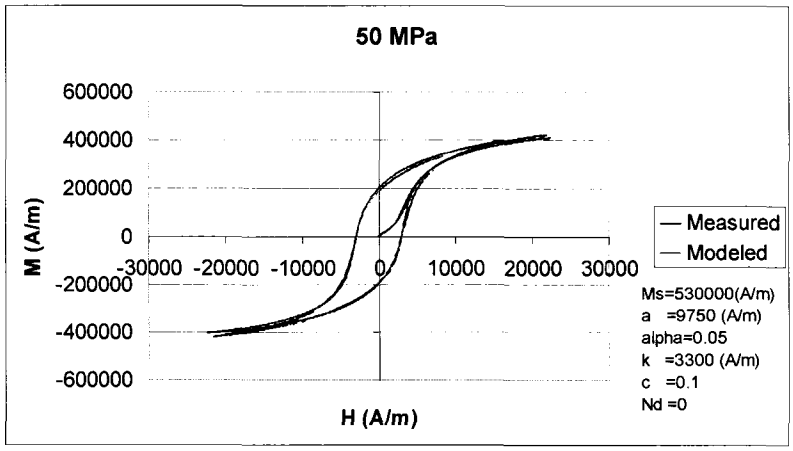
50 MPa
600000
400000
200000
0
-200000
-400000
-600000
-30000 -20000 -10000 0 10000 20000 30000
M (A/m)
H (A/m)
Measured
Modeled
Ms=530000(A/m)
a =9750 (A/m)
alpha=0.05
k =3300 (A/m)
c =0.1
Nd =0

(c)

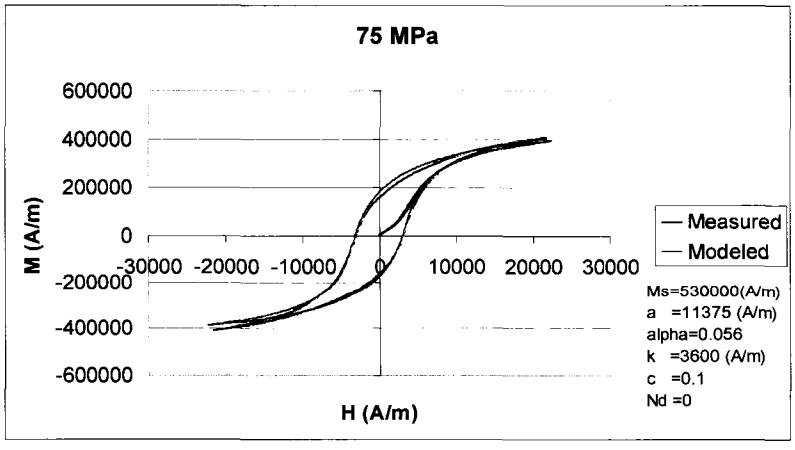
75 MPa
600000
400000
200000
0
-200000
-400000
-600000
-30000 -20000 -10000 0 10000 20000 30000
M (A/m)
H (A/m)
Measured
Modeled
Ms=530000(A/m)
a =11375 (A/m)
alpha=0.056
k =3600 (A/m)
c =0.1
Nd =0

(d)

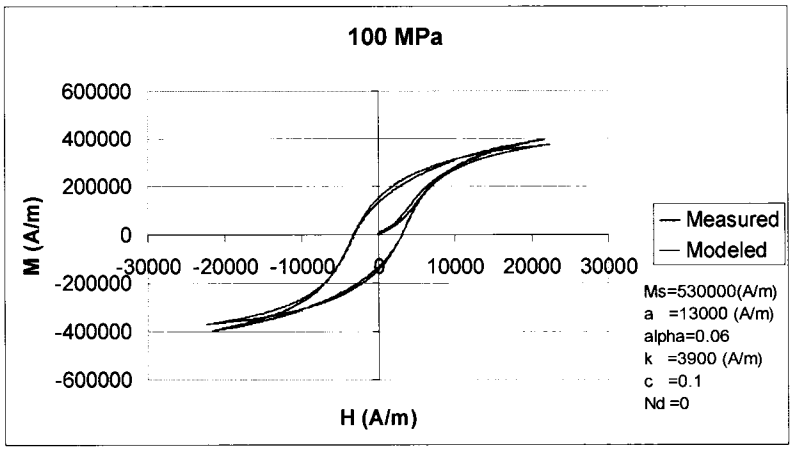

(e)

Figure 3.16 Hysteresis loop simulations for cold-worked nickel under various tensile stresses: (a) 0MPa, (b) 25MPa, (c) 50MPa, (d) 75MPa, (e) 100MPa.

The reason for the difference between modeled and experimental data at loop tip can be explained as follows. Since the linearity of model parameters with respect to stress exists only within certain ranges, at the two ends of these ranges, the linearity becomes weak, so the simulation will also become inaccurate, as seen in Figure 3.11.

As a comparison, the simulation results using the old model which considers only one stress dependent parameter – domain coupling α - are shown in Figure 3.17. From this figure, one can easily see that the old model can not give satisfied simulations. The percentage errors at coercivity H_c and remanence M_r are shown in Table 3.2.

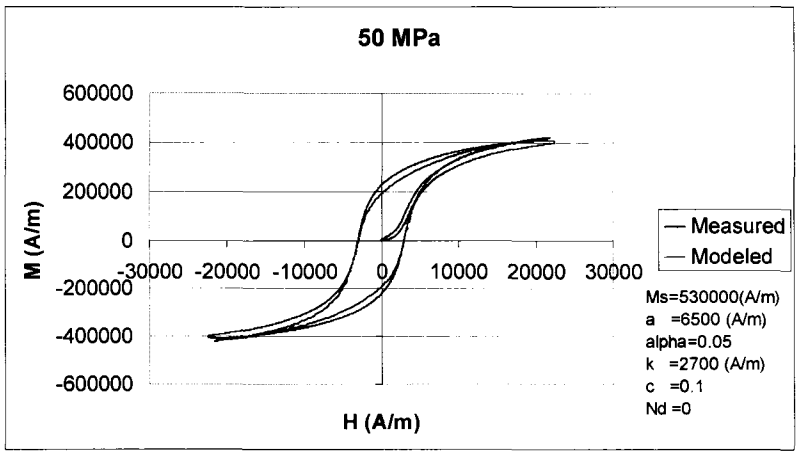

(a)

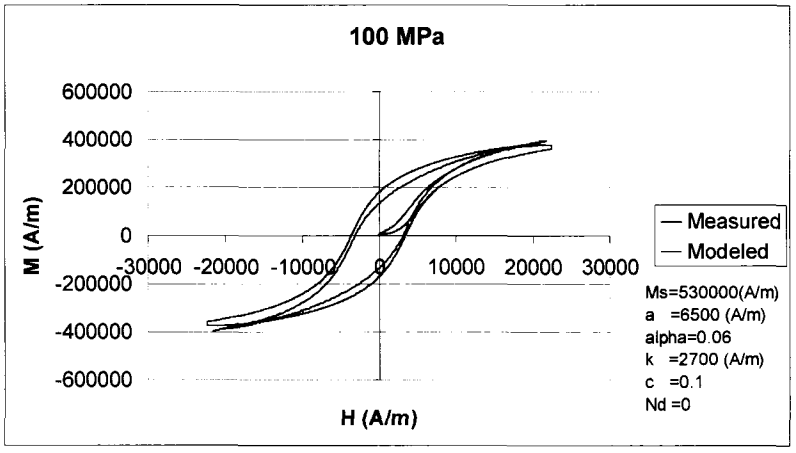

(b)

Figure 3.17 Simulation results from old model under the same condition of Figure 3.16 for the same sample: (a) 50MPa, (b) 100MPa.

Table 3.2 Errors of old and new models at (a) 50MPa, (b) 100MPa.

50MPa	Error at Hc (%)	Error at Mr (%)
Old model	1.4	17
New model	0.71	3.6

(a)

100MPa	Error at Hc (%)	Error at Mr (%)
Old model	13	30
New model	2.6	11

(b)

The same kind of simulation was repeated on the stainless steel 410 sample. Figure 3.18 shows these simulation results. The difference between measured and modeled data can be explained similarly as that for the nickel sample. On the other hand, the measured data also have errors because the steel sample's mechanical properties are similar as the testing machine's adapters. When stresses are applied, both sample and adapters have strain of themselves. When the stresses are removed, they will undergo a short period of time of relaxation. The relaxation of adapters can affect the accuracy of the measured signal of magnetic induction.

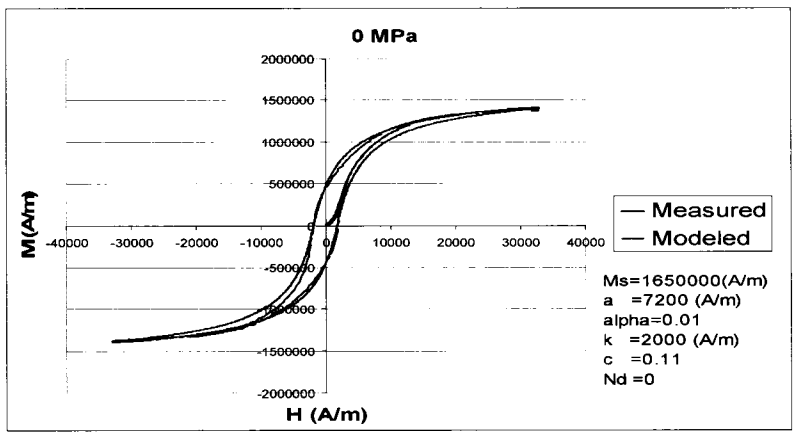

(a)

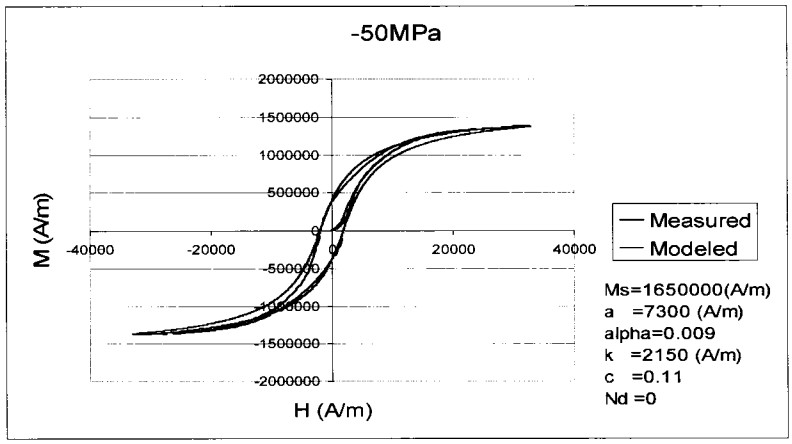
-50MPa
2000000
1500000
1000000
500000
0
-500000
-1000000
-1500000
-2000000
-40000
-20000
20000
40000
M (A/m)
H (A/m)
Measured
Modeled
Ms=1650000(A/m)
a =7300 (A/m)
alpha=0.009
k =2150 (A/m)
c =0.11
Nd =0

(b)

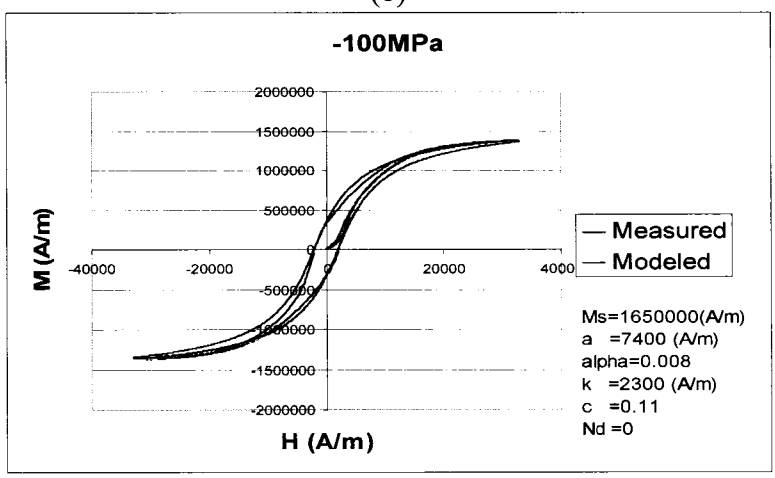
-100MPa
2000000
1500000
1000000
500000
0
-500000
-1000000
-1500000
-2000000
-40000
-20000
20000
40000
M (A/m)
H (A/m)
Measured
Modeled
Ms=1650000(A/m)
a =7400 (A/m)
alpha=0.008
k =2300 (A/m)
c =0.11
Nd =0

(c)

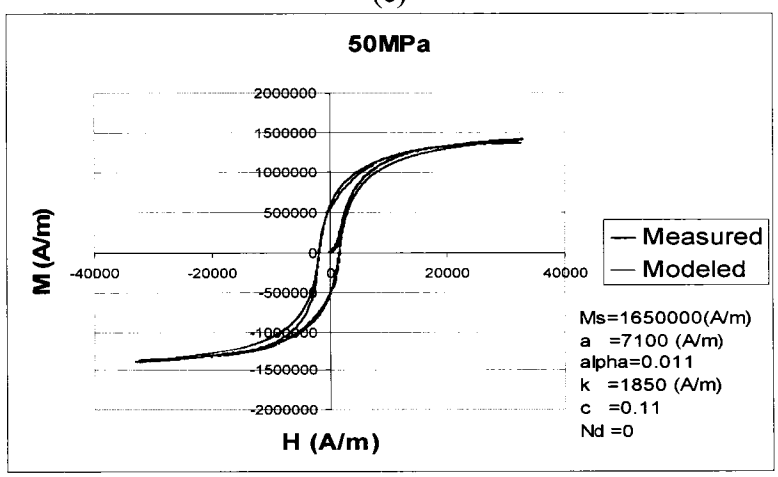
50MPa
2000000
1500000
1000000
500000
0
-500000
-1000000
-1500000
-2000000
-40000
-20000
20000
40000
M (A/m)
H (A/m)
Measured
Modeled
Ms=1650000(A/m)
a =7100 (A/m)
alpha=0.011
k =1850 (A/m)
c =0.11
Nd =0

(d)

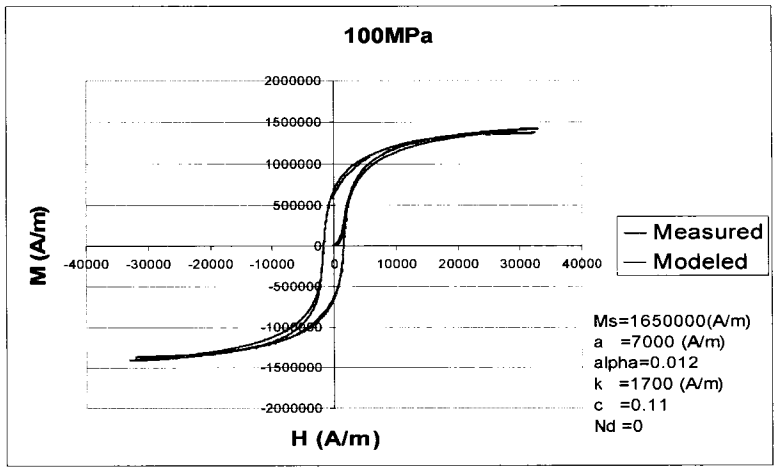

(e)

Figure 3.18 Hysteresis loop simulations for steel under various stresses: (a) 0MPa, (b) -50MPa, (c) -100MPa, (d) 50MPa, (e) 100MPa.

A similar simulation can also be conducted on annealed nickel sample. Again, similar results have been obtained.

It is interesting that the stress dependence of hysteresis can be described correctly in both qualitative and quantitative ways by considering the parameter dependence on phenomenological constants of anisotropy and magnetostriction. The benefit for engineering applications is the straight forward model identification and the rapid calculation as compared to other models.

The anhysteretic functions of the magnetization curve could be exchanged in these models, although the shapes of the curves are determined by different principles used to derive the functions. Usually, the two model parameters of the anhysteretic curve allow for an agreement with respect to χ_a' and at maximum magnetization M_m.

From the above simulation results, we can calculate every set of parameters for the hysteresis loops under different stress levels. Figure 3.19 through Figure 3.21 show the domain density *a*, pinning coefficient *k*, domain coupling α as a function of stress.

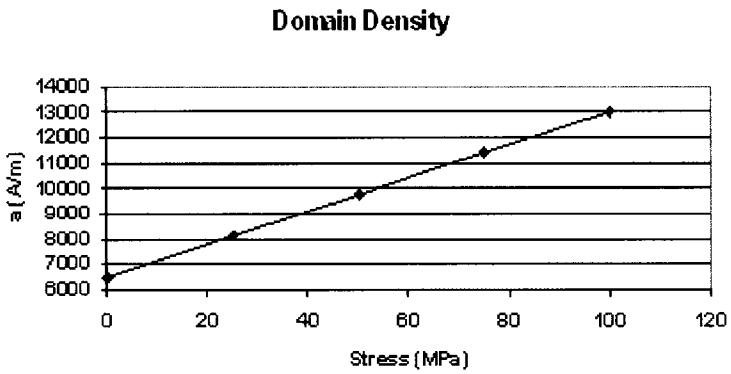

Figure 3.19 Domain density *a* under different stresses for the cold-worked nickel sample.

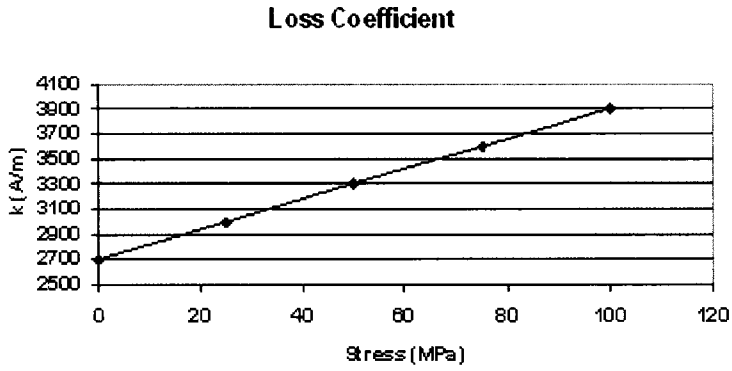

Figure 3.20 Pinning coefficient *k* under different stresses for the cold-worked nickel sample.

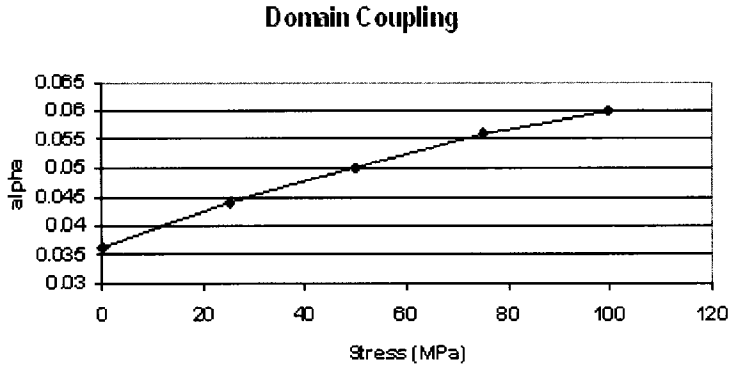

Figure 3.21 Domain coupling α under different stresses for the cold-worked nickel sample.

It can be seen that all the parameters increase almost linearly with stress within a range of applied stress. The most interesting thing is the domain coupling parameter, because it can be seen that the linear relationship does not always hold with respect to stresses. The domain coupling is on the other hand a piecewise linear function of stress within different ranges. The reason for the change of domain coupling is the change of stress dependent components of magnetostriction, according to Equation (2.13). Domain coupling is proportional to $d\lambda/dM$. So according to Equation (2.13), the situation is more complicated, since λ will depend on M whereas the differential equation of M is an function of λ and therefore M is an implicit function of itself. Keeping this in mind, a suggested explanation is as the stress increases, the stress related components (γ_{12} and γ_{22} in this study) become the dominant components of the magnetostriction. After that point, the stress dependent components dominate the magnetostriction all the way until the stress changes the sign.

Based on the evidence, the model theory can be modified by including the stress dependence of the model parameters which are mentioned above. That is to say, not only domain coupling affects the hysteresis loop under various stresses, but also other parameters do. However, in-depth study of the physical meaning of the relationship between these parameters and stress is needed. For example, what the linear function is within some stress range for different materials remains unsolved.

CHAPTER 4. THE MAGNETOMECHANICAL EFFECTS

This chapter investigates the previous model theory of the changes in magnetization that a ferromagnetic material undergoes when subjected to an applied uniaxial stress. The magnetomechanical effects are different from that of the changes in the hysteresis curve under a series of constant applied stresses, which was introduced in chapter 2.

The magnetomechanical effect can be defined as the change of magnetization of a magnetic material resulting from the application of stress. It is related to many technological phenomena such as the observation of previous unmagnetized large structures to become magnetized when stressed in the presence of the earth's magnetic field. The magnetomechanical effects can be used in magnetoelastic stress or torque sensors which are made of magnetic materials for non-destructive evaluation applications. The tendency of magnetized materials to have their magnetization reduced after stressing and applications of magnetic field is also attractive in industry.

Following the general introduction of the magnetomechanical effects, the previous model theories of magnetomechanical effects are discussed. These involve the so called effective field theory and the law of approach. The concept of reversible and irreversible magnetization is also explained in this chapter.

4.1 Introduction to the magnetomechanical effects

Figure 4.1 is a typical curve of the changes of magnetic induction depending on the change of applied stress. Under a constant magnetic field, when the material (nickel in this example) is subjected to stress, whether tensile or compressive, the material's magnetic induction or magnetization will change accordingly. Although the changes in magnetization are not as large as the changes caused by applied magnetic field, they are the characteristics of magnetostrictive materials. So if it is applied to a sensor, the sensor can tell the stress applied on some material, which is a very useful technique for non-destructive evaluation of mechanical conditions of engineering components or structures.

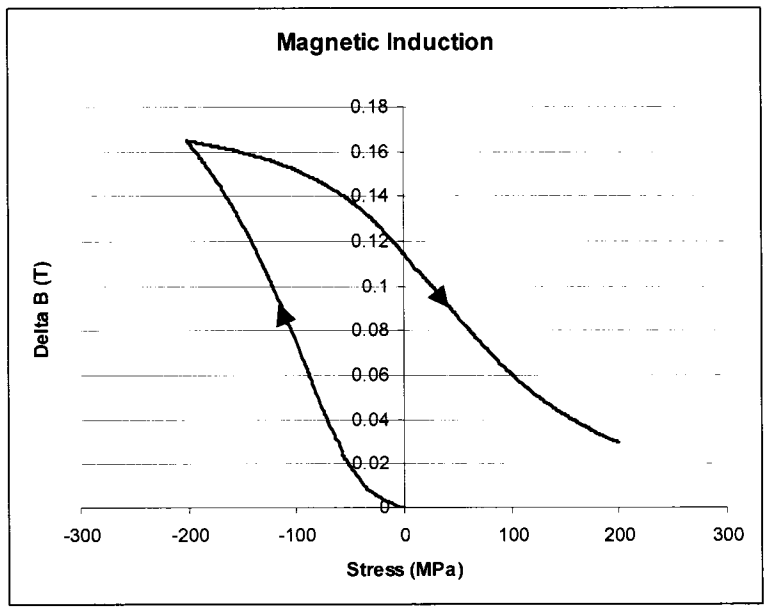

Figure 4.1 Typical changes in magnetic induction versus applied stress curve.

The investigation on this phenomenon was continued for many years, but it was never adequately explained. In recent years there has been a resurgence of interest in the

problem. This work gives a further study on this problem. Basically, the magnetization process in ferromagnetic materials is hysteretic and therefore inherently irreversible in nature, although reversible changes in magnetization are superposed on the irreversible changes. It has been proposed that the change in magnetic induction under varying stress might be proportional to the displacement of the initial magnetic induction from the anhysteretic magnetic induction. A better understanding of reversible and irreversible changes of stress induced magnetization will be a good beginning of this topic.

On the other hand, computer modeling and simulation of the behavior of magnetic materials is becoming feasible due to the ever increasing computation power, although it still remains a challenging task because of the complex nature of the phenomenon. Simulations of the magnetic hysteresis and magnetomechanical responses of materials is also increasingly important in nondestructive evaluation to aid interpretation of magnetic NDE measurement result and design of magnetoelastic stress on torque sensors for NDE application.

4.2 Previous model theories of magnetomechanical effects

4.2.1 Effective field theory

Recent research has shown that the magnetization curves of materials can be modeled in a variety of configurations [23]. In addition stress, whether uniaxial [41] or torsional [42], strongly affects the measured magnetic properties. This is the main content of chapter 4 and 5. The effect of stress on magnetization can be described as a

perturbation of the magnetic field, since the stress affects the orientation of magnetic moments through the magnetoelastic coupling [21].

As shown in previous research [43], an applied uniaxial stress σ acts in some respects like an applied magnetic field operating through the magnetostriction λ. This additional 'field' H_σ can be described by considering the energy A of the system along the reversible anhysteretic magnetization curve, namely

$$A = \mu_0 HM + \frac{\mu_0}{2}\alpha M^2 + \frac{3}{2}\sigma\lambda + TS, \tag{4.1}$$

where T is temperature, S is entropy and $\mu_0\alpha M^2/2$ is the self-coupling magnetic energy. The dimensionless term α has been defined previously in chapter 2 and represents the strength of the coupling of the individual magnetic moments to the magnetization M. The effective magnetic field causes a change in magnetization, and therefore is determined by the derivative of this energy with respect to magnetization M. The derivative of entropy with respect to bulk magnetization M in a ferromagnet will be negligible in the cases under consideration because the fields applied here do not increase the ordering within the domain, although they change the direction of domain magnetization and hence do lead to a change in the bulk magnetization M. Therefore the effective field is given by

$$H_{eff} = \frac{1}{\mu_0}\frac{dA}{dM} = H + \alpha M + \frac{3}{2}\frac{\sigma}{\mu_0}\frac{d\lambda}{dM}. \tag{4.2}$$

This means that a correction needs to be made to the anhysteretic magnetization as a result of the application of stress. In the case in which the applied stress σ_0 is not co-axial with the direction along which λ and M are measured, the stress σ used in Equation

(4.2) is simply the component of applied stress along this direction. For isotropic materials this is given by

$$\sigma = \sigma_0\left(\cos^2\theta - \nu\sin^2\theta\right), \tag{4.3}$$

where θ is the angle between the axis of the applied stress σ_0 and the axis of the magnetic field H, and ν is Poisson's ratio. So the total effective field H_{eff}, including the stress contribution, can be represented as

$$H_\sigma = \frac{3}{2}\frac{\sigma}{\mu_0}\frac{d\lambda}{dM}, \quad H_{eff} = H + \alpha M + H_\sigma, \tag{4.4}$$

where the effects of stress have been incorporated into the equivalent effective field. That is to say the stress on the magnetization can be considered as an effective field which can be derived from thermodynamics as the derivative of the appropriate free energy with respect to the magnetization,

$$H_\sigma = \frac{3}{2}\frac{\sigma_0}{\mu_0}\left(\frac{d\lambda}{dM}\right)\left(\cos^2\theta - \nu\sin^2\theta\right), \tag{4.5}$$

where σ_0 is the stress which is negative for compression and positive for tension, λ is the magnetostriction, M is the magnetization of the material, and μ_0 is the permeability of free space. This equation can be used under suitable conditions for the description of uniaxial, multiaxial and torsional stresses on anhysteretic magnetization.

Then the total effective field H_{eff}, including the stress contribution, is

$$H_{eff} = H + \alpha M + \frac{3}{2}\frac{\sigma_0}{\mu_\circ}\left(\frac{d\lambda}{dM}\right)_\sigma(\cos^2\theta - \upsilon\sin^2\theta) \tag{4.6}$$

Therefore, if the magnetostriction λ can be described as a function of magnetization and stress, H_σ can be determined. The anhysteretic magnetization at field H and stress σ is identical to the anhysteretic at field $H+H_\sigma$ and zero stress. In other words, this theory says that the change in energy of the magnetization in a particular direction can be described either in terms of the stress or, equivalently, in terms of the effective magnetic field that causes the same change in energy. This requires a description of the bulk magnetostriction, which depends on the domain configuration throughout the material.

Figure 3.8 in chapter 3 shows a typical curve of magnetostriction versus magnetization. Based on symmetry, an empirical model for magnetostriction is given by the theory as

$$\lambda = \sum_{i=1}^{\infty} \gamma_i M^{2i} . \tag{4.7}$$

An approximation to the magnetostriction by including the terms up to $i = 1$, this gives

$$H_{eff} = H + \alpha M + \frac{3\gamma_1 \sigma_0}{\mu} (\cos^2 \theta - \upsilon \sin^2 \theta) M . \tag{4.8}$$

The detailed description of stress dependent magnetostriction can be found in chapter 2. A more sophisticated approach to describing the magnetostriction curve, which includes hysteresis, has been given by Sablik and Jiles [28]. Improvements to the description of the magnetostriction as a function of magnetization can also be achieved by the inclusion of higher order terms in Equation (4.7).

However this "effective field theory" has its limitations. Experimental results of Craik and Wood are shown in Figure 4.2 (which is taken from Figure 5 of [44]). At zero stress, the slope of the magnetic induction versus stress curve is positive, either on the positive stress side or the negative stress side.

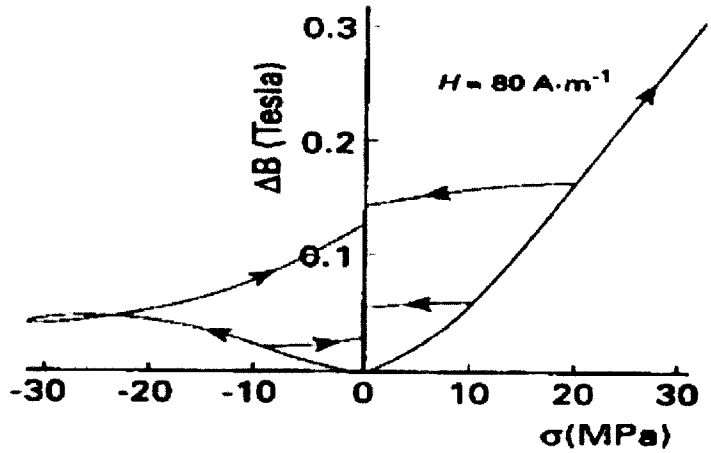

Figure 4.2 The variation in magnetic induction B with stress for a specimen of mild steel, after Craik and Wood [44]. The slope at zero stress is positive.

Figure 4.3 is the calculated result based on Equation (4.8) which uses the effective field theory. From this figure, we can see that the slope of magnetization versus stress curve at zero stress is zero, which is not in total agreement with experimental results.

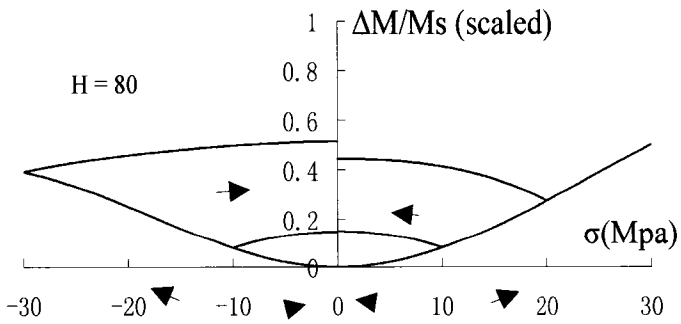

Figure 4.3 Calculated result using effective field theory. Under conditions similar to those employed in reference [44].

In many cases the stress can be included in the form of a perturbation to the magnetic field. The key to this description is to provide a means by which both magnetic field and stress can be treated similarly in the equations. However not all magnetomechanical behavior can be explained by the effective field theory. For example, at larger stresses this approximation is no longer valid since magnetic field and stress have different effects on magnetization.

4.2.2 Stress-dependent irreversible and reversible magnetizations

The energy lost to domain wall pinning is expressed as a function of the irreversible change in magnetization M_{irr} by the equation [40]

$$E_{pin}(M_{irr}) = \frac{n\langle \varepsilon_\pi \rangle}{2m} \int_0^{M_{irr}} dM_{irr} , \tag{4.9}$$

where n is the number density of pinning sites, $<\varepsilon_\pi>$ is the average pinning energy of the sites for 180° domain walls, and m is the magnetic moment of a typical domain. The hysteresis equation for irreversible changes in magnetization can be derived and can be shown to be

$$M_{irr} = M_{an} - \frac{\delta n\langle \varepsilon_\pi \rangle}{\mu_o 2m} \frac{dM_{irr}}{dH_e} , \tag{4.10}$$

where H_e is the effective field (it is different from the H_{eff} in 4.2.1), defined as

$$H_e = H + \alpha M , \tag{4.11}$$

and δ is a directional parameter having the value +1 for $dH/dt > 0$ and -1 for $dH/dt < 0$.

In previous work [21], it has been shown that the reversible component of magnetization M_{rev} reduces the difference between the prevailing irreversible magnetization M_{irr} and the anhysteretic magnetization M_{an} at the given field strength. This can be expressed as

$$M_{rev} = c\left(M_{an} - M_{irr}\right), \tag{4.12}$$

where M_{an} is the anhysteretic magnetization and M_{irr} is the irreversible magnetization, which is achieved when all domain walls are returned to their planar condition and all reversible rotations of domain magnetizations are relaxed back to zero. The coefficient c describes the flexibility of the magnetic domain walls.

It has been found in previous studies [44, 45, 46] that the direction of the change in magnetization with applied stress is independent of the sign of the stress for small stresses when the magnetization is sufficiently distant from the anhysteretic. This means that the direction of change is not directly dependent on the stress, but rather on some other related quantity, which is independent of the sign of the stress. A reasonable hypothesis [21] is to consider the elastic energy per unit volume W supplied to the material by the changing applied stress.

$$W = \frac{\sigma^2}{2E}, \tag{4.13}$$

where E is the relevant elastic modulus. It may reasonably be anticipated that some of this elastic energy causes unpinning of domain walls.

This equation can be transformed into a derivative with respect to stress σ. From Equation (4.13) the differential of the elastic energy dW is given by

$$dW = (\frac{\sigma}{E})d\sigma . \tag{4.14}$$

Equation (4.12) can then be differentiated with respect to the elastic energy W supplied to the material as a result of applied stress

$$\frac{dM_{rev}}{dW} = c\left(\frac{dM_{an}}{dW} - \frac{dM_{irr}}{dW}\right), \tag{4.15}$$

and based on the law of approach, in which the magnetization moves irreversibly towards the anhysteretic on application of stress,

$$\frac{dM_{irr}}{dW} = \frac{1}{\xi}(M_{an} - M_{irr}), \tag{4.16}$$

where ξ is a coefficient with dimensions of energy per unit volume, which relates the derivative of irreversible magnetization with respect to elastic energy to the displacement of the irreversible magnetization from the anhysteretic magnetization. The derivative of the total magnetization with respect to the elastic energy is then obtained by summing the irreversible and reversible components from Equation (4.15) and (4.16):

$$\frac{dM}{dW} = \frac{(1-c)}{\xi}(M_{an} - M_{irr}) + c\frac{dM_{an}}{dW} . \tag{4.17}$$

Considering Equation (4.14), therefore Equation (4.17) becomes

$$\frac{dM}{d\sigma} = \frac{1}{\varepsilon^2}\sigma(1-c)(M_{an} - M_{irr}) + c\frac{dM_{an}}{d\sigma}, \tag{4.18}$$

and Equation (4.16) can be written as

$$\frac{dM_{irr}}{d\sigma} = \frac{1}{\varepsilon^2}\sigma(M_{an} - M_{irr}), \tag{4.19}$$

where $\varepsilon = (E\xi)^{1/2}$ is a coefficient that has the dimensions of stress.

This equation can predict the measurement data under some circumstances, but is not always correct in general. So, it needs to be modified to accurately describe the experimental data.

Figure 4.4 is a calculated result based on Equation (4.18) and (4.19). The slope of the magnetization versus stress curve is zero at zero stress. This does not occur very often in practice and is not a general result. In other words, this model equation needs to be modified in order to give predictions that are in agreement with observations.

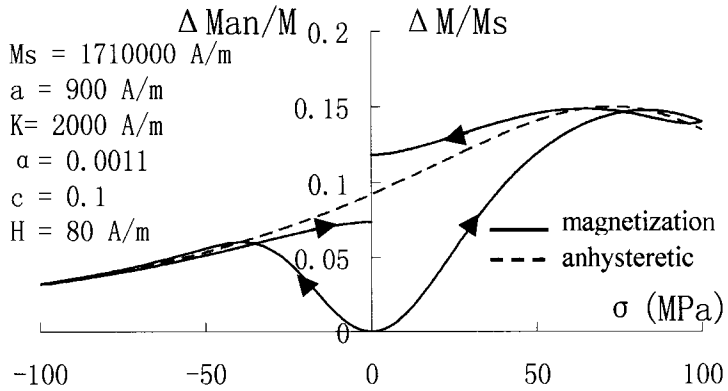

Figure 4.4 The calculated variation of magnetization with stress under conditions similar to those employed in reference [44]. The slope at zero stress is zero.

4.2.3 Extension of this hypothesis

Many works are concerned with improving the modeling of magnetization changes under constant magnetic field and varying stress, i.e. the so called $H-\sigma$ process. Viable modeling of these processes can allow us to predict the behavior of magnetic materials under stress.

As mentioned previously [47] in Figure 4.5, it is seen that the computed magnetization near zero stress appears to increase in unlimited fashion rather than ultimately tending to a limiting hysteretic pattern, as seen experimentally [48, 49, 50]. Also the slope of the magnetization versus stress curve is zero at zero stress.

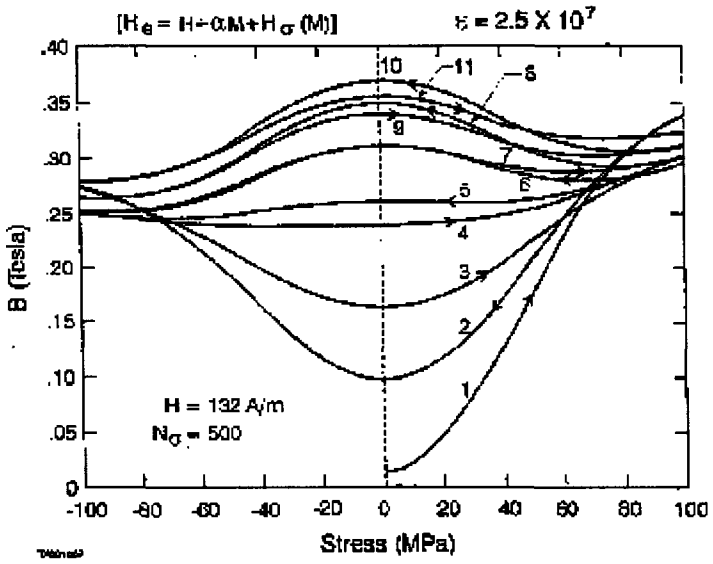

Figure 4.5 Variation of the magnetization according to the original magnetomechanical model after repeated stress cycling at constant field *H*. The numbers represent the magnetization curve obtained during each succeeding leg of the stress variation (cited from [47]).

Previous study [21] gives two possible approaches to generalizing the model that seem reasonable. The first one is proposed to use two different relaxation constants, ξ_a and ξ_r, with $\xi_r > \xi_a$ (i.e., ε_a and ε_r, with $\varepsilon_r > \varepsilon_a$), as seen by the following equations,

$$\frac{dM}{d\sigma} = \frac{1}{\varepsilon_a^{\,2}}\sigma(1-c)(M_{an} - M_{irr}) + c\frac{dM_{an}}{d\sigma}, \tag{4.20}$$

$$\frac{dM}{d\sigma} = \frac{1}{\varepsilon_r^{\,2}}\sigma(1-c)(M_{an} - M_{irr}) + c\frac{dM_{an}}{d\sigma}. \tag{4.21}$$

The physical concept for this is that stress application (denoted by a) is different from stress release (denoted by r). Stress application (i.e. increasing stress) essentially "reshapes" domain boundaries, causing some irreversible wall movement and some bowing of domain walls. Of the walls that move, some get so strongly pinned that they do not move on stress release (i.e. decreasing stress). Wall reshaping is therefore different on stress release, implying a different relaxation constant, ξ or ε, for the release process.

By using this revised model, the limiting stress hysteresis loop for magnetization is approached very quickly in some cases. In others, it is approached more slowly or not quite reached. Clearly, the behavior seen experimentally can now be produced by the revised version of the model, at least qualitatively, but not always.

The second approach introduces a "turning point stress" in Equation (4.19), i.e. it is the stress that existed the last time the sign of the changing stress was changed.

$$\frac{dM}{d\sigma} = \frac{1}{\varepsilon^2}(\sigma - \sigma_o)(1-c)(M_{an} - M_{irr}) + c\frac{dM_{an}}{d\sigma} \tag{4.22}$$

It can be seen that a limiting stress hysteresis loop is again approached using this second revised model. The limiting loop does not show quite as much hysteresis as the first revised model. However, it is still possible to produce cases where the magnetization quickly goes to the limiting behavior, more slowly approaches the limiting behavior, or does not quite reach the limiting behavior after several cycles of applying stress. Thus, qualitatively, the second model also exhibits agreement with behavior seen experimentally to some extent.

However, these two approaches have their difficulties respectively. The first one uses different relaxation constants which add extra dimensions to this problem and is difficult to justify. One problem with the second approach is that it would imply that

$$dW = [(\sigma - \sigma_o)/E]d\sigma, \tag{4.23}$$

$$dM_{irr} = \frac{(\sigma - \sigma_o)d\sigma}{\varepsilon^2}(M_{an} - M_{irr}), \tag{4.24}$$

and if σ is decreasing ($d\sigma<0$) from σ_{max} , then with $\sigma > 0$ and $M_{an} > M_{irr}$, it follows that dM_{irr} is positive and M_{irr} continues to approach M_{an}. Although it gives good practical results, the reformulation is hard to physically justify, because if we take algebraic integral with respect to σ for Equation (4.23), it will imply $W = \frac{(\sigma - \sigma_o)^2}{2E}$ which can not be easily explained.

This work also does some extended study on the original model. The detailed works are stated as follows.

The Rayleigh law, which describes hysteretic behavior in magnetization at low field strengths, can be expressed as

$$M = \chi_a H \pm \eta H^2, \tag{4.25}$$

where for the initial magnetization curve χ_a is the initial susceptibility and η is called the Rayleigh constant; + for positive field, - for negative field.

Rayleigh also showed that the hysteresis loop was composed of two parabolas:

$$M = (\chi_a - \eta H_-)H + \frac{\eta}{2}(H^2 - H_-^2), \tag{4.26}$$

$$M = (\chi_a + \eta H_+)H - \frac{\eta}{2}(H^2 - H_+^2), \tag{4.27}$$

where Equation (4.26) and (4.27) present ascending and descending portions of the loop, respectively. H_+ and H_- are the maximum fields applied. These equations are the same except for the sign change on the quadratic term and the sign change on the linear term. When the value of H is reduced to zero, the remnant magnetization on the descending (upper) branch is $M_{R+} = \frac{1}{2}\eta H_+^2$ while on the ascending (lower) branch it is $M_{R-} = -\frac{1}{2}\eta H_-^2$.

From Equation (4.25), we will have $M_+ = \chi_a H_+ + \eta H_+^2$ and $M_- = \chi_a H_- - \eta H_-^2$ where M_+ and M_- are the magnetization at maximum applied magnetic field H_+ and H_- respectively.

Substituting these into Equation (4.26) and (4.27), we obtain

$$M - M_+ = \chi_a (H - H_+) - \frac{\eta}{2}(H - H_+)^2, \tag{4.28}$$

$$M - M_- = \chi_a (H - H_-) + \frac{\eta}{2}(H - H_-)^2. \tag{4.29}$$

According to Brown [43] the effect of stress on magnetization can be expressed using an equation that is very similar to the Rayleigh law. In Figure 4.6 this derivation the fractional change in volume as a result of stress-induced domain wall motion is

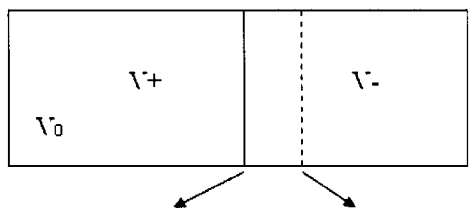

Figure 4.6 The simplest case of spin-up and spin-down domains.

$$\Delta V = \frac{V - V_0}{V_{tot}} = \alpha|\sigma| + \beta\sigma^2, \tag{4.30}$$

where V_0 is the original volume before any domain wall movement and V_{tot} is the total volume of the sample; α and β are constants depending on domain wall type. From this, in the simplest case of spin-up and spin-down domains, it is easily shown [51] that

$$\Delta M = 2M_s\Delta V. \tag{4.31}$$

Therefore if there is a change in volume of the domains ΔV a corresponding change of magnetization ΔM occurs. Beginning from these definitions and Equation (4.31), we can see that the equivalent expression for the change in magnetization is

$$\Delta M = 2M_s(\alpha|\sigma| + \beta\sigma^2). \tag{4.32}$$

This equation is true whether stress is increasing in the positive direction (tension) or the negative direction (compression). So when σ = 0, ΔM = 0 and ΔV = 0 which is the starting condition. Subsequently change in magnetization can be represented as change of ΔM.

From this we can develop equations for the stress dependence of magnetization in the Rayleigh region. Consider the similarity between Brown's hypothesis (Equation (4.30)) and the Rayleigh law (Equation (4.25)), when the stress is being reduced from σ_+ along the descending branch, referring to Equation (4.26), the equation governing this is

$$\Delta M - \Delta M_+ = 2M_s\left[\alpha(|\sigma - \sigma_+|) - \frac{\beta}{2}(\sigma - \sigma_+)^2\right], \tag{4.33}$$

when the stress is being reduced from σ_- along the ascending branch, referring to Equation (4.29), the equation governing this is

$$\Delta M - \Delta M_{-} = 2M_s\left[\alpha(|\sigma - \sigma_{-}|) + \frac{\beta}{2}(\sigma - \sigma_{-})^2\right], \tag{4.34}$$

where ΔM_{+} and ΔM_{-} represent the change of magnetization at the maximum tensile and compressive stresses respectively.

There is an important difference between this stress dependent equation and the normal field dependent Rayleigh region equation. In particular, these ΔM-σ curves are actually symmetric, unlike the analogous curve of magnetization versus field. Also when the value of σ is reduced to zero, the remanent magnetization on the descending (upper) branch is $\Delta M_{R+} = \frac{2M_s}{2}\beta\sigma_{+}^{2}$ while on the ascending (lower) branch it is $\Delta M_{R-} = \frac{2M_s}{2}\beta\sigma_{-}^{2}$.

Based on the above equations, a hypothesis which is unjustified yet can be further shown that the elastic energy per unit volume W supplied to the material by the changing applied stress is given by

$$W = \eta\,|\,\sigma\,| + \frac{\sigma^2}{2E}, \tag{4.35}$$

where E is the relevant elastic modulus and η is a coefficient which denotes the rate at which magnetization approaches the anhysteretic magnetization.

This equation can be transformed into a derivative with respect to stress σ. From Equation (4.35) the differential of the elastic energy dW is given by

$$dW = (\eta + \frac{\sigma}{E})d\sigma \qquad \sigma \geq 0, \tag{4.36}$$

$$dW = (-\eta + \frac{\sigma}{E})d\sigma \qquad \sigma < 0. \tag{4.37}$$

Equation (4.12) can then be differentiated with respect to the elastic energy W supplied to the material as a result of applied stress:

$$\frac{dM_{rev}}{dW} = c\left(\frac{dM_{an}}{dW} - \frac{dM_{irr}}{dW}\right), \tag{4.38}$$

and based on the law of approach, there is also

$$\frac{dM_{irr}}{dW} = \frac{1}{\xi}\left(M_{an} - M_{irr}\right), \tag{4.39}$$

where ξ is a coefficient with dimensions of energy per unit volume, which relates the derivative of irreversible magnetization with respect to elastic energy to the displacement of the irreversible magnetization from the anhysteretic magnetization. The derivative of the total magnetization with respect to the elastic energy is then obtained by summing the irreversible and reversible components from Equation (4.38) and (4.39):

$$\frac{dM}{dW} = \frac{(1-c)}{\xi}\left(M_{an} - M_{irr}\right) + c\frac{dM_{an}}{dW}. \tag{4.40}$$

Considering Equation (4.36) and (4.37), therefore Equation (3-27) now becomes

$$\frac{dM}{d\sigma} = \frac{1}{\varepsilon^2}(1-c)(M_{an} - M_{irr})(\sigma \pm \eta E) + c(\frac{\sigma}{E} \pm \eta)\frac{dM_{an}}{d\sigma}, \tag{4.41}$$

where M_{an} is the anhysteretic magnetization, σ is the stress, M_{irr} presents the irreversible component of magnetization , E is the relevant elastic modulus, c describes the flexibility of the magnetic domain walls. ε has been defined previously [45], η is a coefficient which represents irreversible change in the magnetization with the action of a stress [46]. Equation (4.39) can then be written as

$$\frac{dM_{irr}}{d\sigma} = \frac{1}{\varepsilon^2}(M_{an} - M_{irr})(\sigma \pm \eta E), \tag{4.42}$$

where $\varepsilon = (E\xi)^{1/2}$ is a coefficient that has dimensions of stress.

Both Equation (4.41) and Equation (4.42) contain an additional term compared with Equation (4.18) and (4.19). This is due to the use of the Rayleigh law equivalent.

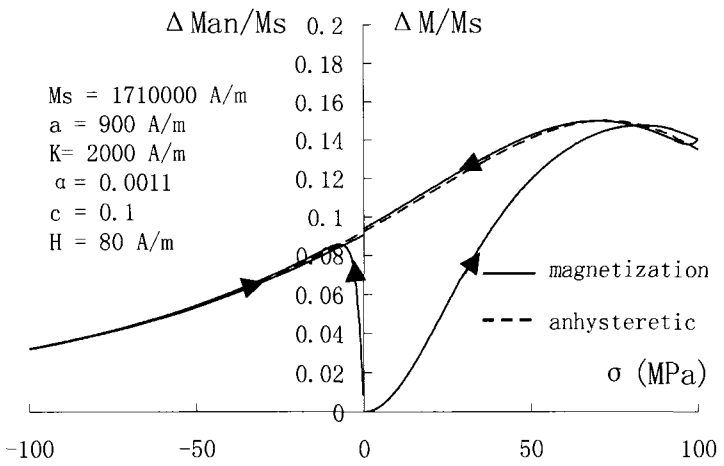

Figure 4.7 The calculated variation of magnetization with stress under conditions similar to those employed in reference [44]. The slope at zero stress is positive.

The calculated result using model Equation (4.42) is shown in Figure 4.7. At zero stress, the slope of induction versus stress curve is positive, either on the positive stress side or the negative stress side. Also it is seen that the changes of magnetization follows the stress dependent anhysteretic magnetization. This is the result of model theory.

4.3 Conclusion

In reversible cases the stress can be included in the form of a perturbation to the magnetic field, so both magnetic field and stress can be treated similarly in the equations.

This is the so called "effective field theory". Because there are irreversible and hysteretic effects, not all magnetomechanical behaviors can be explained by this simple theory. The Law of Approach model can simulate well on the initial magnetization curve, but not always so well on the descending and ascending branch on the hysteresis loop simulation in chapter 3. The model theory mentioned in chapter 4 is an extension of that in chapter 2. So one can expect that the simulation of ΔM - σ will not be good enough, especially for the reversible part of the magnetization curves. The slope $(dM/d\sigma)_{\sigma=0}$ is also not found to be zero in practice, although the previous theory of the magnetomechanical effect suggests that it should be. At larger stresses this simple approximation is no longer valid since magnetic field and stress have different effects on magnetization. So the "Effective Field Theory" and the "Law of Approach" have their limitations. Rayleigh's Law gives us a basis for improving the model theory by including both linear and non-linear terms. The "Law of Approach" is still valid under this extension because it can be modified by including the linear component into the equation. The new model equation gives results that are in better agreement both qualitatively and quantitatively with observations. But due to the limitation of Rayleigh's Law, which can only be used at low field, the extended model is still limited to the low stress region.

It can be seen that the shape of the measured ΔM vs σ curves shows a good agreement with those modeled based on the magnetomechanical theory which is the basis for further development of magnetoelastic NDE sensors. Detailed studies of the effects of these factors on magnetic measurement parameters are also essential to the development of magnetic inspection techniques for residual stress determination. The

experimental data need to be analyzed and will be validated by the magnetomechanical hysteresis model.

CHAPTER 5. MEASUREMENT AND MODELING OF MAGNETOMECHANICAL EFFECTS

It has been shown that the parameters of the anhysteretic functions of JAM model depend approximately linearly on the effective anisotropy. This can be utilized to build relationships between these phenomenological parameters and with the spontaneous magnetization and the constants of anisotropy and magnetostriction.

In this study, the magnetomechanical effects which refer to the changes of magnetization in response to varying magnetic field under constant applied stresses and their applications have been systematically investigated experimentally, theoretically and numerically. The effects of stress on magnetic properties of bulk material with both positive and negative magnetostriction have also been studied using the Jiles-Atherton modeling approach.

For comparison magnetic induction versus stress curves were measured in materials subjected to various tensile and compressive stresses within their elastic limits. The stress dependent magnetic induction signals were found to be in good agreement with the experimental results.

In order to verify if this model theory works on both hard and soft materials, measurements on the nickel and steel sample have been conducted.

5.1 Measurement of magnetic induction under stress

Figure 5.1 shows connection of equipment for measurement. The measurement is very similar to that of hysteresis measurement, except for the different measurement procedures and connection of equipment. A servo-hydraulic mechanical testing system (Model 8500, Instron, Inc.) was used to apply stress on the samples; solenoid to vary the applied magnetic field; pickup coil to collect magnetic induction signals. Both magnetic induction signal and load signal were recorded by computer. An important point to note is that the magnetic induction signal was often weak from the pick-up coil with some background noise. So a low-pass filter needs to be used to screen the noise and amplify the useful signal. The samples studied include steel and nickel. The experiment involved applying an external stress to a sample at up to 60% of the estimated yield strength in order to stay within its elastic limit.

The objective of this measurement was to perform systematic experimental studies of connection between micro-structural changes due to stress and magnetic properties of ferromagnetic Fe-based materials. The nickel rod sample is the same as in chapter 3. The stainless steel 410 is a dog-bone like sample which is also the same as in chapter 3. All the measurements were conducted within the sample's elastic limit in order to ensure a completely reversible mechanical response.

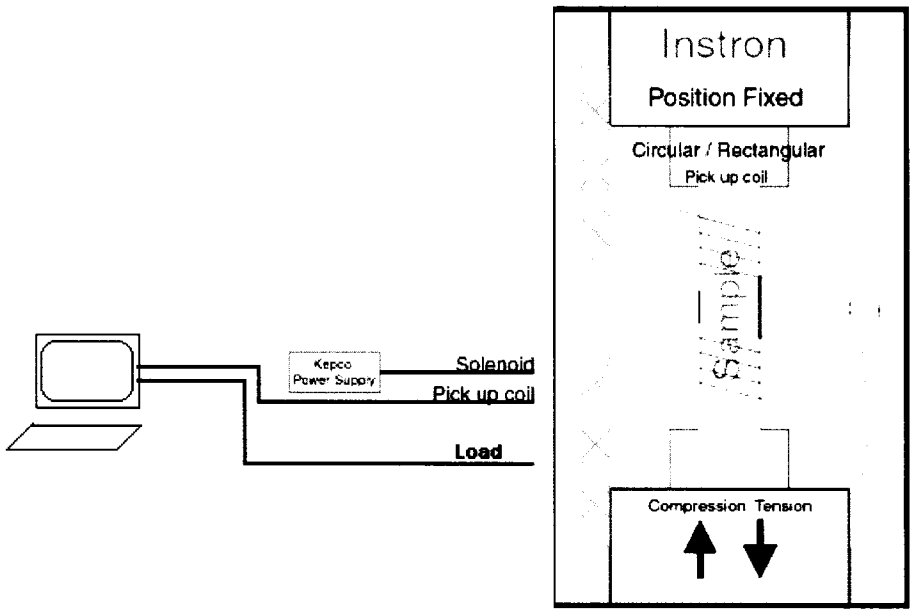

Figure 5.1 Magnetic induction versus stress curve measurement.

During the test the sample was first demagnetized using an a.c. magnetic field with decaying field amplitude. The sample was then subjected to cyclic stresses with different profiles: applying a tensile stress up to maximum stress level (different for different samples dependent on the yield strengths of the samples) and then decreasing it to zero; applying a compressive stress up to maximum stress level and then decreasing it to zero. The results are shown in Figure 5.2, Figure 5.3, and Figure 5.4 for the cold-worked, annealed nickel and 410 stainless steel samples respectively.

These stress profiles were used to investigate the stress-induced irreversible changes in magnetization, which in general is asymmetric depending on the sign of stress. The measurements were repeated under different magnetic field strengths for different samples. The output of the sensing coil was filtered and amplified before it was subjected to data analysis and storage.

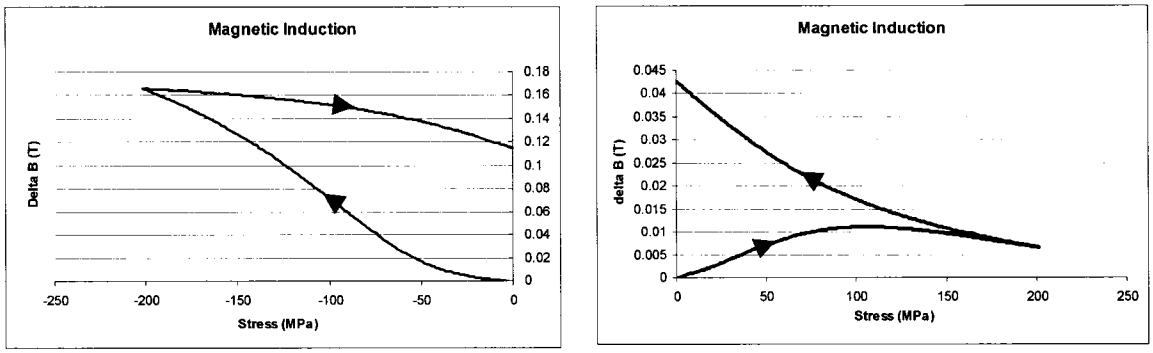

(a)

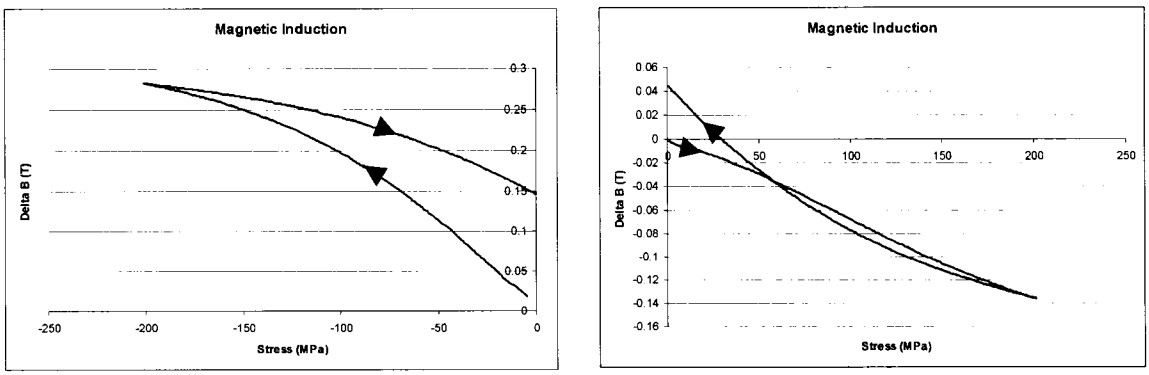

(b)

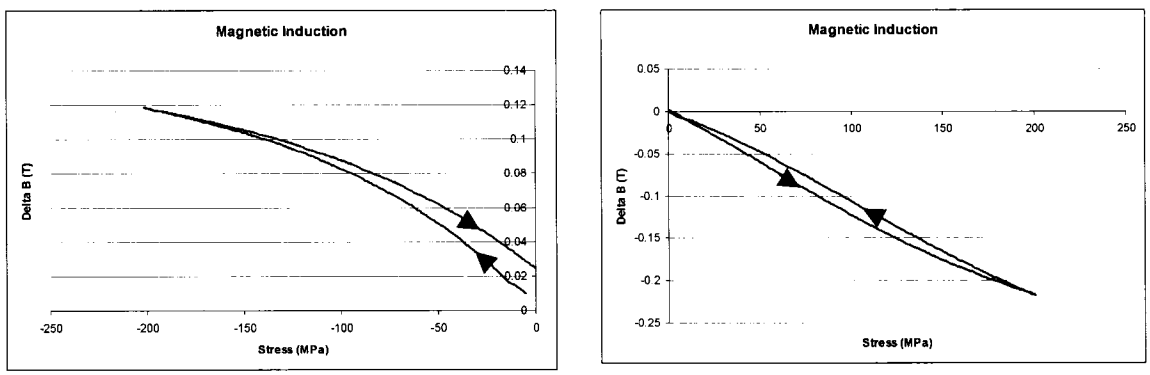

(c)

Figure 5.2 Magnetic induction versus stress for cold-worked nickel sample. The magnetic field: (a) 1kA/m, (b) 3kA/m, (c) 10kA/m.

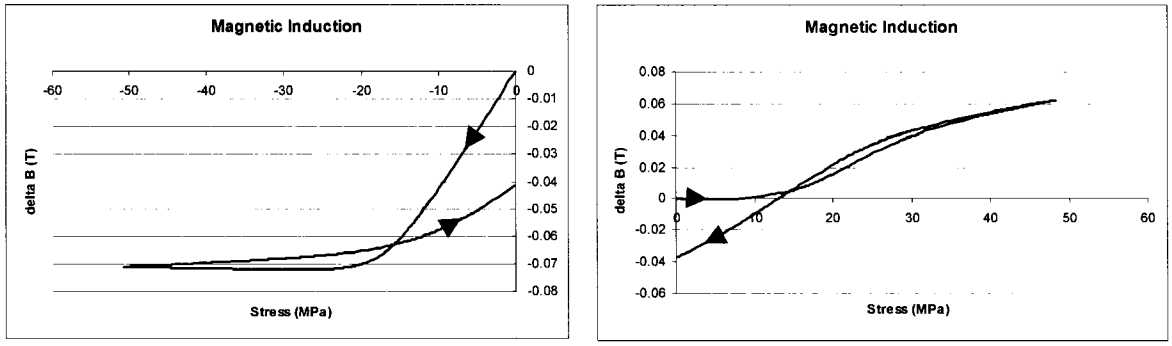

(a)

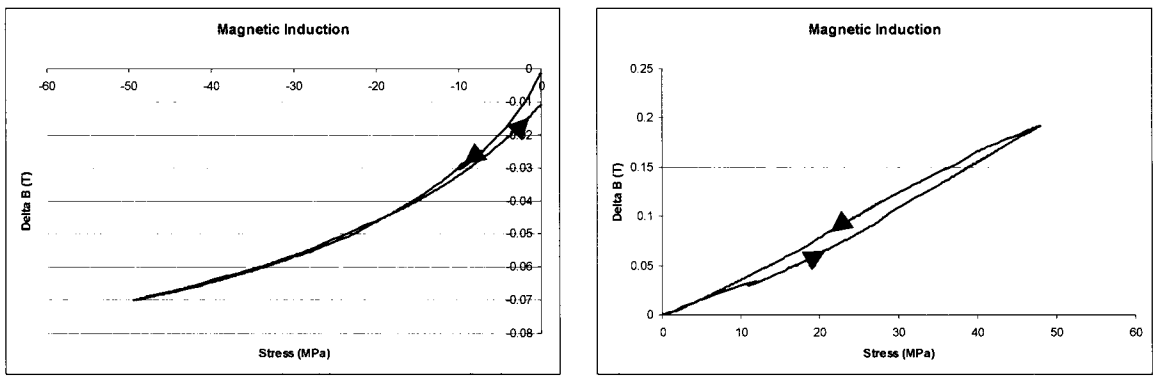

(b)

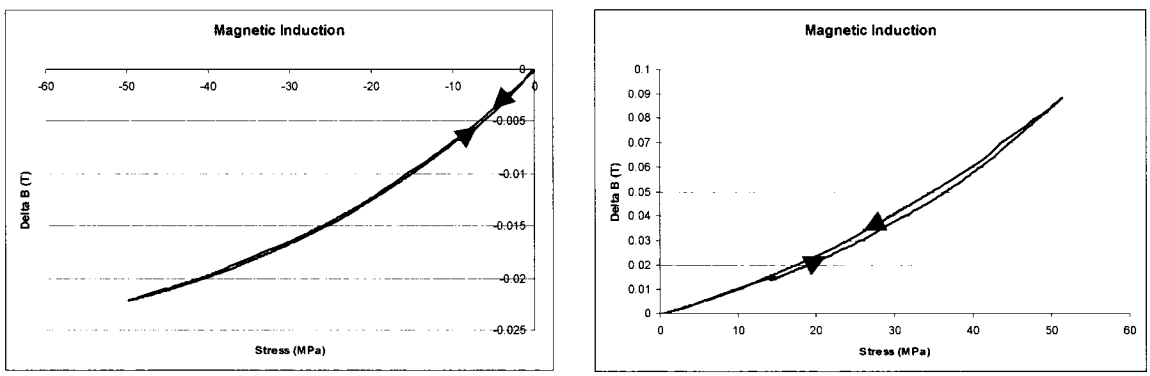

(c)

Figure 5.3 Magnetic induction versus stress for annealed nickel sample. The magnetic field: (a) 1kA/m, (b) 3kA/m, (c) 10kA/m.

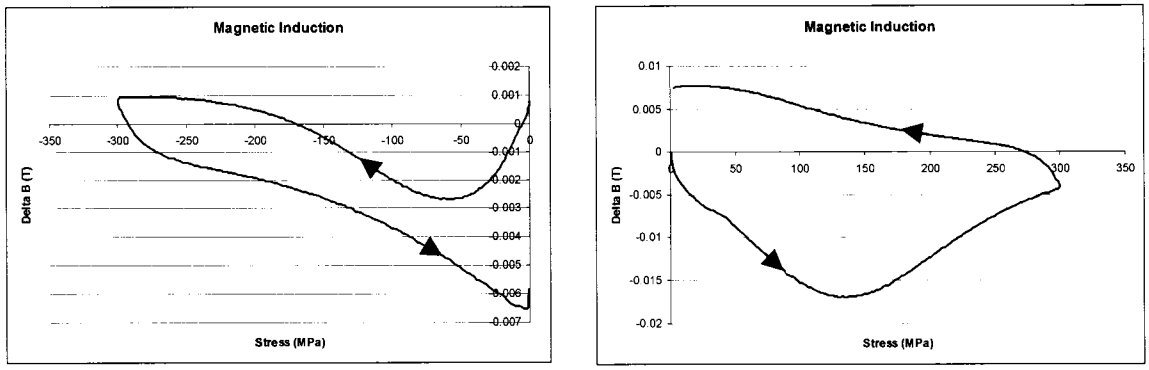

(a)

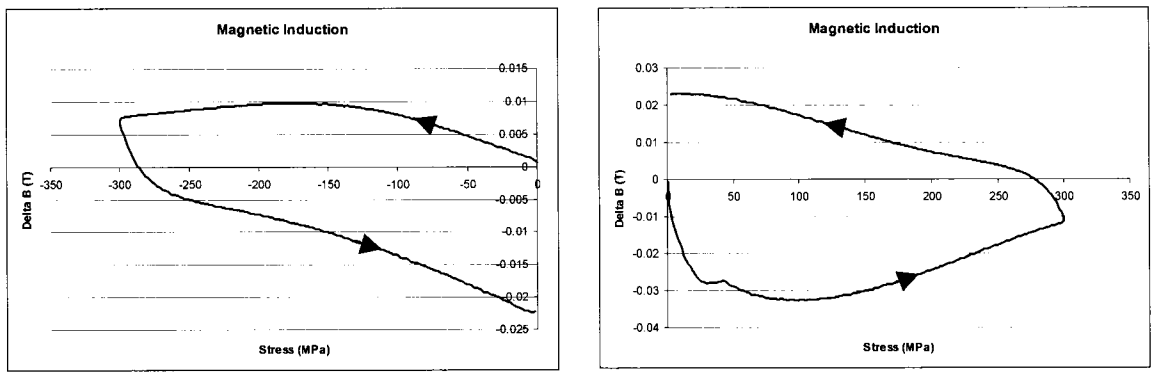

(b)

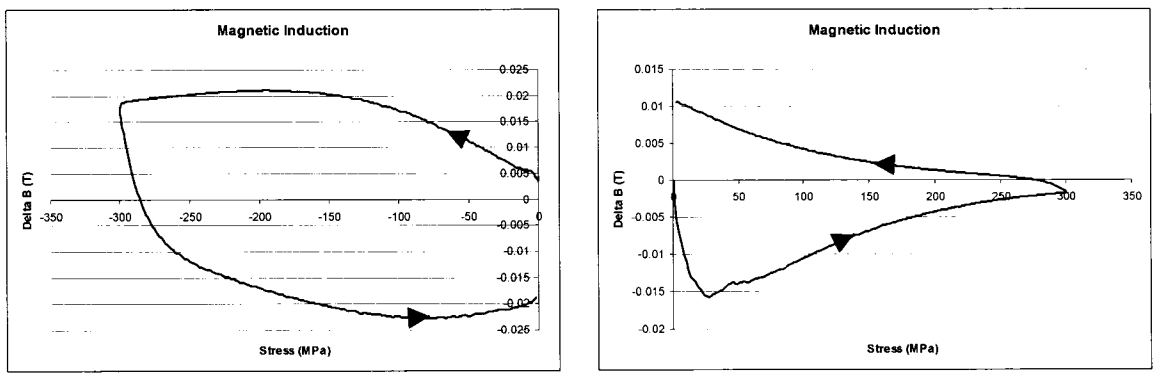

(c)

Figure 5.4 Magnetic induction versus stress for steel sample. The magnetic field: (a) 1kA/m, (b) 3kA/m, (c) 10kA/m.

5.2 Model parameter calculation

Considering the symmetric parabola shape of the typical magnetostriction curve as shown in Figure 5.5, it is reasonable to use a simplified approximation to the magnetostriction by including the power terms up to 2 in Equation (4.7) and ignoring the constant term, which is simply the elastic strain and does not play an active role in the magnetomechanical effect.

The stress-dependence of magnetostriction curve λ (M, σ) can be described in terms of the stress dependence of γ_1 and γ_2 using a Taylor series expansion as described by Equation (2.15). This can be done by the best curve fitting procedure on Figure 5.5. Then, $\gamma_{11} \sim \gamma_{22}$ can be obtained from the linear curve fitting from γ_1 and γ_2 versus stress graph, as seen in Figure 5.6.

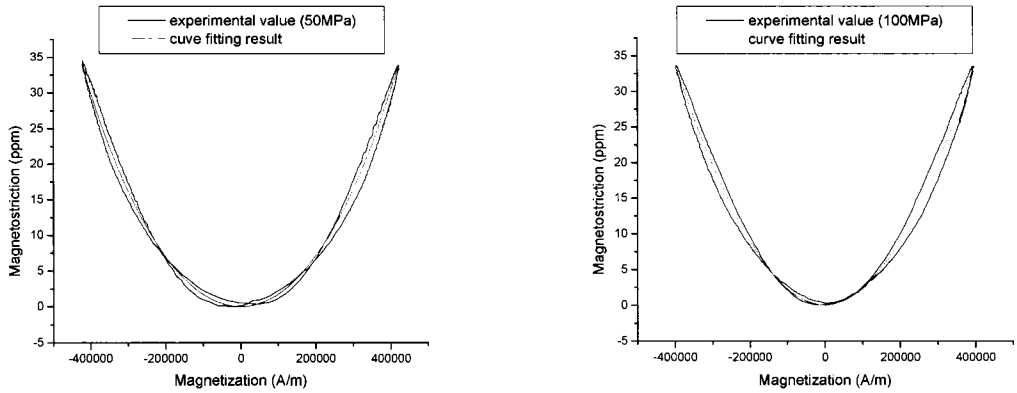

(a) cold-worked nickel

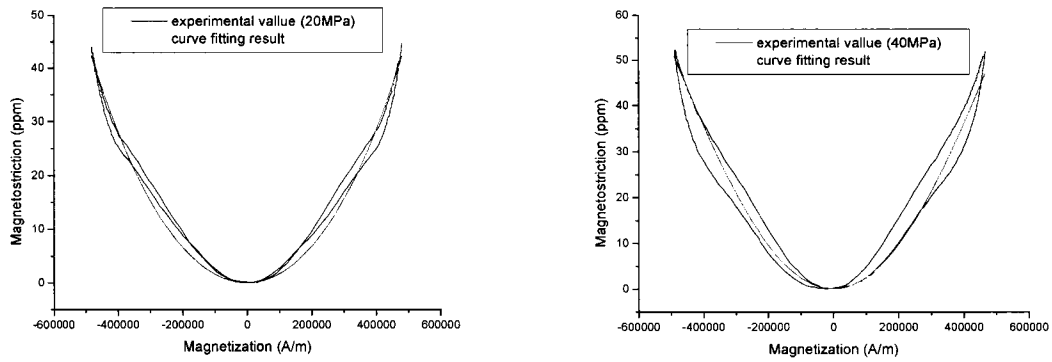

(b) annealed nickel

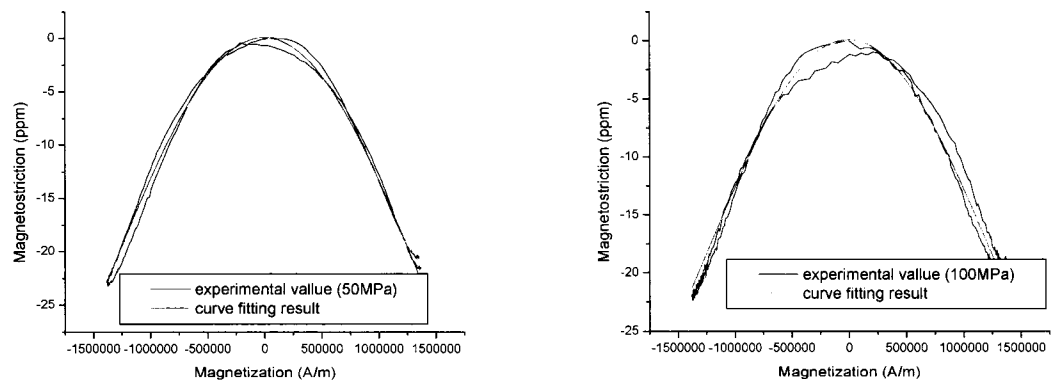

(c) steel sample

Figure 5.5 Best curve fitting results of magnetostriction against magnetization at various tensile stresses for (a) cold-worked nickel; (b) annealed nickel; (c) steel sample.

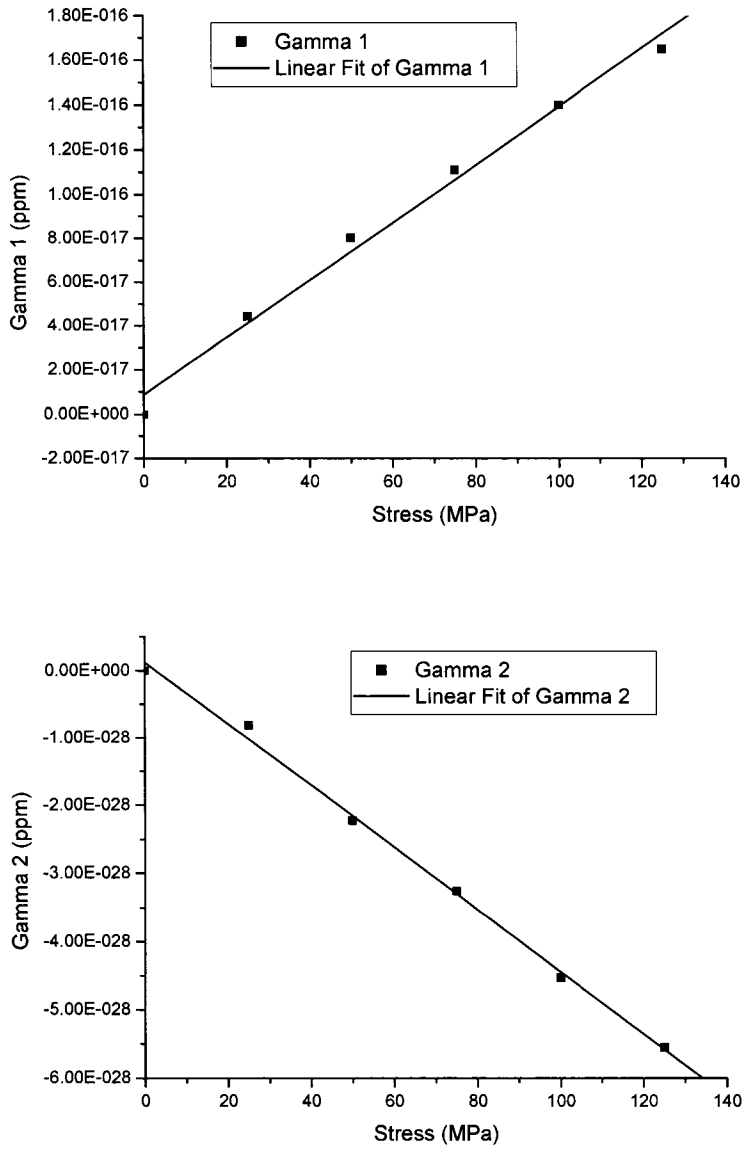

Figure 5.6 Linear curve fitting results of magnetostriction components against tensile stress for the cold-worked nickel sample.

The parameters, γ_1 and γ_2, in Equation (2.13) about magnetostriction are approximately linearly proportional to stress as shown in Figure 5.6. That is to say the hypothesis of Equation (2.15) is consistent with the experimental result. The same

procedure can be conducted on annealed nickel and steel samples. Table 5.1 shows the results obtained on these samples by this method.

Table 5.1 Linear curve fitting for $\gamma_{11} \sim \gamma_{22}$ for different samples.

Sample	γ_{11} (m^2A^{-2})	γ_{12} ($m^2A^{-2}Pa^{-1}$)	γ_{21} (m^4A^{-4})	γ_{22} ($m^4A^{-4}Pa^{-1}$)
Nickel (cold-worked)	8.51E-24	1.31E-24	1.22E-35	-4.56E-36
Nickel (annealed)	-7.21E-18	-6.11E-18	-5.01E-28	1.67E-29
Steel	1.88E-17	-6.31E-20	-2.57E-30	1.27E-32

Figure 5.7 tells how to get the required parameters from hysteresis loop. All the magnetic properties such as different susceptibilities, coercivity, and remanence can be measured from the experimental hysteresis loops. Table 5.2 shows the hysteresis model parameters obtained by the inversion algorithm from the same software package. One should note that when proceeding the simulation, the basic parameters obtained by this inverse calculation routine need to be adjusted in order to obtain a reasonable fit to the hysteresis and anhysteretic curves measured data.

It has been seen that the inversion algorithm works well for mild steel [40]. But by comparing the simulation graphs, this algorithm is not always applicable for all kinds of material, especially for the hard magnetic materials such as cold-worked nickel.

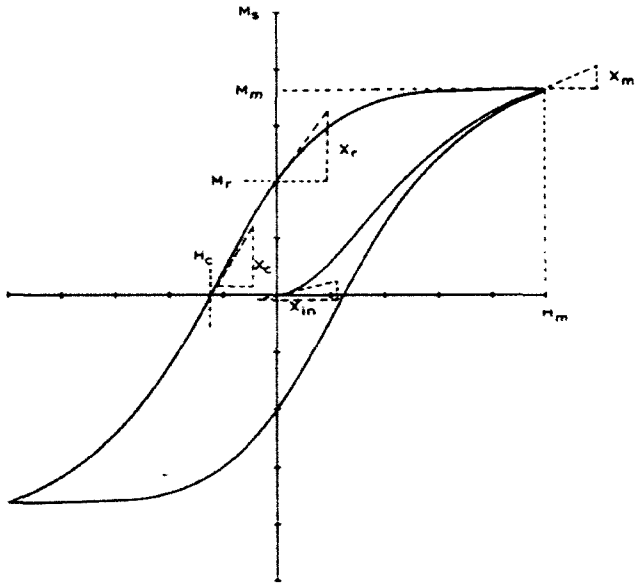

Saturation magnetizaton	M_s		
Slope of anhysterestic at the origin	χ_{an}	Field at loop tip (field maximum)	H_m
Slope of initial curve at the origin	χ_{in}	Magnetization at loop tip (maximum)	M_m
Slope at coercive point	χ_c	Slope at loop tip	χ_m
Remanence	M_r	Demagnetization factor	N
Slope at remanence	χ_r	Coercivity	H_c

Figure 5.7 The various data from the experimental hysteresis curve that are used in the parameter calculation routine.

Table 5.2 Hysteresis parameters of different samples under zero stress level.

Sample	Ms (A/m)	a (A/m)	k (A/m)	α	c
Nickel (cold-worked)	530000	6500	2700	0.036	0.1
Nickel (annealed)	530000	400	600	0.00009	0.4
410 Stainless Steel	1650000	7200	200	0.01	0.11

5.3 Model simulation results

Stress-induced changes in magnetization were simulated using the improved model equations of the magnetomechanical effect. The input model parameters were determined by measuring hysteresis loops and magnetostriction curves under various applied stresses using the Magnescope. The stress-strain curve of the sample was also measured to determine the mechanical properties such as the Young's modulus for use in the simulations.

Figure 5.8 and 5.9 show the simulations for cold-worked nickel sample under a constant magnetic field of 1kA/m. The stress effects were simulated for applied stresses up to 200MPa in both tensile and compressive direction, which were then reduced to zero. Although the model parameters are the same as those used in hysteresis loop simulations, one can see that the simulated magnetomechanical effects are not as accurate as those of hysteresis loops. One possible reason is that, as mentioned before, the linear relationship of model parameters and stress only exists within a moderate range of stress. Beyond that range, the linear relationship does not hold or another linear relationship exists. The accumulated calculation errors lead to the inaccurate results. Despite these shortcomings of the improved model, the simulation results still give us a better outcome than the previous model.

Figure 5.10 and 5.11 show the simulations for the annealed nickel sample under a constant magnetic field of 1kA/m. The stress effects were simulated up to 50MPa in both tensile and compressive direction, and then to zero. Unfortunately the reverse part of

magnetization simulation can not be obtained due to the software limitation, as that of the cold-worked nickel sample.

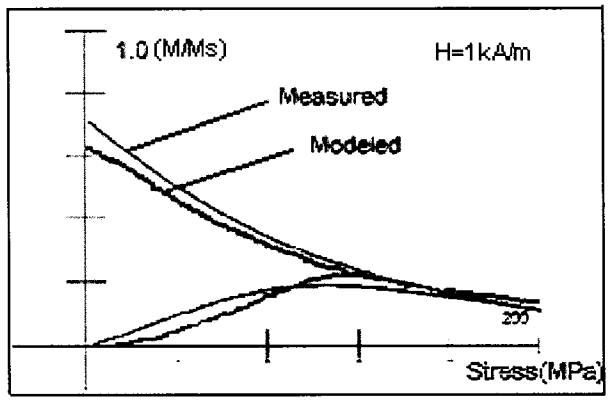

Figure 5.8 Normalized magnetization M versus stress curve for as-received nickel sample at a field of 1 kA/m along the initial magnetization curve. The nickel sample was subjected to 200 MPa first and then reduced to 0 MPa. Model parameters used: M_s = 530000 A/m, a = 6500 A/m, k = 2700 A/m, α = 0.036, c = 0.1.

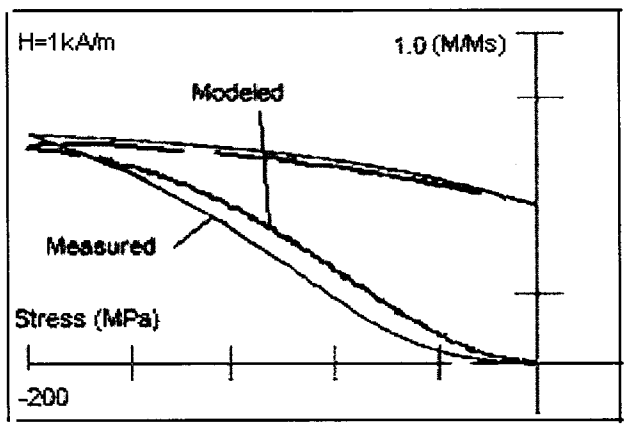

Figure 5.9 Normalized magnetization M versus compressive stress curve for as-received nickel sample at a field of 1 kA/m along the initial magnetization curve. The nickel sample was subjected to -200 MPa first

and then reduced to 0 MPa. M_s = 530000 A/m, a = 6500 A/m, k = 2700 A/m, α = 0.036, c = 0.1.

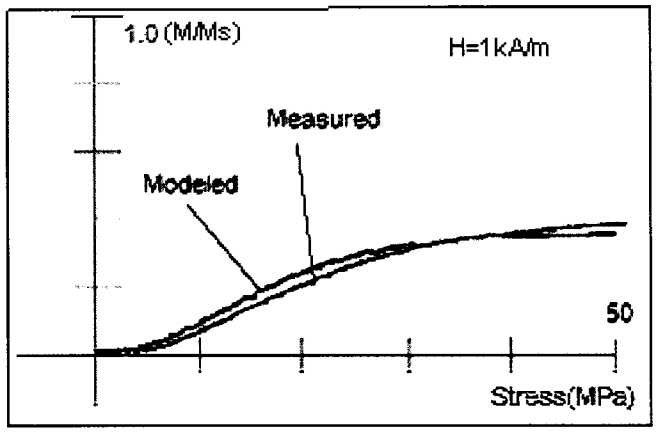

Figure 5.10 Normalized magnetization M versus stress curve for the annealed nickel sample at a field of 1 kA/m along the initial magnetization curve. The nickel sample was subjected to 50 MPa first and then reduced to 0 MPa. M_s = 530000 A/m, a = 400 A/m, k = 600 A/m, α = 0.0009, c = 0.4.

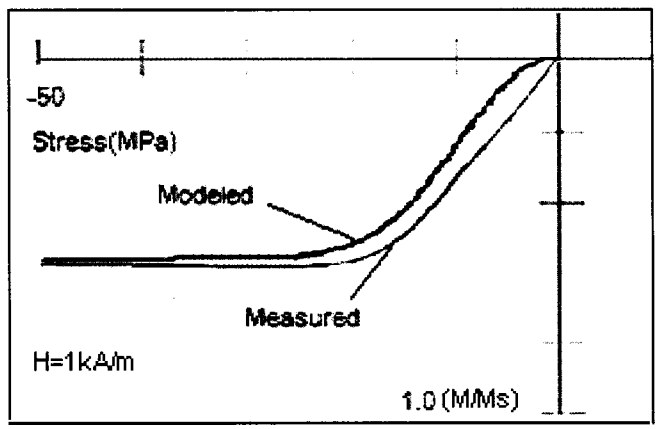

Figure 5.11 Normalized magnetization M versus stress curve for annealed nickel sample at a field of 1 kA/m along the initial magnetization curve. The nickel sample was subjected to -50 MPa first and then reduced to 0 MPa. M_s = 530000 A/m, a = 400 A/m, k = 600 A/m, α = 0.0009, c = 0.4.

Since nickel has unique properties, it has been found that the model equation can not reproduce the experimental data with full agreement. Therefore the model theory still needs to be improved, especially for the modeling parameter calculation routine and the algorithm for convergence of the theoretically predicted loop to the experimentally measured stress loop.

The relationship between model parameters and applied stress is discussed in chapter 3. Experimental data show that most parameters can be described as a linear function of stress, except for the domain coupling which is already considered to be stress dependent in the original model software. This examination has guided the development of the model theory and the simulation software correspondingly.

CHAPTER 6. CONCLUSIONS

In this study, the magnetomechanical effects and their applications had been systematically investigated experimentally, theoretically and numerically.

An accurate model description of the effects of stress on magnetic properties of materials has become increasingly important in situations where the performance characteristics of magnetic materials, such as magnetostrictive sensors or actuators, can be described and if the theoretical model is physically sound, properties and performance outside of a known range of conditions can also be successfully predicted.

The background of magnetism and other related works were introduced in each chapter. By investigating the previous model theories, this work gave a new way to modify the existing and currently used models for describing the effects of applied stresses on magnetization of materials. The previous model is based on the effective field theory and the law of approach, and used one model coefficient as stress dependent parameter. Both effective field theory and the law of approach have their limitations. The previous model works well in most common case within very limited stress levels and in low magnetic field. These limitations had been observed in the recent measurements on steel and nickel samples, including both the cold worked and annealed one.

Rayleigh's Law gives us a basis for the solution to the problems associated with our understanding of the magnetomechanical effect which arose due to disagreement between theory and observation. This idea was used in this work as the first approach to improve the previous model. The law of approach has been modified by adding a linear

component into the equation in addition to the usual quadratic term. The new model equation gives results that are in better agreement with experimental observations, especially for soft magnetic materials such as iron and mild steel. This approach can be thought as a milestone during the thorough study into the topic of the magnetomechanical effects.

However, although better results can be obtained by this approach, there are still a few problems that remain to be resolved. That is to say, the results of hysteresis and magnetomechanical simulations are unsatisfactory under high stress level.

The model of the magnetomechanical effect developed in the previous work provides the basis for describing changes of magnetization under stresses. However there is a need to further improve the model to deal with materials which have different magnetomechanical properties or anisotropy. In this study modeling studies has been performed to investigate how stress induced magnetic anisotropy affects hysteretic and anhysteretic magnetization curves as they approach saturation. The result of this work has led to a model which takes into account the stress dependence of the input model parameters. In this study we derived stress dependence of the other two existing model parameters as stress dependent ones, which were treated as constants previously. The theoretical calculation and proof were also shown in the related chapters. It has been seen that for each of the materials investigated in this work, there exists a linear relationship between those model parameters and stress within some ranges of applied stress. These ranges are different for different materials. For one material such as cold-worked nickel, a piecewise linearity exists within different stress ranges; but for the other

materials such as annealed nickel, a linear relationship between model parameters and stress has been found over the entire range of applied stress studied.

Systematic measurements on nickel and steel samples have been conducted to verify the new model theory of the magnetomechanical effect. These include magnetomechanical effect measurements and hysteresis loop measurements under various applied stress. Anhysteretic magnetization and stress-strain relationships were also measured to determine the material properties and input model parameter for use in the simulations.

The extended model was validated with respect to its capability of describing the changes of magnetization in response to varying mechanical stress under constant applied fields, and to varying magnetic field under constant applied stresses. Simulation results obtained from materials with both positive and negative magnetostrictions, including ferrous alloys and nickel, show improved agreement with the measurement results.

Although the new model equation gave results that were in better agreement both qualitatively and quantitatively with observations, the model did not reproduce the experimental results accurately in all of the situations examined and further discussion and suggestion of the model may still be needed.

As discussed in chapter 3, the hysteresis loops simulated under high stress level show larger discrepancy from the experimental data at the knee of the loops (at high magnetic field). In particular, the reversibility of the modeled hysteresis loop was found to be much less than the measured one. So the reversible part of magnetization is changing respect to stress and magnetic field, unlike the way the model assumes. On the

other hand, the rotation of domain magnetization should also be included in the model, because at the knee of the hysteresis loop this process generally becomes dominant.

The results reported in chapter 5 show improvement over the previous model but also indicate some problems that remain to be solved in the future work. Compared with hysteresis loop simulation, the magnetomechanical effects simulation in general show a larger inaccuracies in reproducing the experimental results. One suggestion is that the relationship between model parameters and stress still needs to be studied and refined, including the number of parameters. The magnetomechanical effects are very complicated phenomena. In-depth study on this topic will have a long way to go but is worth being pursued because of the impact of a valid theoretical description of the effects on a wide variety of applications, such as magnetic NDE and the development of magnetoelastic sensor and actuators.

APPENDIX. REPRINTS OF PAPERS PUBLISHED ON HYSTERESIS AND MAGNETOMECHANICAL EFFECT

Modeling of Stress Effects on Magnetic Hysteresis and Barkhausen Emission Using an Integrated Hysteretic-Stochastic Model

C.C.H. Lo, *Member, IEEE*, S.J. Lee, L. Li, L.C. Kerdus and D.C. Jiles, *Fellow, IEEE**Abstract*-- **An integrated magnetic model has been developed which provides a coherent description of the effects of stress on hysteresis loop and Barkhausen effect (BE) signals. BE signal was calculated based on the hysteretic-stochastic process model of domain wall dynamics, which has been extended to include the magnetomechanical effect. For comparison hysteresis loops and BE signals were measured in materials subjected to various tensile and compressive stresses within the elastic limit. The stress dependence of the modeled hysteresis loop properties and BE signals was found to be in good agreement with the experimental results.**

Index Terms — **hysteresis modeling, Barkhausen effect modeling, magnetoelastic coupling, stress effect .**

I. Introduction

This paper presents an integrated model which provides a description of the effects of stress on both hysteresis loops and Barkhausen emission (BE) signals. It has been proposed in previous studies that an applied stress can be treated as an effective field operating through the magnetoelastic coupling [1,2]. The theory of magnetomechanical effect based on this approach has been found useful in describing the effects of varying stress on magnetization [3,4] and the effects of applied stresses on anhysteretic magnetization curves and BE signals [5]. This approach nevertheless cannot always completely describe the stress dependence of hysteresis loop properties such as coercivity and remanence [6]. In this study the magnetomechanical hysteresis model has been extended by taking into account the effect of applied stresses on domain wall pinning. The extended model has been found capable of reproducing the dependence of magnetic properties such as coercivity and remanence on applied stress. The model has also been incorporated into the hysteretic-stochastic model of Barkhausen effect [7]. In this approach the stress effects on BE signal can be modeled according to the variations of the hysteresis model parameters with applied stress.

II. Effect of Stress on Hysteresis Model Parameters

It has been shown in previous studies [1-3] that the effect of an applied stress σ on magnetization M of ferromagnetic materials can be treated as an effective field given by

$$H_\sigma = \frac{3}{2}\frac{\sigma}{\mu_0}\left(\frac{d\lambda}{dM}\right), \qquad (1)$$

where λ is the magnetostriction and μ_0 is the permeability of free space. If the magnetostriction can be described by an equation of the form $\lambda = \gamma M^2$, where γ is a coefficient dependent on σ, the total magnetic field sensed by a domain can then be written in a particularly simple form,

$$H_{eff} = H + \alpha M + \frac{3\gamma\sigma}{\mu} M = H + \alpha_{eff} M \qquad (2)$$

where $\alpha_{eff} = \alpha + 3\gamma\sigma/\mu$, and α is a mean field parameter representing inter-domain coupling [9] and H is the applied field.

The applied stress changes the anisotropy energies of domains due to the magnetoelastic coupling, and this in turn alters the local energy barrier that a domain wall needs to overcome before it moves irreversibly from one pinning site to another. Therefore the strengths of pinning sites for domain walls become dependent on the applied stress. For simplicity consider inside a isotropic material a domain wall separating two domains which are magnetized along and at an arbitrary angle θ to the stress direction respectively. The difference in magnetoelastic energies between the domains is

$$\Delta E = -\frac{3}{2}\lambda_s \sigma\left(1-\cos^2\theta\right) \qquad (3)$$

Under a constant or zero applied magnetic field the domain wall may break away from the pinning site and move across the energetically unfavorable domain if the internal field is large enough to overcome the pinning force. This causes irreversible changes in magnetization.

For those domain walls which remain pinned after a constant stress σ has been applied, the energy needed to overcome the pinning site becomes dependent on σ because the domains separated by the domain wall will have different magnetoelastic energies. As a result the coercivity of the material changes with the applied stress. This effect can be described based on the theory of ferromagnetic hysteresis [9]. According to this theory the energy E_{pin} dissipated through pinning and unpinning of a domain wall is proportional to the change in magnetization and the pinning coefficient $k_0 = n_0\langle\varepsilon_0\rangle / 2m$, where m is magnetic moment, n_0 is the pinning site density and $\langle\varepsilon_0\rangle$ is the average pinning energy without applied stress. Since the applied stress alters the pinning energy on either side of a domain wall as given in equation (3), the pinning coefficient (denoted by k_{eff}) becomes dependent on stress and can be written as

$$\begin{aligned} k_{eff} &= n(\sigma)\ \langle \varepsilon_0 - \tfrac{1}{2}\lambda_s\sigma(1-\cos^2\theta)\rangle / 2m \\ &\cong n_0\langle\varepsilon_0\rangle/2m - n_0\langle\tfrac{1}{2}\lambda_s\sigma(1-\cos^2\theta)\rangle/2m \\ &= k_0 - n_0\langle\tfrac{1}{2}\lambda_s\sigma(1-\cos^2\theta)\rangle/2m \end{aligned} \qquad (4)$$

where $\langle\ \rangle$ is the value averaged over all the pinning sites and is dependent on σ because the applied stress changes the

orientation of domain magnetization with respect to the stress axis (i.e. θ is a function of σ). Equation (4) was derived based on the assumption that the density of pinning sites (dislocations, secondary phases and precipitates) remains unchanged under applied stresses within the elastic limit of the material. Accordingly the stress-induced change in the pinning coefficient is determined by the product of λ_s and σ. For materials with positive λ_s (e.g. iron at low field strengths) k_{eff} decreases with tension but increases with compression, while for materials with negative λ_s (e.g. nickel) k_{eff} shows the opposite dependence on stress. It is expected that for soft magnetic materials coercivity exhibits a stress dependence similar to that of k_{eff}, since in soft magnetic materials the pinning coefficient k is approximately equal to coercivity [10, 11]. The stress dependence of coercivity predicted by the current model is consistent with that observed in the previous studies on steel [1,3] and nickel [12].

III. Modeling of Stress Effect on Barkhausen Signal

In this study BE signal was simulated based on a hysteretic-stochastic process model of domain wall dynamics [7], which has been extended recently by including the theory of the magnetomechanical effect to provide a description of BE signal under applied stress. According to the extended model BE signal voltage can be expressed in terms of the rate of irreversible changes in magnetization I_{irr} which is governed by [8]

$$\frac{d\dot{I}_{irr}}{dt} = \frac{\chi'_{irr}}{\tau}\left(\frac{dH_a}{dt} - \frac{dH_c}{dt}\right) - \frac{\dot{I}_{irr}}{\tau} \quad , \tag{5}$$

where dH_a/dt is the rate of change of applied field, $\tau = \sigma GS\chi'_{irr}$ and χ'_{irr} is the irreversible differential susceptibility. H_c is the local pinning field governed by

$$\frac{dH_c}{dI_{irr}} + \frac{S(H_c - < H_c >)}{\xi} = \frac{dW}{dI_{irr}} \tag{6}$$

where ξ represents the range of interaction of a domain wall with pinning sites. The function $W(I_{irr})$ describes the Wiener-Lévy (W-L) process [7] which has a zero mean but a finite variance proportional to the intensity of the local pinning field A. i.e. $< dW >= 0$, but $< |dW|^2 >= 2ASdI_{irr}$.

The irreversible susceptibility χ'_{irr} can be computed using the hysteresis model [2] by

$$\chi'_{irr} = \frac{(M_a - M_{irr})}{(k_{eff}\delta/\mu_0) - [\alpha_{eff} + (3\sigma/2\mu_0)(\partial^2\lambda/\partial M^2)](M_a - M_{irr})} . \tag{7}$$

In this approach the effects of the applied stress on BE signal can be modeled via the parameters k_{eff} and α_{eff} which are dependent on stress as shown in equations (2) and (4).

IV. Procedures

In situ hysteresis loop and BE measurements were made on samples under various applied stresses within the elastic limit using a servo-hydraulic mechanical testing system. During the measurement a sample was magnetized using a solenoid. The magnetic field H was measured using a Hall sensor mounted on the sample surface. The output of a search coil wound on the sample was integrated to obtain the hysteresis loop, and was amplified (60 dB) and band pass filtered (10 to 100 kHz) to obtain the BE signals. Magnetostriction was measured using strain gages mounted on the sample surface.

Hysteresis loops were simulated for various stress levels using the following values for the model parameters: B_S = 1.7×10^6A/m, c = 0.605, a = 1300A/m and α = 0.00268. The parameter α_{eff} was calculated for different stress levels using (2). The values of γ were obtained by fitting $\lambda = \gamma M^2$ to the measured magnetostriction curves. The values of k_{eff} for different stress levels were determined by obtaining the best fit to the experimental data.

V. Results and Discussion

As shown in Fig. 1, stress-induced changes in the experimental hysteresis loops can be calculated using the hysteresis model. Good agreement was observed between the experimental and modeled hysteresis loops in the low field regime (that is at field strengths below the coercive field) and for the range of applied stress studied in this work (-533 MPa to 320 MPa). The coercivity and remanence of the simulated hysteresis loops exhibited a stress dependence consistent with that of the experimental data as shown in Fig. 2. Detailed comparison nevertheless revealed that under high compressive stresses (larger than 100 MPa) the modeled hysteresis curves showed deviations from the experimental results in particular at the knee of the hysteresis loops as shown in Fig. 1. A possible explanation is that under high compressive stresses domain magnetization prefers to align perpendicular to the stress axis in steel. At the knee of the hysteresis loop the magnetization reversal processes involve mainly reversible rotation of domain magnetization towards the applied field, as indicated by the small hysteresis in high field regime of the experimental loops. This process is not accounted for by the current model, which is based primarily on the consideration of domain wall motion [9].

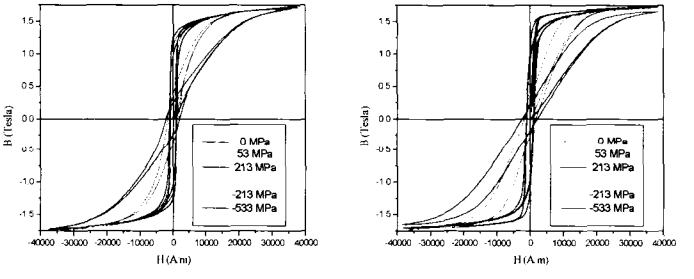

Fig. 1 (a) Measured and (b) modeled hysteresis loops in AISI 410 stainless steel for various applied stresses.

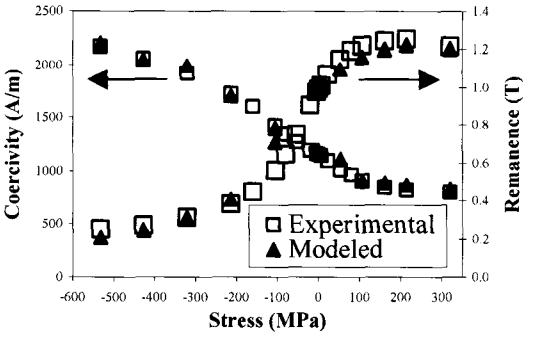

Fig. 2 Measure and modeled coercivity and remanence in AISI 410 stainless steel as a function of stress.

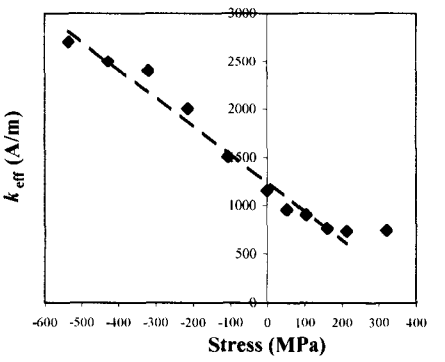

Fig. 3 The pinning coefficient k_{eff} plotted against applied stress σ. The straight line was added as a guide to the eyes.

As shown in Fig. 3, the pinning coefficient k_{eff} appears to vary approximately linearly with stress within the range of -533 MPa to 200 MPa. This experimental result is consistent with that predicted by equation (4). On the other hand k_{eff} becomes relatively insensitive to stress beyond 200 MPa. A possible explanation is that application of large tensile stress favors a domain structure in which domains are magnetized along the stress axis and hence have the same magnetoelastic energy. As a result the magnetoelastic energy does not contribute further to the strength of domain wall pinning and therefore k_{eff} becomes less sensitive to further changes in the applied stress.

The dependence of the normalized root-mean-square (rms) values of the Barkhausen signal (normalized with respect to the values at $\sigma = 0$ MPa) on applied stress is shown in Fig. 4. The measured BE signal increases with tension but decreases with compression. This is consistent with the results reported in previous work [5]. The simulated BE shows a stress dependence which is in agreement with that of the experimental data. The present results indicate that the extended model provides a description of the stress effects on BE signals, which can be exploited for nondestructive evaluation of stress via BE measurements.

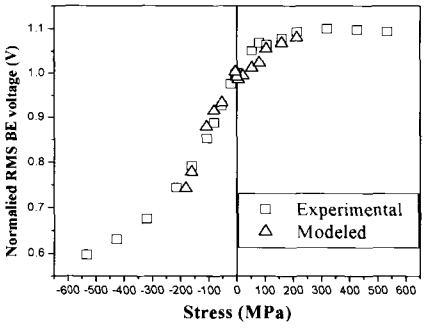

Fig. 4 Measured and modeled rms BE voltage (normalized) as a function of applied stress.

VI. Conclusions

An integrated magnetic hysteresis and Barkhausen effect model has been developed which can be used to describe the effects of applied stresses on hysteresis in magnetization and Barkhausen effect signals. Barkhausen signals were simulated using a hysteretic-stochastic model which has been extended to include the magnetomechanical effect. The dependence of the simulated magnetization hysteresis loop properties and root-mean-square Barkhausen voltage on applied stress were found to be in agreement with experimental results.

References

[1] M.J. Sablik, G.L. Burkhardt, H. Kwun, D.C. Jiles, "A model for the effect of stress on the low-frequency harmonic content of the magnetic induction in ferromagnetic materials", *J. Appl. Phys.*, **63**, 3930, 1988.

[2] M.J. Sablik and D. C. Jiles, "Coupled magnetoelastic theory of magnetic and magnetostrictive hysteresis", *IEEE Trans. Mag.*, 29, 2113, 1993.

[3] D. C. Jiles, "Theory of magnetomechanical effect", *J. Phys. D: Applied Physics*, **28**, 1537, 1995.

[4] M.J.Sablik and R.A.Langman, "Approach to the anhysteretic surface", J. Appl. Phys. 79, 6134, 1996.

[5] M.J. Sablik, "A model for the Barkhausen noise power as a function of applied field and stress", *J. Appl. Phys.*, 74, 5898, 1993.

[6] M.J. Sablik, "A model for asymmetry in magnetic property behaviour under tensile and compressive stress in steel", *IEEE Trans. Mag.*, 33, 3958, 1997.

[7] B. Alessandro, C. Beatrice, G. Bertotti and A. Montorsi, J. Appl. Phys. 68, 2901, 1990.

[8] D. C. Jiles, "Dynamic of domain magnetization and the Barkhausen effect", *Czechoslovak Journal of Physics*, **50**, 893, 2000.

[9] D.C. Jiles and D.L. Atherton, "Theory of ferromagnetic hysteresis", *J. Appl. Phys.*, 55, 2115, 1984.

[10] D.C.Jiles, J.B.Thoelke and M.K.Devine, "Determination of theoretical parameters for modelling bulk magnetic hysteresis properties using the theory of ferromagnetic hysteresis", IEEE Trans. Mag. 28, 27 , 1992.

[11] D. C. Jiles, *Introduction to Magnetism and Magnetic Materials*, 2nd ed., Chapman Hill, London, 1998, pp. 201-204.

[12] D. C. Jiles, T.T. Chang, D.R. Hougen and R. Ranjan, "Stress-induced changes in the magnetic properties of some nickel-copper and nicke-cobalt alloys", *J. Appl. Phys.*, 64(7), 3620, 1988.

Modified Law of Approach for the Magnetomechanical Model: Application of the Rayleigh Law to the Stress Domain

L. L, *Student Member, IEEE* and D.C. Jiles, *Fellow Member, IEEE*

***Abstract*-- Stress is one of the principal external factors affecting the magnetization of materials. A new and improved equation for modeling the magnetomechanical effect has been developed based on extension of the previous equation to include the Rayleigh law. Accordingly the previous theory of the magnetomechanical effect has been refined by including a new linear term in the original model equation.**

***Index Terms*-- magnetization, magnetomechanical, stress**

I. INTRODUCTION

COMPUTER modeling and simulation of the properties of materials is becoming increasingly important. One of the major challenges today is to provide reliable models for non-linear and hysteretic effects in materials. The magneto-mechanical effect, that is the change of magnetization of a magnetic material resulting from the application of stress, has attracted attention because of its complexity. Development of an accurate model description of the magnetomechanical effect becomes increasingly important in applications of stress sensors using magnetostrictive materials and in magnetic measurements for evaluation of stress in materials.

According to the previous theory of the magneto-mechanical effect which is based on the 'law of approach'[1], application of stress induces changes in magnetization towards anhysteretic magnetization. The anhysteretic itself is stress dependent, and the rate of change of magnetization with the input elastic energy is proportional to the displacement of the prevailing magnetization from the anhysteretic magnetization. This model theory has some limitations. For example, as indicated by Sablik [2], it is seen that the computed magnetization stress appears to increase in unlimited fashion rather than tending to a limiting hysteretic pattern, as seen experimentally. It has also been found experimentally that the slope of the magnetization versus stress curve at zero stress is generally non-zero, whereas the model suggests that it should be identically zero.

Manuscript received January 3, 2003. This research was supported by the NSF Industry/University Cooperative Research Program of the Center for Nondestructive Evaluation at Iowa State University.

Lu Li is with Center for NDE and Department of Electrical and Computer Engineering, Iowa State University, Ames, IA 50011, USA (telephone: 515-294-5612, e-mail: cosper@iastate.edu)

David. C. Jiles is with the Ames Laboratory, US Department of Energy, and Department of Materials Science and Engineering, Iowa State University, Ames, IA 50011, USA (telephone: 515-294-9685, e-mail: gauss@ameslab.gov).

II. PREVIOUS MODEL THEORIES OF MAGNETOMECHANICAL EFFECTS

Recent research has shown that the magnetization curves of materials can be modeled in a variety of configurations [3]. In addition stress, whether uniaxial or torsional [4], strongly affects the measured magnetic properties. It has been known that the effect of stress on magnetization can be described as a perturbation of the magnetic field, since the stress affects the orientation of magnetic moments through the magnetoelastic coupling [1].

In many cases the stress can be included in the form of a perturbation to the magnetic field. The key to this description is to provide a means by which both magnetic field and stress can be treated similarly in the equations. However not all magnetomechanical behavior can be explained by the effective field theory. For example, at larger stresses this approximation is no longer valid since magnetic field and stress have different effects on magnetization.

Experimental results of Craik and Wood [5] are shown in Fig. 1 (which is taken from figure 5 of [5]). At zero stress,

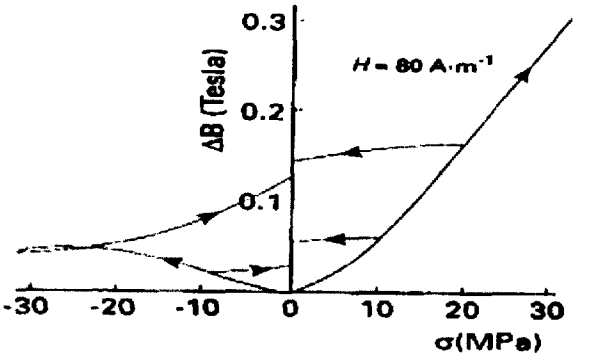

FIGURE 1. The variation in magnetic induction B with stress for a specimen of mild steel, after Craik and Wood [5]. The slope of the curves at zero stress is non-zero.

the slope of the magnetic induction versus stress curve is non-zero, either on the positive stress side or the negative stress side.

The effective field can be derived from thermodynamics as the derivative of the appropriate free energy with respect to the magnetization [1],

$$H_\sigma = \frac{3}{2}\frac{\sigma}{\mu}\left(\frac{d\lambda}{dM}\right) \tag{1}$$

where σ is the stress which is negative for compression and positive for tension, λ is the magnetostriction, M is the magnetization of the material, and μ_0 is the permeability of free space. This equation can be used under suitable

conditions for the description of uniaxial, multiaxial and torsional stresses on anhysteretic magnetization. Ignoring demagnetizing field contributions, the total effective field H_{eff}, including the stress contribution, can be represented as

$$H_{eff} = H + \alpha M + H_{\sigma} \tag{2}$$

where α is a dimensionless mean field parameter representing inter-domain coupling and H is the externally applied field.

If the applied field and applied stress are not coaxial, then

$$H_{eff} = H + \alpha M + \frac{3}{2}\frac{\sigma_0}{\mu}\left(\frac{d\lambda}{dM}\right)_{\sigma}(\cos^2\theta - \upsilon\sin^2\theta) \tag{3}$$

where θ is the angle between the axis of the applied stress σ_0 and the axis of the magnetic field H and v is Poisson's ratio. If the magnetostriction is expressed as a series in even powers of the magnetization, then if one takes only the first term, it follows that $d\lambda/dM$ in Eq. (3) can be replaced by $\gamma_1 M$, where γ_1 is the coefficient of the M^2 term of the series for λ.

A model theory of the changes in magnetization that a ferromagnetic material undergoes when subjected to an applied uniaxial stress has been described previously [1]. The change in magnetization on application of stress can be described by equation Eq. (4), in which the rate of change of magnetization with elastic energy is proportional to the displacement of the magnetization from the anhysteretic magnetization.

$$\frac{dM}{d\sigma} = \frac{1}{\varepsilon^2}\sigma(1-c)(M_{an} - M_{irr}) + c\frac{dM_{an}}{d\sigma} \tag{4}$$

Fig. 2 is a calculated result based on Eq. (4). Without the linear term, the slope of the magnetization versus stress curve must be zero at zero stress. This is not in total agreement with experimental results. In other words, this model equation needs to be modified in order to give predictions that are in agreement with observations.

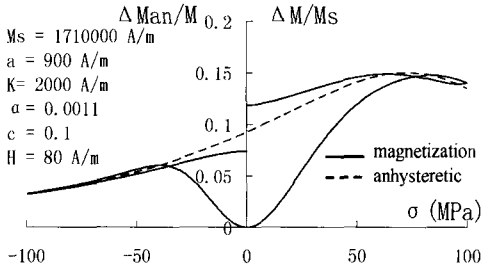

FIGURE 2. The calculated variation of magnetization with stress under conditions similar to those employed in reference [5]. The slope at zero stress is zero.

III. Development Of An Improved Model Theory Of The Magnetomechanical Effect

The Rayleigh law, which describes hysteretic behavior in magnetization at low field strengths, can be expressed as

$$M = \chi_a H \pm \eta H^2 \tag{5}$$

where, for the initial magnetization curve, χ_a is the initial susceptibility and η is called the Rayleigh coefficient; + for positive field use, - for negative field.

Rayleigh also showed that the hysteresis loop can be described by two parabolas:

$$M = (\chi_a - \eta H_-)H + \frac{\eta}{2}(H^2 - H_-^2) \tag{6}$$

$$M = (\chi_a + \eta H_+)H - \frac{\eta}{2}(H^2 - H_+^2) \tag{7}$$

where Eq. (6) and Eq. (7) present ascending and descending portions of the loop, respectively. H_- and H_+ are the maximum fields applied.

From equation (5), we have $M_+ = \chi_a H_+ + \eta H_+^2$ and $M_- = \chi_a H_- - \eta H_-^2$, where M_- and M_+ are the magnetization at maximum magnetic field H_- and H_+.

Substituting these into Eq. (6) and Eq. (7), we obtain

$$M - M_+ = \chi_a(H - H_+) - \frac{\eta}{2}(H - H_+)^2 \tag{8}$$

$$M - M_- = \chi_a(H - H_-) + \frac{\eta}{2}(H - H_-)^2 \tag{9}$$

As shown in [6], the effect of stress on magnetization can be expressed using an equation that is very similar to the Rayleigh law. In this derivation the fractional change in volume is

$$\Delta V = \frac{V - V_0}{V_{tot}} = \alpha|\sigma| + \beta\sigma^2 \tag{10}$$

where V_0 is the original volume before any domain wall movement and V_{tot} is the total volume of the sample; α and β are constants depending on domain wall type [6]. From this, in the simplest case of spin-up and spin-down domains, it is easily shown [7] that

$$\Delta M = 2M_s\Delta V \tag{11}$$

Therefore if there is a change in volume of the domains ΔV a corresponding change of magnetization ΔM occurs.

From these definitions, Eq. (10) and Eq. (11), we can see that the equivalent expression for changes in magnetization is

$$\Delta M = 2M_s(\alpha|\sigma| + \beta\sigma^2) \tag{12}$$

and this equation is true whether stress is increasing in the positive direction (tension) or the negative direction (compression).

From this we can develop stress dependent equations for the Rayleigh region. When the stress is being reduced from σ_+ along the descending branch, the equation governing the magnetization change is

$$\Delta M - \Delta M_+ = 2M_s\left[\alpha(|\sigma - \sigma_+|) - \frac{\beta}{2}(\sigma - \sigma_+)^2\right] \tag{13}$$

and when the stress is being reduced from σ_- along the ascending branch, then the equation governing the magnetization change is

$$\Delta M - \Delta M_- = 2M_s\left[\alpha(|\sigma - \sigma_-|) + \frac{\beta}{2}(\sigma - \sigma_-)^2\right] \tag{14}$$

The calculated result using these model equations is shown in Fig. 3. The positive side represents stress taken from zero stress to maximum tensile stress and back again, whereas the negative side is independent and represents stress taken form zero stress to maximum negative stress and back again. At zero stress, the slope of induction versus stress curve is non-

zero, either on the positive stress side or the negative stress side. This result agrees well with experimental data.

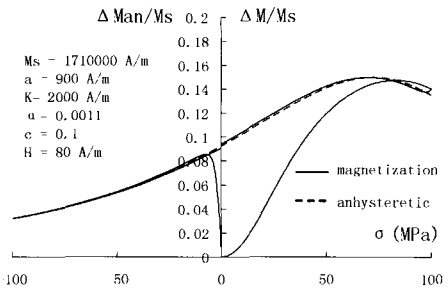

FIGURE 3. The calculated variation of magnetization with stress under conditions similar to those employed in reference [5]. The slope of the curve at zero stress is non-zero.

As a comparison with Ref. [5]'s experimental data, table 1 shows the results obtained by this model. Similar table is used for better comparison with Ref. [1].

H (A/m)	σ max (MPa)	Δ Bmax (T) Measured / Model		Δ Brem (T) Measured / Model	
26	98	0.16	0.09	0.12	0.07
	-98	0.02	0.02	0.10	0.07
80	98	0.37	0.31	0.27	0.20
	-98	-0.02	0.07	0.20	0.20
132	98	0.43	0.60	0.34	0.32
	-98	-0.16	0.11	0.15	0.31

Table 1. A comparison of measured and modeled changes in magnetic induction with stress under various conditions.

IV. Results of New Investigation

In this study, a nickel sample was measured. The sample was first demagnetized and then subjected to various external magnetic field. Under each field level, stress was applied cyclically. Fig. 4 shows the procedure of this measurement under 1019 A/m magnetic field.

Fig. 5 shows the model result for the compressive part of the experimental data. It can be seen that both the shape of the calculated curve and data agree with the measured data. However, this model doesn't give good agreement for the tensile part of the experimental data if use the same set of parameters for the compressive part.

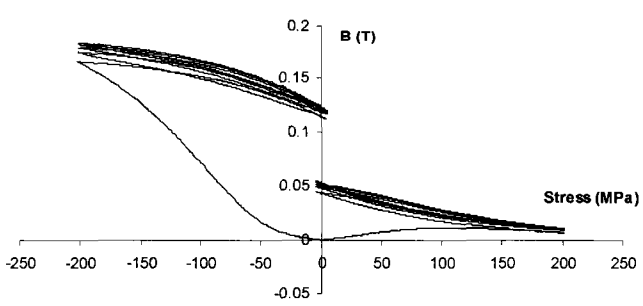

FIGURE 4. Under magnetic field of 1019 A/m, five cycles of applying a tensile and compressive stress up to 200 MPa and then decreasing it to zero.

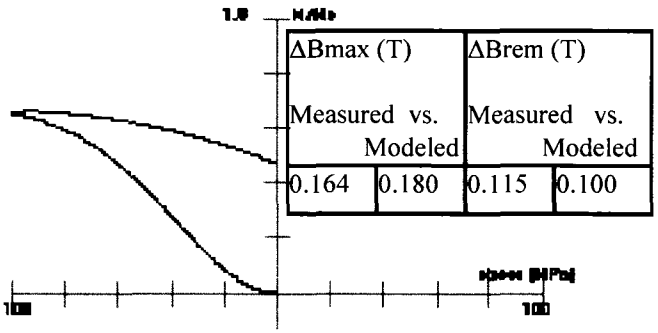

FIGURE 4. Calculated result by the modified model equations.

V. Conclusion

Both effective field theory and the law of approach have their limitations. Rayleigh's Law gives us a basis for the solution of problems with our understanding of the magnetomechanical effect which arose due to disagreement between theory and observation. The law of approach can be modified by adding a linear component into the original model equation. The new model equation gives results that are in better agreement with experimental observations.

References

[1] D.C. Jiles, "Theory of the magnetomechanical effect," Journal of Physics D: Applied Physics, 28, 1537, 1995.

[2] M.J. Sablik, Y.Chen and D.C.Jiles "Modified Law of Approach for the Magnetomechanical Model", *Review of Progress in Quantitative Nondestructive Evaluation*, 1565, 2000.

[3] D.C. Jiles, S.J. Lee, J. Kenkel and K. Metlov, "Superparamagnetic magnetization equation in two dimensions," Appl. Phys. Letts., 77, pp: 1029-1031, 2000.

[4] Y. Chen, B.K.Kriegermeier-Sutton, J.E. Snyder, K.W.Dennis, R.W. McCallum and D.C.Jiles, "Magnetomechanical effects under torsional strain in iron, cobalt and nickel," J.Magn.Magn.Mater., 236, pp: 131-138, 2001.

[5] Craik D J and Wood M J "Magnetization changes induced by stress in a constant applied field" J.Phys. D: Appl.Phys. 4 1009, 1971.

[6] William Fuller Brown, JR. Title: Physical Review, Volume 75, Number1, 1949.

[7] D.C.Jiles, Czech Journal of Physics, 50, 893, 2000.

[8] Jiles D C, Thoelke J B and Devine M K 1992 Determination of theoretical parameters for modeling bulk magnetic hysteresis properties using the theory of ferromagnetic hysteresis *IEEE Trans. Magn.* **28** 27

Modeling of the magnetomechanical effect: application of the Rayleigh law to the stress domain

L. Li [1] and D.C. Jiles[1,2]

[1]Department of Electrical and Computer Engineering

[2]Ames Laboratory, US Department of Energy and Department of Materials Science and Engineering , Iowa State University, Ames, IA 50011, USA

Abstract

Stress is one of the principal external factors affecting the magnetization of materials. The magnetomechanical effect, that is the change of magnetization of a magnetic material resulting from the application of stress, has attracted attention because of its scientific complexity. A new and improved model equation for interpreting the magnetomechanical effect has been developed based on extension of the previous equation to include the Rayleigh Law. According to the previous theory of the magnetomechanical effect which is based on the Law of Approach, application of stress induces changes in magnetization towards anhysteretic magnetization which itself is stress-dependent, and the rate of change of magnetization with the input elastic energy is dependent on the displacement of the prevailing magnetization from the anhysteretic magnetization. The theory has been refined by including a new linear term in the model equation in addition to the well-known quadratic term. It was found that the modified theory provides a much better description of the magnetization changes under stress, particularly at small applied stress amplitudes and when the stress changes sign.

Previous model theories of magnetomechanical effects

Recent research has shown that the magnetization curves of materials can be modeled in a variety of geometrical configurations [1]. In addition stress, whether uniaxial [2] or torsional [3], strongly affects the measured magnetic properties. The effect of stress on magnetization can be described as a perturbation of the magnetic field, since the stress affects the orientation of magnetic moments through the magnetoelastic coupling [4]. But this "effective field theory" and the "law of approach" have their limitations.

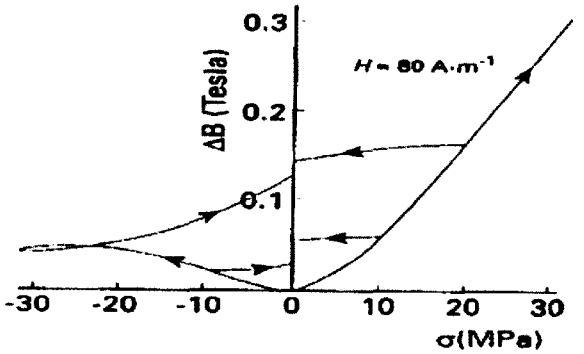

The variation in magnetic induction B with stress for a specimen of mild steel, after Craik and Wood [5].

Figure 1. The variation in magnetic induction B with stress for a specimen of mild steel, after Craik and Wood [5]. The slope at zero magnetic field H and v is Poisson's ratio.

Experimental results of Craik and Wood [5] are shown in figure as 1 (which is taken from figure 5 of [5]). At zero stress, the slope of the magnetic induction versus stress curve is positive, either on the positive stress side or the negative stress side.

As shown in previous research [4], the effect of stress on the magnetization can be considered as an effective field which can be derived from thermodynamics as the derivative of the appropriate free energy with respect to the magnetization,

$$H_\sigma = \frac{3}{2}\frac{\sigma}{\mu}\left(\frac{d\lambda}{dM}\right) \tag{1}$$

where σ is the stress which is negative for compression and positive for tension, λ is the magnetostriction, M is the magnetization of the material, and μ_0 is the permeability of free space. This equation can be used under suitable conditions for the description of uniaxial, multiaxial and torsional stresses on anhysteretic magnetization. The total effective field H_{eff}, including the stress contribution, can be represented as

$$H_{eff} = H + \alpha M + H_\sigma \tag{2}$$

where α is a dimensionless mean field parameter representing inter-domain coupling and H is the applied field.

Then the total effective field H_{eff} includes the stress contribution is

$$H_{eff} = H + \alpha M + \frac{3}{2}\frac{\sigma_0}{\mu_0}\left(\frac{d\lambda}{dM}\right)_\sigma (\cos^2\theta - \upsilon\sin^2\theta) \tag{3}$$

where θ is the angle between the axis of the applied stress σ_0 and the axis of the specimen of mild steel, after Craik and Wood [5]. The slope at zero magnetic field H and v is Poisson's ratio.

stress is positive.

Based on symmetry, an empirical model for magnetostriction can be given as

$$\lambda = \sum_{i=0}^{\infty} \gamma_i M^{2i} \tag{4}$$

If use approximation to the magnetostriction by including the terms up to $i = 1$, this gives

$$H_{eff} = H + \alpha M + \frac{3\gamma_1 \sigma_0}{\mu_0}(\cos^2\theta - \upsilon \sin^2\theta)M = H + \tilde{\alpha} M \tag{5}$$

Figure 2 is the calculated result based on Eq. (5) which uses the effective field theory. From this figure, we can see that the

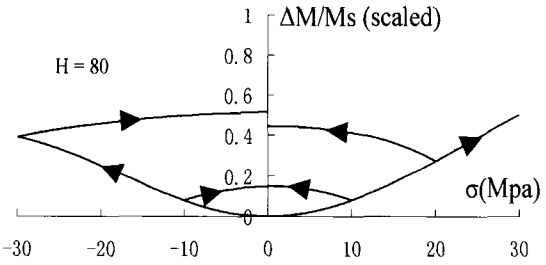

Figure 2. Calculated result using effective field theory. Under conditions similar to those employed by Craik and Wood [5].

slope of magnetization versus stress curve at zero stress is zero, which is not in total agreement with experimental results.

In many cases the stress can be included in the form of a perturbation to the magnetic field. The key to this description is to provide a means by which both magnetic field and stress can be treated similarly in the equations. However not all magnetomechanical behavior can be explained by the effective field theory. For example, at larger stresses this approximation is no longer valid since magnetic field and stress have different effects on magnetization.

A model theory of the changes in magnetization that a ferromagnetic material undergoes when subjected to an applied uniaxial stress has been described previously [6]. The change in magnetization on application of stress can be described by equation Eq. (6), in which the rate of change of magnetization with elastic energy is proportional to the displacement of the magnetization from the anhysteretic magnetization.

$$\frac{dM}{d\sigma} = \frac{1}{\varepsilon^2}\sigma(1-c)(M_{an} - M_{irr}) + c\frac{dM_{an}}{d\sigma} \tag{6}$$

Figure 3 is a calculated result based on Eq. (6). Without the linear term, the slope of the magnetization versus stress curve must be zero at zero stress. This does not occur in practice. In other words, this model equation needs to be modified in order to give predictions that are in agreement with observations.

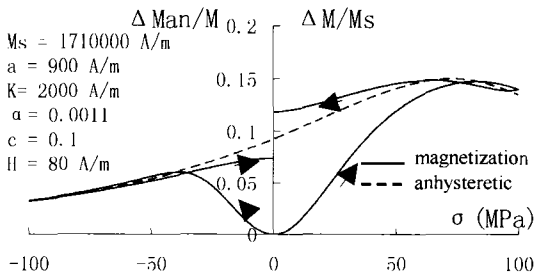

Figure 3. The calculated variation of magnetization with stress under conditions similar to those employed by Craik and Wood [5]. The slope at zero stress is zero.

Development of model theory of magnetomechanical effects

The Rayleigh law, which describes hysteretic behavior in magnetization at low field strengths, can be expressed as

$$M = \chi_a H \pm \eta H^2 \tag{7}$$

where χ_a is the initial susceptibility and η is called the Rayleigh constant; + for positive field use, - for negative field for the initial magnetization curve.

Rayleigh also showed that the hysteresis loop was composed of two parabolas:

$$M = (\chi_a - \eta H_-)H + \frac{\eta}{2}(H^2 - H_-^2) \tag{8}$$

$$M = (\chi_a + \eta H_+)H - \frac{\eta}{2}(H^2 - H_+^2) \tag{9}$$

where Eq. (8) and Eq. (9) present ascending and descending portions of the loop, respectively. H_- and H_+ are the maximum fields applied.

From equation (7), we will have $M_+ = \chi_a H_+ + \eta H_+^2$ and $M_- = \chi_a H_- - \eta H_-^2$ where M_+ and M_- are the magnetization at maximum magnetic field H_+ and H_-.

Substituting these into Eq. (8) and Eq. (9), we obtain

$$M - M_+ = \chi_a(H - H_+) - \frac{\eta}{2}(H - H_+)^2 \tag{10}$$

$$M - M_- = \chi_a(H - H_-) + \frac{\eta}{2}(H - H_-)^2 \tag{11}$$

According to Brown [7] the effect of stress on magnetization can be expressed using an equation that is very similar to the Rayleigh law. In his derivation he wrote the fractional change in volume is

$$\Delta V = \frac{V - V_0}{V_{tot}} = \alpha|\sigma| + \beta\sigma^2 \tag{12}$$

where V_0 is the original volume before any domain wall movement and V_{tot} is the total volume of the sample; α and β are constants depending on

domain wall type. And from this, in the

simplest case of spin-up and spin-down domains, it is easily shown [8] that

$$\Delta M = 2M_s \Delta V \tag{13}$$

therefore if there is a change in volume of the domains ΔV a corresponding change of magnetization ΔM occurs. Beginning from these definitions, Eq. (7) and Eq. (8), we can see that the equivalent expression for changes in magnetization is

$$\Delta M = 2M_s(\alpha|\sigma| + \beta\sigma^2) \tag{14}$$

and this equation is true whether stress is increasing in the positive direction (tension) or the negative direction (compression). That is a important difference between this and the normal Rayleigh region equation.

From this we can develop stress dependent equations for the Rayleigh region. When the stress is being reduced from σ_- along the descending branch, then the equation governing this is

$$\Delta M - \Delta M_+ = 2M_s\left[\alpha\left(|\sigma| - |\sigma_+|\right) - \frac{\beta}{2}\left(\sigma - \sigma_+\right)^2\right] \tag{15}$$

When the stress is being reduced from σ_- along the ascending branch, then the equation governing this is

$$\Delta M - \Delta M_- = 2M_s\left[\alpha\left(|\sigma| - |\sigma_-|\right) - \frac{\beta}{2}\left(\sigma - \sigma_-\right)^2\right] \tag{16}$$

In other words, these curves are actually symmetric, unlike the analogous curve of magnetization versus field.

Results of new investigation

Based on Eq. (15) and Eq. (16), a new model equation, with an additional linear term, has been developed.

$$\frac{dM}{d\sigma} = \frac{1}{\varepsilon^2}(1-c)(M_{an} - M_{irr})(\sigma \pm \eta E) + c\left(\frac{\sigma}{E} \pm \eta\right)\frac{dM_{an}}{d\sigma} \tag{17}$$

where M_{an} is the anhysteretic magnetization, σ is the stress, M_{irr} presents the irreversible component of magnetization , E is the relevant elastic modulus, c describes the flexibility of the magnetic domain walls. ε has been defined previously [6], η is coefficient which represents irreversible change in the magnetization with the action of a stress [7].

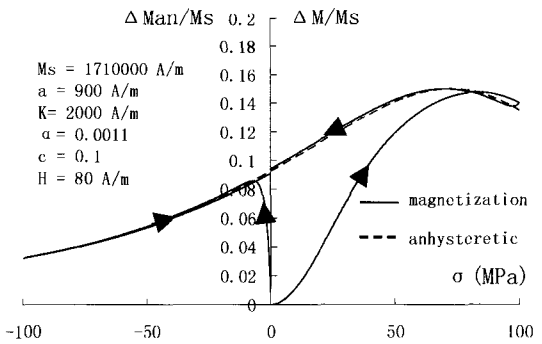

Figure 4. The calculated variation of magnetization with stress under conditions similar to those employed by Craik and Wood [5]. The slope at zero stress is positive.

The calculated result using this model equation is shown in figure 4. At zero stress, the slope of induction versus stress curve is positive, either on the positive stress side or the negative stress side. This result agrees with experimental data very well.

Conclutions

Both Effective Field Theory and the Law of Approach have their limitations. Rayleigh's Law gives us a basis for the solution of current problem which arose due to disagreement between theory and observation. Law of Approach can be modified by adding a linear component into the equation in addition to the usual quadratic term. The new model equation gives results that are in better agreement with observations.

Acknowledgements

This work was supported by the NSF Industry/University Cooperative Research Program at the Center for Nondestructive Evaluation.

References

[1] D.C. Jiles, S.J. Lee, J. Kenkel and K. Metlov, "Superparamagnetic magnetization equation in two dimensions," Appl. Phys. Letts., **77**, pp: 1029-1031, 2000.

[2] M.K. Devine and D.C.Jiles, "Magnetomechanical effect in nickel and cobalt," J.Appl.Phys. **81**, 5603, 1997.

[3] Y. Chen, B.K.Kriegermeier-Sutton, J.E. Snyder, K.W.Dennis, R.W. McCallum and D.C.Jiles, "Magnetomechanical effects under torsional strain in iron, cobalt and nickel," J.Magn.Magn.Mater., **236**, pp: 131-138, 2001.

[4] D.C. Jiles, "Theory of the magnetomechanical effect," Journal of Physics D: Applied Physics, **28**, 1537, 1995.

[5] Craik D J and Wood M J "Magnetization changes induced by stress in a constant applied field" J.Phys. D: Appl.Phys. **4** 1009, 1971

[6] D.C.Jiles, Title: Journal of Physics D: Applied Physics, **28**, 1537-1546, 1995.

[7] William Fuller Brown, JR. Title: Physical Review, Volume 75, Number1, 1949

[8] D.C.Jiles, Czech Journal of Physics, 50, 893, 2000.

A New Approach To Modeling The Magnetomechanical Effect

D.C. Jiles[1,2] *Fellow, IEEE* and L. Li [1], *Student Member, IEEE*
[1]Center for Nondestructive Evaluation
[2] Materials and Engineering Physics Program, Ames Laboratory
Iowa State University, Ames, IA 50011, USA

Abstract

This paper reports on results taken to validate the extension to the theory of the magnetomechanical effect reported recently. This theory is based on a "law of approach" but the underlying equations have been generalized to include linear and non-linear terms which are analogous to those in the well-known Rayleigh law of magnetization. It is shown that the generalized theory can be applied to materials with negative magnetostriction, such as nickel, and that the stress dependent model parameters can be determined from experimental measurements. It has been found that the results show improved agreement with experimental observation compared with the more restricted previous exposition of the model.

Introduction

Development of an accurate model description of the magnetomechanical effect becomes increasingly important in the application of stress sensors using magnetostrictive materials and applications of magnetic measurements to evaluation of stress in materials. One of the major challenges today is to provide reliable models for non-linear and hysteretic effects in materials. The fundamental theory of the magnetomechanical effect is based on the "law of approach" [1]. This has recently been refined by including a linear term in the model equation, which relates to reversible changes in magnetization with stress, as described in a previous paper [2]. Although measurement of magnetomechanical effects in materials with positive magnetostriction had been performed before, there are few experimental data on materials with negative magnetostriction such as nickel that were taken to examine the relationship between the magnetic induction and stress under constant magnetic field.

Selection of model parameters for different materials with positive or negative magnetostriction can be difficult [3]. In order to verify the validity of the generalized model, a series of experiments have been performed on nickel samples which have different magnetostrictive properties. Both experimental and theoretical investigations on nickel samples have been carried out as part of this study in order to determine the relationship between model parameters and material properties. The experimental data have been used to evaluate the generality of two aspects of the new model theory, namely the model parameter determination and magnetomechanical effect simulation.

Model theories of magnetomechanical effects

As shown previously, the effect of stress on the magnetization can be approximated as an effective field described by

$$H_\sigma = \frac{3}{2}\frac{\sigma}{\mu_o}\left(\frac{d\lambda}{dM}\right)(\cos^2\theta - \upsilon\sin^2\theta) \qquad (1)$$

where σ is the stress which is negative for compression and positive for tension, λ is the magnetostriction, M is the magnetization of the material, μ_o is the permeability of free space, θ is the angle between the axis of the applied stress σ and the axis of the magnetic field H and v is Poisson's ratio. Then the total effective field H_{eff} including the stress contribution is

$$H_{eff} = H + \alpha M + H_\sigma \qquad (2)$$

where α is a dimensionless mean field parameter representing inter-domain coupling. In the isotropic limit, supposing that applied stress and magnetic field are applied coaxially, the stress-dependence of the anhysteretic magnetization curve can be determined based on the generalized Langevin function as

$$M_{an} = M_S\left\{\coth\left(\frac{H+\alpha M+H_\sigma}{a}\right) - \frac{a}{H+\alpha M+H_\sigma}\right\} \qquad (3)$$

where $a=k_BT/\mu_o m$ in which k_B is Boltzmann's constant, T is the temperature, and m is the magnetic moment of a typical pseudo-domain. The choice of a function for the anhysteretic

magnetization must depend on the details of the particular material chosen. The model using the above anhysteretic magnetization equation, which applies to isotropic materials, works satisfactorily for soft magnetic materials such as iron and nickel. However other analytic anhysteretic functions are possible [4]

Based on the irreversible, reversible and anhysteretic components of magnetization, the differential equation for the total magnetization is

$$\frac{dM}{d\sigma} = \frac{1}{\varepsilon^2}(\sigma \pm \eta E)(1-c)(M_{an} - M_{irr}) + c\frac{dM_{an}}{d\sigma} \quad (4)$$

where E is the relevant elastic modulus, c is the reversibility coefficient, M_{irr} presents the irreversible component of magnetization, ε is the rate of approach parameter which has been defined previously [1], η is a coefficient which represents the reversible change in the magnetization with the action of a stress [5]. In this work, equation (3) has been used for modeling of anhysteretic magnetization and equation (4) has been used for modeling the stress dependence of magnetization.

Experimental Procedures

Hysteresis loop and magnetization versus stress measurements were made on samples under various applied stresses within the elastic limit using a servo-hydraulic Instron mechanical testing system. The samples used for these measurements were nickel rods 140mm in length and 8mm diameter. All the measurements were conducted within the elastic limit in order to ensure a completely reversible mechanical process. An initial measurement was carried out to obtain the stress-strain curve for the material and for the purpose of obtaining preliminary hysteresis data under both tensile and compressive loading conditions. During the measurement the sample was magnetized using a solenoid. The magnetic field H was measured using a Hall sensor mounted on the sample surface. The output of a search coil wound on the sample was integrated to obtain the hysteresis loop. Magnetostriction was measured using strain gauges mounted on the sample surface. The stress-strain curve of the sample was also measured to determine the mechanical properties such as the Young's modulus for use in the simulations.

Results and discussion

The experimental data include hysteresis parameters such as the coercivity, remanence, initial permeability and maximum differential permeability. Stress-induced changes in magnetization were calculated using the improved model equation. The theoretical parameters were determined from measured hysteresis loops and magnetostriction curves under various applied stresses using the previously published inversion algorithm [6]. Hysteresis loops were modeled under zero stress levels using different sets of parameters for both as-received and annealed nickel samples.

Good agreement was observed between the experimental and modeled hysteresis loops in the low field regime (that is at field strengths below the coercive field). But the modeled hysteresis curves also showed deviations from the experimental results in particular at the knee of the hysteresis loops. A possible explanation is that at the knee of the hysteresis loop the magnetization reversal processes involve mainly reversible rotation of domain magnetization towards the applied field, as indicated by the small hysteresis in high field regime of the experimental loops [7].

Figs. 1 and 2 show the measured and modeled comparison for the as-received and annealed nickel under tensile stress. For the initial part of the magnetization curve, the modeled results show good agreement with the experimental observations both for as-received and annealed nickel samples. But along the reverse part of the curve of annealed nickel the model calculations did not agree so well with the measured results.

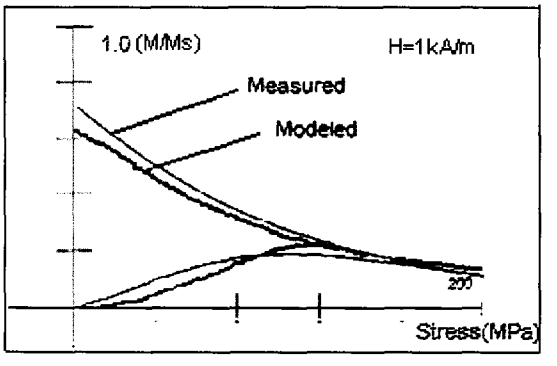

FIGURE 1. Magnetic induction B versus stress curve for as-received nickel sample at a field of 1 KA/m along the initial magnetization curve. The nickel sample was subjected to 200 MPa first and then reduced to 0 MPa. Ms = 530000 A/m, a = 6500 A/m, k = 2700 A/m, α = 0.036, c = 0.1.

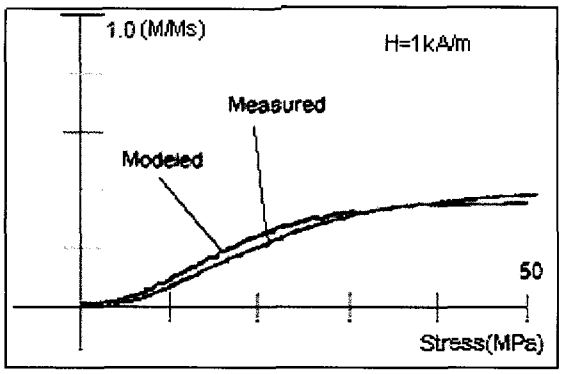

FIGURE 2. Magnetic induction *B* versus stress curve for annealed nickel sample at a field of 1 KA/m along the initial magnetization curve. The nickel sample was subjected to 50 MPa first and then reduced to 0 MPa. *Ms* = 530000 A/m, *a* = 400 A/m, *k* = 600 A/m, α = 0.0009, *c* = 0.4.

Similar results for the compression test on the as-received and annealed nickel samples were obtained following the same method in Figs. 3 and 4. It can be seen that better agreement between theory and experiment was obtained.

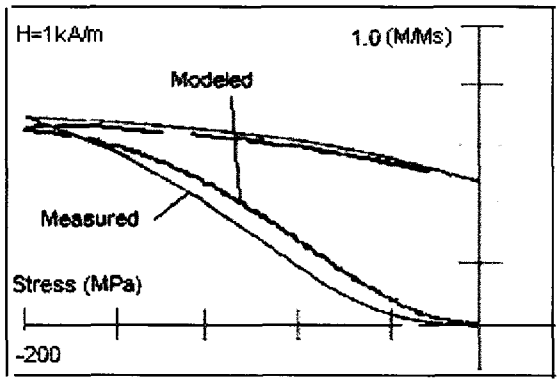

FIGURE 3. Magnetic induction B versus stress curve for as-received nickel sample at a field of 1 KA/m along the initial magnetization curve. The nickel sample was subjected to -200 MPa first and then reduced to 0 MPa. Ms =530000 A/m,a =6500 A/m,k =2700 A/m,α =0.036,c =0.1.

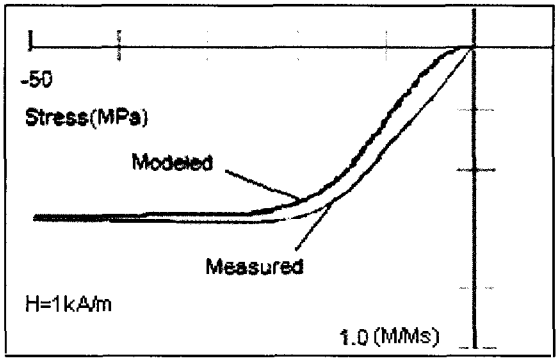

FIGURE 4. Magnetic induction B versus stress curve for annealed nickel sample at a field of 1 KA/m along the initial magnetization curve. The nickel sample was subjected to -50 MPa first and then reduced to 0 MPa. Ms = 530000 A/m, a = 400 A/m, k = 600 A/m, α = 0.0009, c = 0.4.

Conclusions

A modification of the "law of approach" for the magnetomechanical effect was achieved by taking into account both linear and non-linear terms. In order to verify the generality of the improved model, a series of experiments were made on two different nickel samples. The new model equation gave results that were better agreement both qualitatively and quantitatively with observations. However the model did not reproduce the experimental results accurately in all of the situations examined and further refinement of the model may still be needed.

Acknowledgements

This work was supported by the NSF Industry/University Cooperative Research Program at the Center for Nondestructive Evaluation, Iowa State University.

References

1. D.C.Jiles, *Journal of Physics D: Applied Physics, 28, 1537-1546, 1995.*

2. L. Li and D.C. Jiles, *IEEE Trans. Magn., vol.39, No.5, 3037-3039, Sept. 2003.*

3. P.R. Wilson, J.N. Ross, and A.D. Brown, *IEEE Trans. Magn., vol.37, No.2, 989-993, Mar. 2001.*

4. D.C.Jiles, S.J.Lee J.Kenkel and K.Metlov, *Applied Physics Letters, 77, 1029, 2000.*

5. W. F. Brown, *Physical Review, Volume 75, 541, Number1, 1949.*

6. D.C. Jiles, J.B. Thoelke, and M.K. Devine, *IEEE Trans. Magn., vol 28, No.1, 27-35, Jan. 1992*

7. C. C. H. Lo, S. J. Lee, L. Li, L. C. Kerdus and D.C. Jiles, *IEEE Trans. Magn., vol.38, No.5, 2418-2420 Sept. 2002.*

A NEW MODEL EQUATION FOR INTERPRETING THE MAGNETOMECHANICAL EFFECT USING A GENERALIZATION OF THE RAYLEIGH LAW

L. Li [1]and D.C. Jiles[1,2]

[1]Department of Electrical and Computer Engineering
[2]Ames Laboratory, US Department of Energy and Department of Materials Science and Engineering , Iowa State University, Ames, IA 50011, USA

ABSTRACT. Stress is one of the principal external factors affecting the magnetization of materials. A new and improved model equation for interpreting the magnetomechanical effect has been developed based on extension of the previous equation to include the Rayleigh law. The previous theory "law of approach" has been refined by including a new linear term in the model equation in addition to the well-known quadratic term. It was found that the modified theory provides a much better description of the magnetization changes under stress.

INTRODUCTION

The magnetomechanical effect, that is the change of magnetization of a magnetic material resulting from the application of stress, has attracted attention because of its scientific complexity. According to the previous theory of the magnetomechanical effect which is based on the "law of approach", application of stress induces changes in magnetization towards anhysteretic magnetization which itself is stress-dependent, and the rate of change of magnetization with the input elastic energy is dependent on the displacement of the prevailing magnetization from the anhysteretic magnetization. In this study, the theory has been refined by including a new linear term in the model equation in addition to the well-known quadratic term. An understanding of the complex relationships between microstructural properties of materials and magnetic measurements is being aided by the development of the new models and computer simulations. The extended model developed based on the law of approach is being validated and refined for simulations of NDE measurements on different materials under various conditions, such as different applied stresses or different applied field strengths. This approach will aid design and optimization of NDE measurements and will also improve efficiency and cost effectiveness. It was found that the modified theory provides a much better description of the magnetization changes under stress, particularly at small applied stress amplitudes and when the stress changes sign.

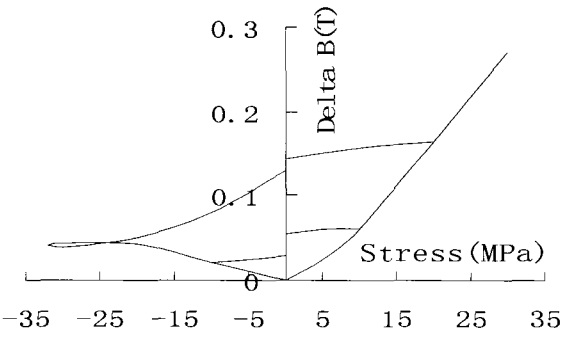

FIGURE 1. The variation in magnetic induction B with stress for a specimen of mild steel. The slope at zero stress is non-zero.

PREVIOUS MODEL THEORIES OF MAGNETOMECHANICAL EFFECTS

Recent research has shown that the magnetization curves of materials can be modeled in a variety of configurations [1]. In addition stress, whether uniaxial [2] or torsional [3], strongly affects the measured magnetic properties. The effect of stress on magnetization can be described as a perturbation of the magnetic field, since the stress affects the orientation of magnetic moments through the magnetoelastic coupling [4]. But this "effective field theory" and the "law of approach" have their limitations.

Experimental results similar to Craik and Wood [5] are shown in figure 1. At zero stress, the slope of the magnetic induction versus stress curve is positive, either on the positive stress side or the negative stress side.

As shown in previous research [4], the effect of stress on the magnetization can be considered as an effective field which can be derived from thermodynamics as the derivative of the appropriate free energy with respect to the magnetization,

$$H_\sigma = \frac{3}{2}\frac{\sigma}{\mu_o}\left(\frac{d\lambda}{dM}\right) \tag{1}$$

where σ is the stress which is negative for compression and positive for tension, λ is the magnetostriction, M is the magnetization of the material, and μ_o is the permeability of free space. This equation can be used under suitable conditions for the description of uniaxial, multiaxial and torsional stresses on anhysteretic magnetization. The total effective field H_{eff}, including the stress contribution, can be represented as

$$H_{eff} = H + \alpha M + H_\sigma \tag{2}$$

where α is a dimensionless mean field parameter representing inter-domain coupling and H is the applied field. Then the total effective field H_{eff}including the stress contribution is

$$H_{eff} = H + \alpha M + \frac{3}{2}\frac{\sigma_0}{\mu_0}\left(\frac{d\lambda}{dM}\right)_\sigma (\cos^2\theta - \upsilon \sin^2\theta) \tag{3}$$

where θ is the angle between the axis of the applied stress σ_0 and the axis of the magnetic field H and v is Poisson's ratio.

Based on symmetry, an empirical model for magnetostriction can be given as

$$\lambda = \sum_{i=0}^{\infty} \gamma_i M^{2i} \tag{4}$$

If use the first two terms as an approximation to the magnetostriction, i.e. by including the terms up to $i = 1$, this gives

$$H_{eff} = H + \alpha M + \frac{3\gamma_1\sigma_0}{\mu_0}(\cos^2\theta - \upsilon \sin^2\theta)M \tag{5}$$

Figure 2 is the calculated result based on Equation (5) which uses the effective field theory. From this figure, we can see that the slope of magnetization versus stress curve at zero stress is zero, which is not in total agreement with experimental results.

In many cases the stress can be included in the form of a perturbation to the magnetic field. The key to this description is to provide a means by which both magnetic field and stress can be treated similarly in the equations. However not all magnetomechanical behavior can be explained by the effective field theory. For example, at larger stresses this approximation is no longer valid since magnetic field and stress have different effects on magnetization.

A model theory of the changes in magnetization that a ferromagnetic material undergoes when subjected to an applied uniaxial stress has been described previously [6]. The change in magnetization on application of stress can be described by equation Equation (6), in which the rate of change of magnetization with elastic energy is proportional to the displacement of the magnetization from the anhysteretic magnetization.

$$\frac{dM}{d\sigma} = \frac{1}{\varepsilon^2}\sigma(1-c)(M_{an} - M_{irr}) + c\frac{dM_{an}}{d\sigma} \tag{6}$$

Figure 3 is a calculated result based on Equation (6). Without the linear term, the slope of the magnetization versus stress curve must be zero at zero stress. This does not occur in practice. In other words, this model equation needs to be modified in order to give predictions that are in agreement with observations.

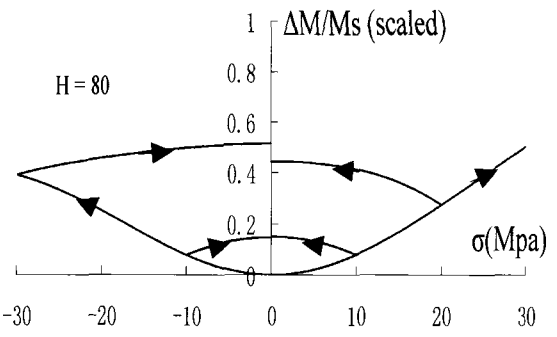

FIGURE 2. Calculated result using effective field theory. Under conditions similar to those employed in reference [5].

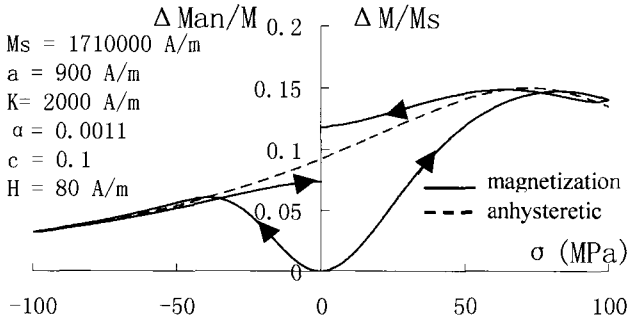

FIGURE 3. The calculated variation of magnetization with stress under conditions similar to those employed in reference [5]. The slope at zero stress is zero.

DEVELOPMENT OF MODEL THEORY OF MAGNETOMECHANICAL EFFECTS

The Rayleigh law, which describes hysteretic behavior in magnetization at low field strengths, can be expressed as

$$M = \chi_a H \pm \eta H^2 \tag{7}$$

where χ_a is the initial susceptibility and η is called the Rayleigh constant; + for positive field use, - for negative field for the initial magnetization curve. Rayleigh also showed that the hysteresis loop was composed of two parabolas:

$$M = (\chi_a - \eta H_-)H + \frac{\eta}{2}(H^2 - H_-^2) \tag{8}$$

$$M = (\chi_a + \eta H_+)H - \frac{\eta}{2}(H^2 - H_+^2) \tag{9}$$

where Equation (8) and Equation (9) present ascending and descending portions of the loop, respectively. H_+ and H_- are the maximum fields applied.

From equation (7), we will have $M_+ = \chi_a H_+ + \eta H_+^2$ and $M_- = \chi_a H_- - \eta H_-^2$ where M_+ and M_- are the magnetization at maximum magnetic field H_+ and H_-.

Substituting these into Equation (8) and Equation (9), we obtain

$$M - M_+ = \chi_a (H - H_+) - \frac{\eta}{2}(H - H_+)^2 \tag{10}$$

$$M - M_- = \chi_a (H - H_-) + \frac{\eta}{2}(H - H_-)^2 \tag{11}$$

According to Brown [7] the effect of stress on magnetization can be expressed using an equation that is very similar to the Rayleigh law. In this derivation the fractional change in volume is

$$\Delta V = \frac{V - V_0}{V_{tot}} = \alpha|\sigma| + \beta\sigma^2 \tag{12}$$

where V_0 is the original volume before any domain wall movement and V_{tot} is the total volume of the sample; α and β are constants depending on domain wall type. From this, in the simplest case of spin-up and spin-down domains, it is easily shown [8] that

$$\Delta M = 2M_s \Delta V \tag{13}$$

therefore if there is a change in volume of the domains ΔV a corresponding change of magnetization ΔM occurs. Beginning from these definitions, Equation (7) and Equation (8), we can see that the equivalent expression for changes in magnetization is

$$\Delta M = 2M_s(\alpha|\sigma| + \beta\sigma^2) \tag{14}$$

and this equation is true whether stress is increasing in the positive direction (tension) or the negative direction (compression). That is a important difference between this stress dependent equation and the normal field dependent Rayleigh region equation.

From this we can develop stress dependent equations for the Rayleigh region. When the stress is being reduced from σ_+ along the descending branch, then the equation governing this is

$$\Delta M - \Delta M_+ = 2M_s\left[\alpha(|\sigma| - |\sigma_+|) - \frac{\beta}{2}(\sigma - \sigma_+)^2\right] \tag{15}$$

when the stress is being reduced from σ_- along the ascending branch, then the equation governing this is

$$\Delta M - \Delta M_- = 2M_s\left[\alpha(|\sigma| - |\sigma_-|) - \frac{\beta}{2}(\sigma - \sigma_-)^2\right] \tag{16}$$

In other words, these curves are actually symmetric, unlike the analogous curve of magnetization versus field.

RESULTS OF NEW INVESTIGATION

Based on Equation (15) and Equation (16), a new model equation, with an additional linear term, has been developed.

$$\frac{dM}{d\sigma} = \frac{1}{\varepsilon^2}(1-c)(M_{an} - M_{irr})(\sigma \pm \eta E) + c(\frac{\sigma}{E} \pm \eta)\frac{dM_{an}}{d\sigma} \qquad (17)$$

where M_{an} is the anhysteretic magnetization, σ is the stress, M_{irr} presents the irreversible component of magnetization , E is the relevant elastic modulus, c describes the flexibility of the magnetic domain walls. ε has been defined previously [6], η is coefficient which represents irreversible change in the magnetization with the action of a stress [7].

The calculated result using this model equation is shown in figure 4. At zero stress, the slope of induction versus stress curve is positive, either on the positive stress side or the negative stress side. This result agrees well with experimental data.

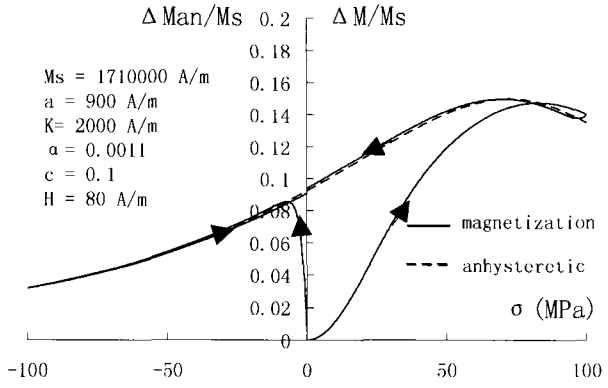

FIGURE 4. The calculated variation of magnetization with stress under conditions similar to those employed in reference [5]. The slope at zero stress is positive.

CONCLUTIONS

Both effective field theory and the law of approach have their limitations. Rayleigh's Law gives us a basis for the solution of problems which arose due to disagreement between theory and observation. The law of approach can be modified by adding a linear component into the equation in addition to the usual quadratic term. The new model equation gives results that are in better agreement with experimental observations.

ACKNOWLEDGEMENTS

This work was supported by the NSF Industry/University Cooperative Research Program at the Center for Nondestructive Evaluation.

REFERENCES

1. D.C. Jiles, S.J. Lee, J. Kenkel and K. Metlov, *Superparamagnetic magnetization equation in two dimensions*, *Appl. Phys. Letts.*, 77, pp: 1029-1031, 2000.
2. M.K. Devine and D.C.Jiles, *Magnetomechanical effect in nickel and cobalt*, *J.Appl.Phys.* **81**, 5603, 1997.
3. Y. Chen, B.K.Kriegermeier-Sutton, J.E. Snyder, K.W.Dennis, R.W. McCallum and D.C.Jiles, *Magnetomechanical effects under torsional strain in iron, cobalt and nickel*, *J.Magn.Magn.Mater.*, 236, pp: 131-138, 2001.
4. D.C. Jiles, *Theory of the magnetomechanical effect*, *Journal of Physics D: Applied Physics*, 28, 1537, 1995.
5. Craik D J and Wood M J *Magnetization changes induced by stress in a constant applied field J.Phys. D: Appl.Phys.* 4 1009, 1971
6. D.C.Jiles, *Journal of Physics D: Applied Physics*, 28, 1537-1546, 1995.
7. William Fuller Brown, JR. *Physical Review*, Volume 75, Number1, 1949
8. D.C.Jiles, Czech *Journal of Physics*, 50, 893, 2000.

Keywords

Magnetomechanical
Magnetization
Rayleigh

FURTHER APPROACH TO MODELING THE MAGNETOMECHANICAL EFFECT

L. Li [1]and D.C. Jiles[1,2]

[1]Department of Electrical and Computer Engineering
[2]Ames Laboratory, US Department of Energy and Department of Materials Science and Engineering , Iowa State University, Ames, IA 50011, USA

ABSTRACT. The magnetomechanical effect is the change of magnetization of a magnetic material resulting from the application of stress. One of the major challenges today is to provide reliable models for non-linear and hysteretic effects in materials. Development of an accurate model description of the magnetomechanical effect becomes increasingly important in the development of stress sensors using magnetostrictive materials and applications of magnetic measurements to evaluation of stress in materials. Selection of model parameters for materials with positive or negative magnetostriction can be difficult. Investigations based on experiments have been done in order to determine the relationship between model parameters and material properties. These have been used to evaluate the generality of the new model theory.

INTRODUCTION

Development of an accurate model description of the magnetomechanical effect becomes increasingly important in the development of stress sensors using magnetostrictive materials and applications of magnetic measurements to evaluation of stress in materials. One of the major challenges today is to provide reliable models for non-linear and hysteretic effects in materials. The fundamental theory on magnetomechanical effect based on 'law of approach' [1] has been refined by including a new linear term in the model equation as described in previous paper [2]. Theoretical results have been compared with published experimental data for various steel specimens [1]. Although the measurement on magnetomechanical effects in steel samples had been done before, there are few experimental data on nickel samples to examine the relationship between the magnetic induction and stress under constant magnetic field. It can be seen that in some circumstances, the refined model provides a better description of the magnetization changes under stress. However in others, it does not, especially when the stress decrease from the maximum value. The key point for this problem is to choose a correct set of model parameters for different materials. However, selection of parameters for different materials with positive or negative magnetostriction can be difficult [3]. In order to verify the generality of the improved model, a series of experiments were made on nickel samples which have different magnetostrictive properties. The experiment involved applying an external stress

to the materials at up to 60% of the estimated yield strength and detecting the changes in magnetic induction *in situ* using an encircling coil. With this object, both experimental and theoretical investigations on cold-worked and annealed nickel samples have been carried out recently in order to determine the relationship between model parameters and material properties. The experimental data has also been used to evaluate the generality of two aspects of the new model theory, namely the model parameters calculation and magnetomechanical effects simulation. The calculated results and experimental results are compared both qualitatively and quantitatively in this research.

MODEL THEORIES OF MAGNETOMECHANICAL EFFECTS

As shown in previous research [1], the effect of stress on the magnetization can be considered as an effective field described as

$$H_\sigma = \frac{3}{2}\frac{\sigma}{\mu_o}\left(\frac{d\lambda}{dM}\right), \quad H_{eff} = H + \alpha M + H_\sigma \tag{1}$$

where σ is the stress which is negative for compression and positive for tension, λ is the magnetostriction, M is the magnetization of the material, and μ_o is the permeability of free space, α is a dimensionless mean field parameter representing inter-domain coupling and H is the applied field. Then the total effective field H_{eff}including the stress contribution is

$$H_{eff} = H + \alpha M + \frac{3}{2}\frac{\sigma_0}{\mu_o}\left(\frac{d\lambda}{dM}\right)_\sigma (\cos^2\theta - \upsilon\sin^2\theta) \tag{2}$$

where θ is the angle between the axis of the applied stress σ_0 and the axis of the magnetic field H and v is Poisson's ratio. In the isotropic limit, supposing the of applied stress and magnetic field have the same direction, the stress-dependence of the anhysteretic magnetization curve can be determined as

$$M_{an} = M_S\left[\coth\left(\left(H + \alpha M + \frac{3}{2}\frac{\sigma}{\mu_o}\left(\frac{d\lambda}{dM}\right)_\sigma\right)/a\right) - a/\left(H + \alpha M + \frac{3}{2}\frac{\sigma}{\mu_o}\left(\frac{d\lambda}{dM}\right)_\sigma\right)\right] \tag{3}$$

where $a=k_BT/\mu_o m$ in which k_B is Boltzmann's constant, T is the temperature, and m is the magnetic moment of a typical domain. In the uniaxial case and planar case, the stress-dependence of the anhysteretic magnetization can be expressed by other formats. That is to say, the choice of a function for the anhysteretic magnetization must depend on the details of the particular material chosen. The phenomenological model using the above anhysteretic magnetization equation applies to isotropic material, also works satisfactorily for soft magnetic materials such as iron, steel and annealed nickel.

Based on the irreversible, reversible and anhysterestic components of magnetization described in [1], the differential equation for the total magnetization [4] is

$$\frac{dM}{d\sigma} = \frac{1}{\varepsilon^2}(\sigma \pm \eta E)(1-c)(M_{an} - M_{irr}) + c\frac{dM_{an}}{d\sigma} \tag{4}$$

where E is the relevant elastic modulus, c describes the flexibility of the magnetic domain walls, M_{irr} presents the irreversible component of magnetization, ε has been defined previously [1], η is coefficient which represents irreversible change in the magnetization with the action of a stress [5].

PROCEDURES

The objective of this research is to perform systematic experimental studies of connection between micro-structural changes due to stress and magnetic properties of ferromagnetic materials. *In situ* hysteresis loop and B-Stress measurements were made on samples under various applied stresses within the elastic limit using a servo-hydraulic mechanical testing system. The samples used for these measurements are nickel pods with 5.4 inch length and 0.318 inch diameter. All the measurements were conducted within the sample's elastic limit in order to make a completely reversible process. An initial measurement was carried out using the Magnescope to obtain the stress-strain curve for the material and for the purpose of obtaining preliminary hysteresis data under both tensile and compressive loading conditions. During the measurement a sample was magnetized using a solenoid. The magnetic field H was measured using a Hall sensor mounted on the sample surface. The output of a search coil wound on the sample was integrated to obtain the hysteresis loop. Magnetostriction was measured using strain gages mounted on the sample surface.

RESULTS AND DISCUSSION

The results, all carried out under positive (tensile) and negative (compressive) loading conditions for both cold-worked and annealed nickel samples, are obtained directly from Magnescope. The results include magnetic (hysteresis) parameters such as the coercivity, remanence, initial permeability and maximum differential permeability. Stress-induced changes in magnetization were simulated using the improved model equation of the magnetomechanical effect. The input model parameters were determined by measuring hysteresis loops and magnetostriction curves under various applied stresses using the Magnescope. The stress-strain curve of the sample was also measured to determine the mechanical properties such as the Young's modulus for use in the simulations. Hysteresis loops were simulated for zero stress levels using different sets of parameters for cold-worked and annealed nickel samples. By the inversion algorithm, modeled hysteresis loops and measured curves are compared in figure 1 and figure 2.

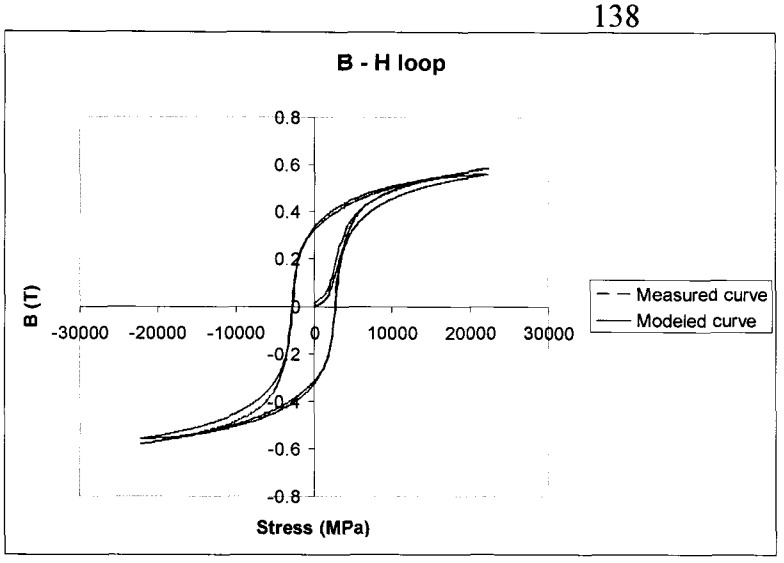

FIGURE 1. Comparison of experimental and modeled data for cold-worked nickel sample using calculated parameters Ms = 530000 A/m, a = 6500 A/m, k = 2700 A/m, α = 0.036, c = 0.1.

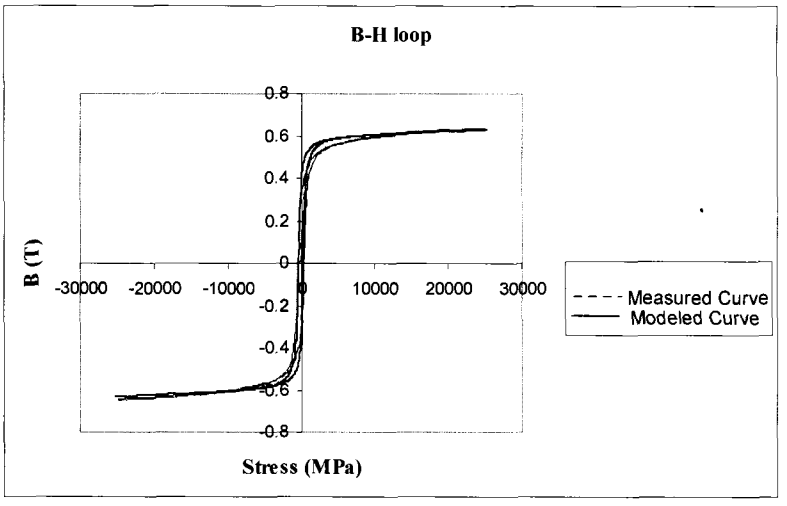

FIGURE 2. Comparison of experimental and modeled data for annealed nickel sample using calculated parameters Ms = 530000 A/m, a = 400 A/m, k = 600 A/m, α = 0.0009, c = 0.4.

Good agreement was observed between the experimental and modeled hysteresis loops in the low field regime (that is at field strengths below the coercive field). But the modeled hysteresis curves also showed deviations from the experimental results in particular at the knee of the hysteresis loops. A possible explanation is that at the knee of the hysteresis loop the magnetization reversal processes involve mainly reversible rotation of domain magnetization towards the applied field, as indicated by the small hysteresis in high field regime of the experimental loops [6]. The stress-dependence of magnetostriction curve λ (M, σ) can be described in terms of the stress dependence of γ_1 and γ_2 using a Taylor series expansion as described by [1]. And the stress related model parameter $\gamma_{11} \sim \gamma_{22}$ can be obtained from curve fitting from γ_1 and γ_2 versus stress graph which can be draw from anhysteretic experimental data.

Based on these parameters, the calculated curve of cold-worked nickel sample is shown in figure 4, compared with measured curve shown in figure 3. It can be seen that the

curve shapes agree well with each other except the initial magnetic induction part. The quantitatively comparison is shown in table 1.

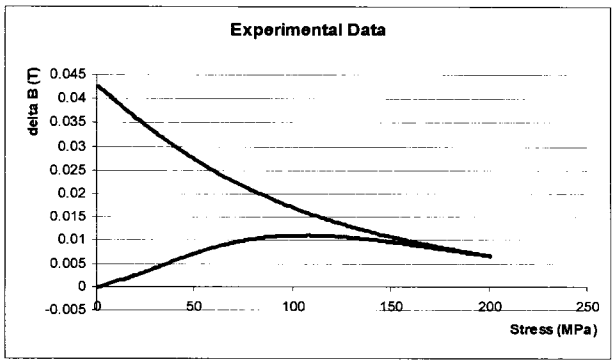

FIGURE 3. Magnetic induction *B* versus stress curve for cold-worked nickel sample. The nickel sample is subjected to 200 MPa first and then reduced to 0 MPa.

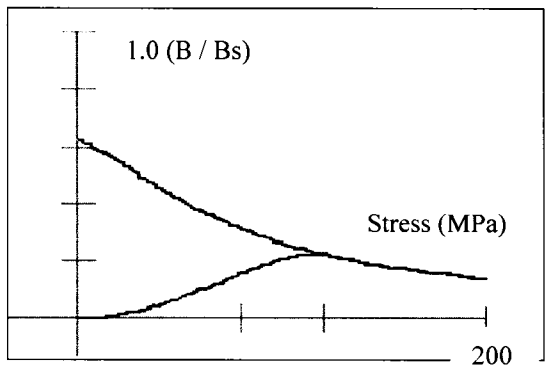

FIGURE 4. Calculated curve using parameter *Ms* = 530000 A/m, *a* = 6500 A/m, *k* = 2700 A/m, α = 0.036, *c* = 0.1. The curves are normalized by Ms.

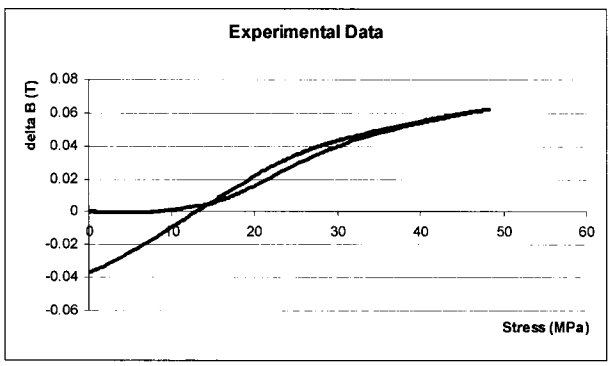

FIGURE 5. Magnetic induction *B* versus stress curve for annealed nickel sample. The nickel sample is subjected to 50 MPa first and then reduced to 0 MPa.

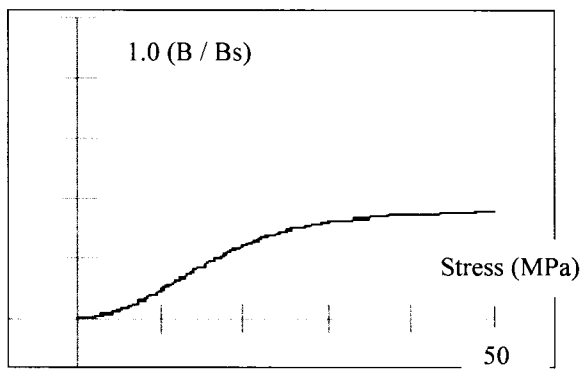

FIGURE 6. Calculated curve using parameter *Ms* = 530000 A/m, *a* = 400 A/m, *k* = 600 A/m, α = 0.0009, *c* = 0.4. The curves are normalized by Ms.

Figure 5 and figure 6 show the measured and modeled comparison for the annealed nickel sample using the parameters obtained from figure 2. For the initial part of the magnetic induction curve, the calculated data shows good agreement to the experimental data. But opposite to the cold-work situation, the reverse part of the modeled curve doesn't agree with the measured one, neither quantitatively nor qualitatively. Due to the model software's problem, this part of curve isn't shown in figure 6. The quantitative comparison is shown in table 1.

Compressive measurements were also conducted to both the cold-worked and annealed nickel sample. The nickel sample was subjected to maximum load within the elastic limit and then reduced to zero load. Several cycles were carried out in order to get the mean value of the measurement. Figure 5 ~ figure 8 show the experimental data and calculated results. It can be seen that better results can be obtained for the cold-worked nickel, but again the reverse part of magnetic induction curve of annealed nickel can not agree with the experimental data. The quantitative comparison is shown in table 2.

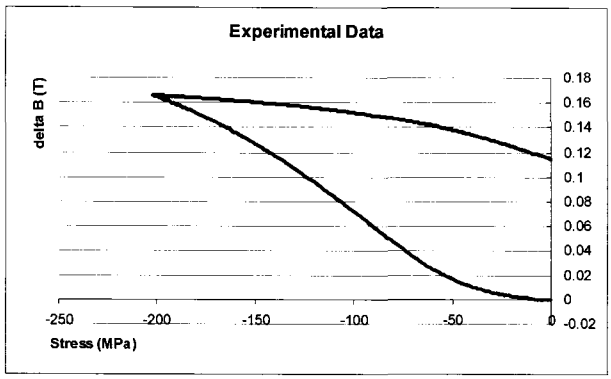

FIGURE 5. Magnetic induction *B* versus stress curve for cold-worked nickel sample. The nickel sample is subjected to -200 MPa first and then reduced to 0 MPa.

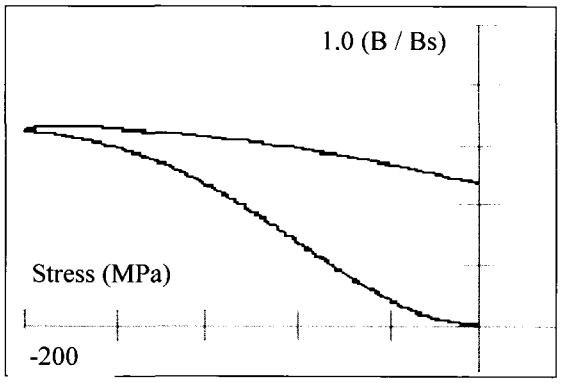

FIGURE 6. Calculated curve using parameter *Ms* = 530000 A/m, *a* = 6500 A/m, *k* = 2700 A/m, α = 0.036, *c* = 0.1. The curves are normalized by Ms.

Tensile load	ΔB_{max} (T)		ΔB_{rem} (T)	
	Measured	Modeled	Measured	Modeled
Cold-worked	0.007	0.005	0.043	0.061
Annealed	0.062	0.050	n/a	n/a

TABLE 1. Comparison of measured and experimental data of nickel sample under tensile load.

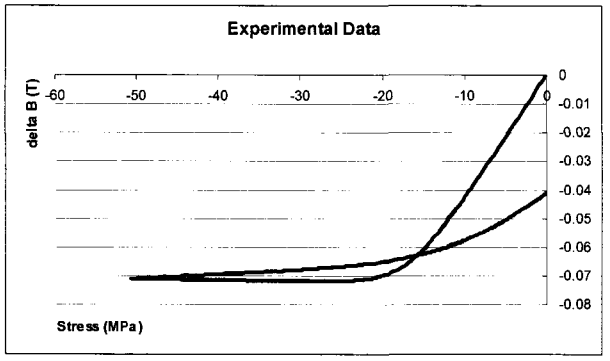

FIGURE 7. Magnetic induction *B* versus stress curve for annealed nickel sample. The nickel sample is subjected to -50 MPa first and then reduced to 0 MPa.

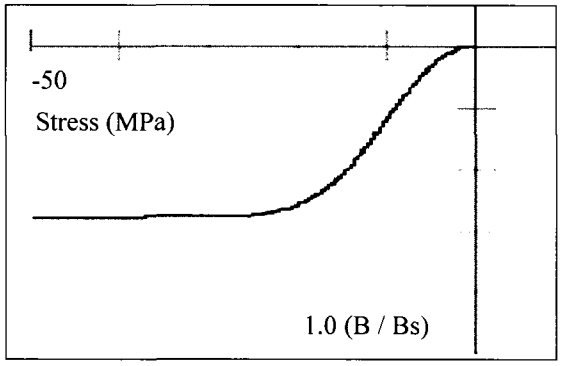

FIGURE 8. Calculated curve using parameter *Ms* = 530000 A/m, *a* = 400 A/m, *k* = 600 A/m, α = 0.0009, *c* = 0.4. The curves are normalized by Ms.

Compressive load	ΔB_{max} (T)		ΔB_{rem} (T)	
	Measured	Modeled	Measured	Modeled
Cold-worked	0.164	0.180	-0.072	-0.059
Annealed	0.115	0.100	n/a	n/a

TABLE 2. Comparison of measured and experimental data of nickel sample under compressive load.

CONCLUTIONS

Modification of Law of Approach was done by taking into account both linear and non-linear terms. In order to verify the generality of the improved model, a series of experiments were made on nickel samples which have different magnetostrictive properties. The new model equation gives results that are in better agreement both qualitatively and quantitatively with observations. But it still needs to be revised since the model can not reproduce the experimental results in all kinds of situations.

ACKNOWLEDGEMENTS

This work was supported by the NSF Industry/University Cooperative Research Program at the Center for Nondestructive Evaluation.

REFERENCES

1. D.C.Jiles, *Journal of Physics D: Applied Physics, 28, 1537-1546, 1995.*
2. L. Li and D.C. Jiles, *IEEE Trans. Magn., vol.39, No.5, Sept. 2003.*
3. Peter R. Wilson, J. Neil Ross, and Andrew D. Brown, *IEEE Trans. Magn., vol.37, No.2, Mar. 2001.*
4. L. Li and D.C. Jiles, *Review of Progress in Quantitative Nondestructive Evaluation, Bellingham, Washington, 2002.*
5. William Fuller Brown, JR. *Physical Review, Volume 75, Number1, 1949.*
6. C. C. H. Lo, S. J. Lee, L. Li, L. C. Kerdus and D.C. Jiles, *IEEE Trans. Magn., vol.38, No.5, Sept. 2002.*

Keywords

Magnetomechanical
Magnetization
Model parameter

REFERENCES

[1] G. Bertotti, Hysteresis in Magnetism, *Academic Press,* London, 1998.

[2] E. Della Torre, Magnetic Hysteresis, *IEEE Press,* Piscataway, 1999.

[3] A. Iv´anyi, Hysteresis Models in Electromagnetic Computation, *Akad´emiai Kiad´o,* Budapest, 1997.

[4] I. D. Mayergoyz, Mathematical Models of Hyseresis, *Springer,* New York, 1991.

[5] Rayleigh, Lord, *Phil. Mag.*, **23**, 225, 1887.

[6] Becker, R. and Doring, W., *Ferromagnetismus*, Springer, Berlin, 1938.

[7] Bozorth, R. M., *Ferromagnetism*, Van Nostrand, New York, 1951.

[8] Fröhlich, O., *Electrotech* **Z.**, **2**, 134, 1881.

[9] Kennelly, A. E., *Trans. Am. IEE.*, **8**, 485, 1891.

[10] Weiss, P., *J. Phys.*, **9**, 373, 1910.

[11] D.C. Jiles and D.L. Atherton, Theory of ferromagnetic hysteresis, *J. Magn. Magn. Mater.*, **48**, 1986.

[12] B.D. Cullity, Introduction to Magnetic Materials, *Addison-Wesley*, New York, 1972.

[13] H.J. Williams, *Phys. Rev.* **52**, 747, 1937.

[14] S. Chikazumi, *Physics of Magnetism*, Wiley, New York, 1964.

[15] F. Preisach, Zeit, *Für Physik* **94**, 277, 1935.

[16] L. Nëel, *J. de Phys. Rad.* **11**, 49, 1950.

[17] L. Nëel, *Advan. Phys.* **4**, 191, 1955.

[18] W. F. Brown, *J. Appl. Phys.* **30**, 62S, 1959.

[19] A. Aharoni, *J. Appl. Phys.* **30**, 70S, 1959.

[20] M. Langevin, Ann. De Chem. et. al., *Phys.* **5**, 70, 1905.

[21] D. C. Jiles, Theory of the magnetomechanical effect, *J. Phys. D: Appl. Phys.* **28** 1537-1546, 1995.

[22] D. A. Kaminski, D. C. Jiles and M. J. Sablik, Angular dependence of the magnetic properties of polycrystalline iron under the action of uniaxial stress, *J. Magn. Magn. Mater.* **104**, 382, 1992.

[23] D. C. Jiles, S. J. Lee, and J. Kenkel, Superparamagnetic magnetization equation in two dimensions, *Applied Physics Letters,* **Vol. 77**, No. 7, 2000.

[24] M. J. Sablik and R. A. Langman, Approach to the anhysteretic surface, *J. Appl. Phys.* **79**, 6134, 1996.

[25] M. J. Sablik, A model for the Barkhausen noise power as a function of applied field and stress, *J. Appl. Phys.*, **74**, 5898, 1993.

[26] D. C. Jiles, Dynamic of domain magnetization and the Barkhausen effect, *Czechoslovak Journal of Physics*, **50**, 893, 2000.

[27] M. J. Sablik, G. L. Burkhardt, H. Kwun, D. C. Jiles, A model for the effect of stress on the low-frequency harmonic content of the magnetic induction in ferromagnetic materials, *J. Appl. Phys.*, **63**, 3930, 1988.

[28] M. J. Sablik and D. C. Jiles, Coupled magnetoelastic theory of magnetic and magnetostrictive hysteresis, *IEEE Trans. Mag.*, **29**, 2113, 1993.

[29] M. J. Sablik, A model for asymmetry in magnetic property behaviour under tensile and compressive stress in steel, *IEEE Trans. Mag.*, **33**, 3958, 1997.

[30] D. C. Jiles and D. L. Atherton, Theory of ferromagnetic hysteresis, *J. Appl. Phys.*, **55**, 2115, 1984.

[31] D. C. Jiles, Introduction to Magnetism and Magnetic Materials, 2nd ed., *Chapman Hill*, London, pp. 201-204, 1998.

[32] D. C. Jiles, T. T. Chang, D. R. Hougen and R. Ranjan, Stress-induced changes in the magnetic properties of some nickel-copper and nickel-cobalt alloys, *J. Appl. Phys.*, **64(7)**, 3620, 1988.

[33] N. S. Akulov, *Z. Phys.* **69**, 822, 1931.

[34] L. Ne´el, *J. Phys. Rad.* **9**, 193, 1948.

[35] W. Gerling, Z. Angew. *Phys.* **28**, 4, 1969.

[36] M. Vazquez, W. Fernegel, H. Kronm¨uller, *Phys. Stat. Sol. A* **115**, 547, 1989.

[37] J. M. Makar and D. L. Atherton, *IEEE Trans. Magn.* **30**, 1380, 1994.

[38] A. Saito, T. Yamamoto, and H. Iwasaki, *IEEE Trans. Magn.* **36**, 3078, 2000.

[39] A. Notoji, M. Hayakawa, and A. Saito, *IEEE Trans. Magn.* **36**, 3074, 2000.

[40] Jiles D C, Thoelke J B and Devine M K, Determination of theoretical parameters for modelling bulk magnetic hysteresis properties using the theory of ferromagnetic hysteresis, *IEEE Trans. Magn.* **28**, 27, 1992.

[41] M. K. Devine and D. C.Jiles, Magnetomechanical effect in nickel and cobalt, *J.Appl.Phys.* **81**, 5603, 1997.

[42] Y. Chen, B.K.Kriegermeier-Sutton, J. E. Snyder, K.W.Dennis, R.W. McCallum and D. C. Jiles, Magnetomechanical effects under torsional strain in iron, cobalt and nickel, *J.Magn.Magn.Mater.*, **236**, pp: 131-138, 2001.

[43] William Fuller Brown, JR. Title: Physical Review, Volume **75**, Number1, 1949.

[44] D. J. Craik and M. J. Wood, Magnetization changes induced by stress in a constant applied field, *J. Phys. D: Appl. Phys.* **4**, 1009, 1971.

[45] Birss R. R., Faunce C. A. and Isaac E. D., Magnetomechanical effects in iron and iron-carbon alloys, *J. Phys. D: Appl. Phys.* **4** 1040, 1971.

[46] Jiles D. C. and Atherton D. L., Theory of the magnetization process in ferromagnets and its application to the magnetomechanical effect, J. Phys. D: Appl. Phys. 17 1265, 1984.

[47] Review of Progress in Quantitative Nondestructive Evaluation, *American Institute of Physics*, 2000.

[48] D.P. Craik and R.J. Fairholme, *J. de Physique Colloq.* C1, **32**, 681, 1971.

[49] D.L. Atherton and J.A. Szpunar, *IEEE Trans. Magn.* **22**, 514, 1986.

[50] I.M. Robertson, *IEEE Trans. Magn.* **29**, 2078, 1993.

[51] D. C. Jiles, Dynamic of domain magnetization and the Barkhausen effect, *Czechoslovak Journal of Physics*, **50**, 893, 2000.